Contaminant spreading in areas with a high density of Seasonal Aquifer Thermal Energy Storage (SATES) systems

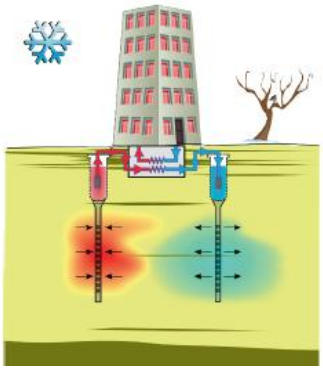

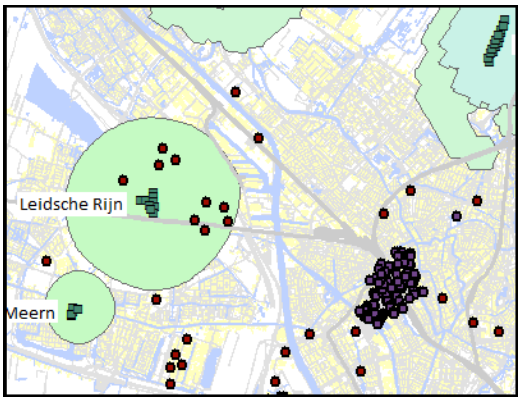

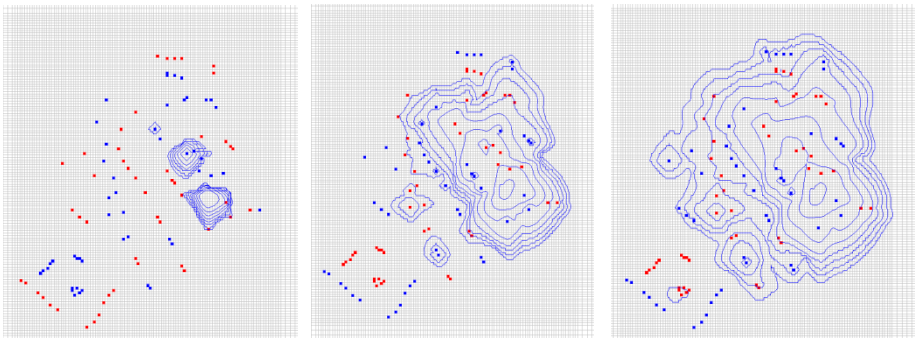

Universiteit Utrecht

KWR Watercycle Research Institute

I.H. Phernambucq

February 2015

Contaminant spreading in areas with a high density of Seasonal Aquifer Thermal Energy Storage (SATES) systems

Describing and quantifying the causes and consequences of spreading by SATES systems in the Dutch subsurface

As a thesis for	Master Study Earth Surface and Water Track Hydrology Faculty of Geosciences University of Utrecht (UU) Budapestlaan 4 3584 CD Utrecht
Host organization	KWR Watercycle Research Institute (KWR) Groningenhaven 7 3433 PE Nieuwegein
Supervisors	Ir. M. Bloemendal (KWR) Dr. N. Hartog (KWR) Prof. Dr. Ir. S. M. Hassanizadeh (UU)
Date	1 March 2015
Author	I.H. Phernambucq 3472000

Universiteit Utrecht

KWR
Watercycle Research Institute

Abstract

Seasonal Aquifer Thermal Energy Storage (SATES) is an increasingly popular type of renewable energy. Hereby summer heat and winter cold is stored in the subsurface for use in the opposite seasons. SATES systems are realized in high density in urban areas, where large amounts of contaminants are present. It is not fully understood to what extent interactions between the different SATES systems cause spreading of contaminants and to what extent SATES systems are a threat for the water quality, as groundwater protection zones are often present close by the urban area. In this study, analytical solutions, a theoretical model and a case study model of the city of Utrecht are used to describe, quantify and explain contaminant spreading in a high density SATES system area. Furthermore, these results are used to place the effects it in a regional perspective.

Model simulations showed that SATES systems contribute significantly to contaminant spreading, by two mechanisms.

1. Recirculation is the extraction of (contaminated) water by a SATES well and re-injection in the other SATES well. More wells within a SATES system and a larger distance between the extraction and injection wells increase the spreading effect of recirculation. As there is no straightforward way to model recirculation, the most realistic method, cross coupling of wells, is chosen out of several options.
2. SATES induced head changes increase spreading significantly, also in the vertical direction, and contribute to contamination dilution from a dense non-aqueous phase liquid (DNAPL).

Interaction between SATES systems is determined by overlapping capture zones. SATES induced head changes enlarge capture zones and increase the hydrological interaction of SATES systems. This results in more contaminant spreading.

Spreading is increased in such a degree, that on a timescale of decades all contaminations in a cluster of SATES systems are mixed to a single contamination plume. Contaminant travel times within a SATES system area are very small, but a buffer zone without SATES systems between the contaminated area and drinking water wells can extend the travel time significantly. In a regional perspective, other extraction wells (e.g. on building sites) are at least as important for the water quality as SATES systems, because of their purely extracting character and their much larger discharge.

This study shows how contaminant spreading is significantly increased in a high density SATES system area. It provides hands-on analytical relationships to describe the impact of several well variables on the amount of spreading. Besides, this report contains methods to properly model SATES specific processes that affect contaminant spreading. Also, the modeled contaminant spreading is placed in a larger perspective. Future research should focus on how this knowledge can be applied in regional subsurface planning.

Contents

Abstract ... 3

Contents ... 4

1. Introduction ... 6

1.1 The working of SATES systems ... 6
1.2 Increasing activity in a polluted subsurface ... 7
1.3 Problem statement and goal ... 8
1.4 Study approach and structure of report ... 9

2. Theoretical framework ... 10

2.1 Energy efficiency of SATES systems ... 10
2.1.1 Energy efficiency of an individual SATES system ... 10
2.1.2 Energy efficiency in high density SATES system areas ... 12
2.1.3 Common well patterns ... 12
2.2 The effect of SATES systems on groundwater quality ... 13
2.2.1 Groundwater quality affected by an individual SATES system ... 13
2.2.2 Contaminant spreading in high density SATES system areas ... 14

3. Methods ... 15

3.1 Modeling software ... 15
3.1.1 MODFLOW ... 15
3.1.2 MT3DMS ... 15
3.1.3 PMPATH ... 16
3.2 Setup of the theoretical model ... 17
3.3 Case study model setup ... 18
3.3.1 Setting of case study Utrecht ... 18
3.3.2 Case study model setup ... 24

4. Contaminant spreading mechanisms of SATES systems ... 29

4.1 Qualifying mechanisms and variables: the analytical approach ... 29
4.1.1 Mixing effects ... 29
4.1.2 Increased flow ... 32
4.1.3 Transport by recirculation ... 34
4.2 Qualifying mechanisms and variables using a theoretical model ... 35

4.2.1 Modeling well discharge 35

4.2.2 Modeling recirculation 37

4.2.3 Sensitivity analysis on the mechanisms 42

5. SATES systems spreading effects in a case study: Utrecht, the Netherlands 47

5.1 Spreading in a high density SATES systems area 47

5.2 Spreading by SATES systems in a regional perspective 52

5.2.1 Spreading effects on a regional scale 52

5.2.2 The effect of other extraction wells 58

6. Discussion 60

6.1 SATES system induced contaminant spreading 60

6.1.1 Recirculation is most important contaminant spreading mechanism of an individual SATES system 60

6.1.2 Overlapping of capture zones is causes hydrological interaction between SATES systems and increases contaminant spreading 61

6.1.3 A higher well discharge causes increased groundwater flow and contaminant spreading 62

6.1.4 Combining mechanisms: total spreading effect 63

6.2 SATES system induced spreading in a regional perspective 64

6.2.1 Spreading effects on a regional scale 64

6.2.2 Implications for planning 65

6.3 Further research 66

7. Conclusions 68

Acknowledgements 69

References 70

List of symbols and units 73

List of figures 75

List of tables 78

Appendix I: Recovery ratio of the warm and cold well 79

1. Introduction

The subsurface of many countries in the world is polluted. In the past it was not known to what degree pollution is harmful and waste legislation was not developed very well. Waste was dumped unconsciously or illegally. The aquifers under cities are often polluted as a consequence of activities in the past [Zuurbier *et al.*, 2013]. The pollution is present as a contamination plume or as a dense non-aqueous phase liquid (DNAPL). Common DNAPLs are Dense Non-Aqueous Phase Liquids (DNAPLs), which are often used for dry chemical cleaning and metal degreasing processes [Zuurbier *et al.*, 2013]. DNAPLs are mainly immobile and located at the bottom of the first aquifer. When a DNAPL dissolves, a plume of chlorinated hydrocarbon (CHC) grows. CHCs have also been released directly from the textile and chemical industry.

In the Netherlands the polluted subsurface is a problem, too. In 1987 it was decided that companies are obligated to remediate the subsurface that they are responsible for. However, still much contamination is present because the source is unknown or the case became barred. Contamination can dissolve in groundwater and then be transported by natural groundwater flow. This way the contamination is spread and the potential harm increased. Contaminant spreading can be a threat for the groundwater quality, the environment and the human use of the groundwater, for example for drinking water.

Contaminant spreading can be significantly increased by human activity in the subsurface. A relatively new technology that is widely applied in urban areas is Seasonal Aquifer Thermal Energy Storage (SATES). Because SATES systems have multiple pumps that cause increased groundwater flow and mixing, they increase the spreading of contaminants. Therefore SATES systems are possibly a large threat for the groundwater quality.

1.1 The working of SATES systems

Seasonal Aquifer Thermal Energy Storage is a type of shallow (< 400 m) geothermal energy. It is a so-called open system, as heating and cooling water is pumped directly into the aquifer. The most common type of a SATES system is a doublet. A doublet consists of a warm and a cold well, which are typically separated by 50 to 200 m. During summer, cold water is extracted from the 'cold well' and used to cool buildings, after which the warmed water is injected into the aquifer at the 'warm well'. During winter, the system is reversed and the stored warm water is used to heat the building, whereupon the cold water is injected by the cold well into the subsurface (Fig. 1). SATES systems for larger buildings often consist of multiple hot and cold wells. Water extracted from either warm or cold wells is collected and becomes mixed. The water is transported together and used to control the temperature of the building. Thereafter it is re-injected in the several w ells of the other type.

According to Bonte [2013], the Dutch groundwater is typically 9-12 °C. Cold water from SATES systems is 5-10 °C; warm water has temperatures from 15-20 °C. Because this temperature is too low to heat up a building, a heat pump is used to bring the water to a warmer temperature. cooling it is generally not necessary to additionally cool the water from the cold well. A heat pump can produce the heating much more efficient than a conventional heater and for cooling only pumping energy from the groundwater pump is required, instead of mechanical cooling machines. A SATES-system therefore has a much lower energy use and operational cost. SATES systems are more expensive than conventional heating and cooling systems. The payback time for the additional cost compared to a conventional system is in the Netherlands generally about 10 years [Li, 2014], but varies from 7 to 40 years, as it is also dependent on energy prices [SKB, 2013]. After the large initial investment the operational costs are low [Li, 2014].

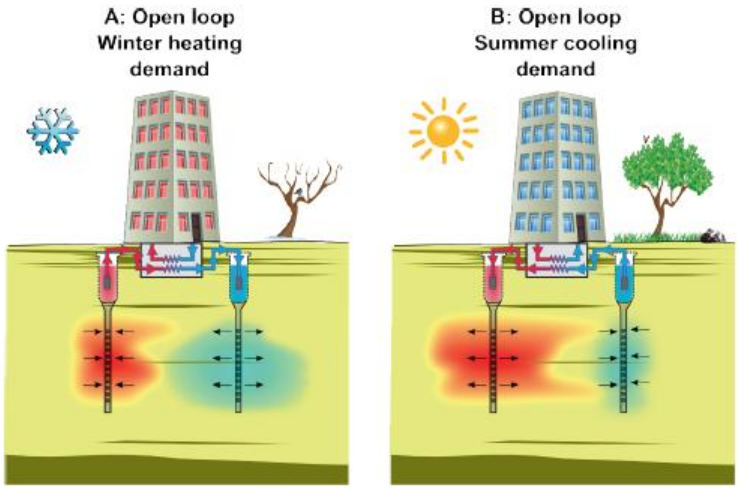

Fig. 1: The working of a SATES system [Bonte, 2013].

The other type of shallow geothermal energy is Borehole Thermal Energy Storage (BTES). BTES consists of a circuit of closed pipes in the subsurface, in which a fluid flows (often water with anti-freeze) [SKB, 2013]. Via conduction heat is exchanged with the surrounding subsurface, which can be used to control the building's temperature. Because conduction is the transport method, the fluid of BTES systems is not in contact with aquifers and the effects on groundwater flow and contaminant spreading are minimal. Therefore this study focuses on SATES systems.

1.2 Increasing activity in a polluted subsurface

In the Netherlands the use of SATES systems started in the early 1980s [Haehnlein *et al*, 2010]. The subsurface of the Netherlands is suitable for these systems, because of its 20-150 m thick permeable aquifers and a low hydraulic gradient. As SATES systems work with thermal energy storage, it needs a thermal energy surplus in one season and a deficit in the other. The moderate Dutch climate fits these conditions.

While in 1995 only 29 SATES licenses were given, in 2013 this was increased to more than 2500 (Fig. 2). This estimation excludes small SATES (discharge < 10 m^3 $hour^{-1}$) and BTES systems that were installed before 1 July 2013, as it could be done without license [Bonte, 2013]. SATES systems are expected to keep increasing in numbers at a rate of more than 10 % per year [Taskforce WKO, 2009]. Shallow geothermal energy systems will consequently be the largest groundwater user in the Netherlands before 2020 [Bonte, 2013]. Also in the rest of Europe and North America the growth rate of shallow geothermal energy systems is high [Bonte, 2013; Bloemendal *et al.*, 2013].

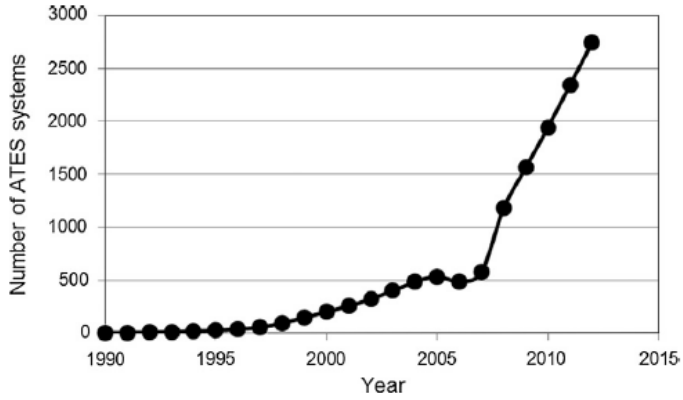

Fig. 2: The increase of SATES systems in the utilities sector in the Netherlands [Sommer, 2015].

The demand for SATES systems is high because of their contribution to sustainable energy, energy savings and CO_2 emission reduction. Yet shallow geothermal energy covers only 4 % of the total renewable energy production in the Netherlands [CBS, 2013], but it has the potential to contribute significantly to the Dutch targets. With 40 % heating is the largest energy-consumer in the Netherlands. Low temperature heating comprises about a third of the total fossil energy consumption. SATES systems could save up to 30 % compared with conventional heating and cooling systems [Bonte, 2013]. Most SATES systems are used in utility buildings. In this sector energy savings by SATES systems could amount to 11 % [Bloemendal *et al.*, 2013] and CO_2 reductions to 2 % [Taskforce WKO, 2009].

The application of SATES systems thus increases fast, but legislation lags behind. Before 2013 every province in the Netherlands had its own regulations with regard to shallow geothermal energy. In July 2013 the Order in Council on shallow geothermal energy was approved, which provided nationwide regulations. Small shallow geothermal energy systems need to be reported and large SATES and BTES systems need a license [Bonte, 2013]. The guideline for well distance is 3 times the thermal radius of a well, where well distance is the distance between individual SATES wells [Bloemendal *et al.*, 2013]. Negative thermal interference between systems is not allowed and has to be reported [De Jonge *et al.*, 2012]. Over a period of five years there should be a thermal balance [DWA and IF, 2012].

1.3 Problem statement and goal

The present guidelines thus are based on the thermal influence and effects of SATES systems. Besides, most research done on SATES systems is focused on the energy efficiency. However, contaminant spreading is affected by hydrological effects of SATES systems. As the hydrological radius of a well is about 1.5 times the thermal radius, hydrological interaction is expected. This problem is particularly present in urban areas. Due to the high density of buildings, the demand for SATES systems is the highest in urban areas. However, SATES systems require subsurface space. In many places the demand for SATES systems exceeds the available subsurface space [Bloemendal *et al.*, 2013]. At the same time, the subsurface of urban areas is contaminated. SATES systems increase contaminant spreading, which makes them a threat for the groundwater quality. However, it is not fully understood to what extent interactions between the different systems cause spreading of contaminants. Also the regional consequences for water quality are unknown. The water quality is of special importance for drinking water companies. In the Netherlands, 60% of the drinking water comes from groundwater [Bonte, 2013]. In many urban areas SATES systems are realized

close to groundwater protection zones, inducing a tenstion between different interests [Bonte *et al.*, 2008]. Authorities aim to use the subsurface as optimal and sustainable as possible, while at the same time negative spreading effects have to be minimized.

In short, because many SATES systems are mixing and spreading these contaminated sites nearby drinking water extraction wells, it is important to understand the causes and consequences of SATES induced contaminant spreading. Therefore, this study aims to 1) Clarify the mechanisms and variables that play a role in contaminant spreading by SATES systems; 2) Describe and where possible quantify the spreading within an urban area with a high density of SATES systems and the resulting impact on the groundwater quality of the surrounding region.

1.4 Study approach and structure of report

To reach the goals and get reliable results, different research methods are used in this study: analytical solutions, a theoretical model and a case study model. For the case study model a realistic and representative simulation of a subsurface with SATES systems is needed. In Utrecht, located in the center of the Netherlands, the density of SATES systems around the city center is high, while old contamination is abundantly present. This might be a threat for drinking water extractions located around the city. Besides, detailed information is available about the subsurface, the present contamination and the well locations and discharges. This makes Utrecht a suitable case study to investigate the impact of SATES system induced contaminant spreading within and beyond the SATES system area.

Hereafter, the report continues with a review of the theoretical background relevant for this research (chapter 2). Then the used modeling software and the setup of the models are described (chapter 3). In the results section I am zooming out from an individual SATES system to a regional scale. Firstly, analytical solutions that describe contaminant spreading mechanisms on small scale are presented (section 4.1) and validated by a sensitivity analysis (section 0). Subsequently, contaminant spreading within the cluster of SATES systems in Utrecht is described and quantified (section 5.1). Then the effects on a larger, regional scale are studied (section 5.2). In the discussion (chapter 6), the results of the different research methods and scale levels are combined. The consequences for regional subsurface planning are discussed and recommendations for future research are given. Finally, chapter 7 comprises the conclusions.

2. Theoretical framework

As stated in the introduction much research has been done on the energy efficiency of SATES systems, but less on the consequences for contaminant spreading. This chapter contains a literature review of the research relevant for this study.

2.1 Energy efficiency of SATES systems

2.1.1 Energy efficiency of an individual SATES system

The performance of a SATES system depends on several factors, depending on the heat demand, the heat pump and subsurface conditions. For this study the underground performance of a SATES system is relevant. This is determined by the degree of recovery of the stored thermal energy.

The recovery ratio represents the performance of a well underground. It is defined as the volume of extracted water that in the former period has been injected by the well, divided by the total volume that has been extracted. [Bear and Jacobs, 1965]. For a SATES system this can be rewritten to the real recovery of temperature over the theoretical recovery of temperature [Sommer, 2015]. The recovery ratio in a two-dimensional horizontal plane is affected by the well capture zone, which is the shape of the injection or extraction volume. Sometimes it can be assumed these volumes are cylinders and that the capture zone in two dimensions can be represented by a circle, but with a relatively large ambient groundwater flow the shape of the capture zone becomes more like an ellipse.

The parameter that determines the shape of the capture zone is defined as the dimensionless parameter $\bar{t}$ [Bear and Jacobs, 1965], that is defined in equation (1):

$$\bar{t} = \frac{2\pi D q^2 t}{\theta Q} \quad (1)$$

Where D = aquifer depth (L), q = specific discharge of ambient groundwater flow (L T^{-1}), t = length of injection or extraction period (T), θ = porosity of the aquifer (-) and Q = well discharge (L^3 T^{-1}).

$\bar{t}$ can be different for the injection and extraction stage, when the duration or the discharge differs. The higher the ambient groundwater flow, the more ellipse shaped the circle is and the higher $\bar{t}$ becomes, as shown in Fig. 3A. However, a higher well discharge can compensate and result in a lower $\bar{t}$ and a more circular shape. $\bar{t}$ is partly determined by aquifer characteristics (D, q and θ), but can partly be controlled (t and Q). As the capture zone of the injection stage is elongated downstream and the capture zone of the extraction stage upstream, this has consequences for the temperature of water that is recovered, as shown in Fig. 3B. The more ellipse shaped the capture zone is, the higher the value for $\bar{t}$ is and the lower the recovery ratio.

Next to $\bar{t}$, Bear and Jacobs [1965] estimated another parameter β that affects the recovery ratio: $\beta = \frac{Q_{ex}}{Q_{inj}}$. The larger the extraction discharge Q_{ex} relative to the injection discharge Q_{inj}, the more of the injected water is recovered by the well. For each well the recovery ratio can be determined using $\bar{t}_{\text{injection}}$, $\bar{t}_{\text{extraction}}$ and β.

Only under some limitations all of the injected water can be recovered (also shown Fig. 3B). The capture zone of the pumping stage reaches a limit downstream, the 'water divide' of the pump. No matter how large the extraction discharge is or how long the duration of the extraction stage, it is not possible to recover

injected water that has passed the water divide. For every β, a limiting $\bar{t}$ value for the injection stage exists, up to which water can be recovered. If $\bar{t}_{\text{injection}}$ is larger than that, not all injected water can be recovered.

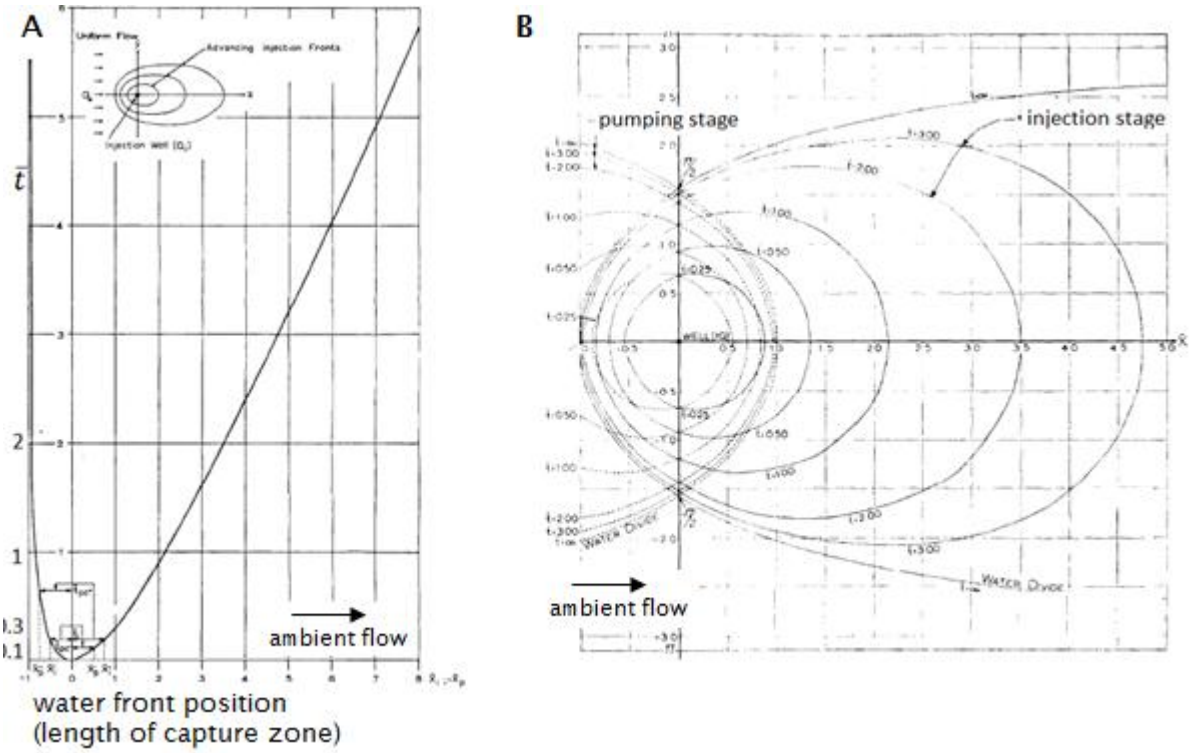

Fig. 3: (A) The length of the capture zone (x-axis) vs. the elongation as parameter $\bar{t}$ (y-axis). (B) The view from above of the shapes of the pumping (extraction) and injection capture zones. Again the length of the capture zone is projected on the x-axis. Larger circles represent more elongated capture zones (larger $\bar{t}$ values) [after Bear and Jacob, 1965].

Whether a capture zone, the hydrological influence zone of a well, can be described as a circle or as an ellipse, depends on $\bar{t}$. The critical value for $\bar{t}$ is analyzed by Ceric and Haitjema [2005]. They stated that for the interval $0 \leq \bar{t} \leq 0.1$, a radial capture zone can be assumed. The capture zone can be described as a circle with hydraulic radius, shown in equation (2):

$$r_H = \sqrt{\frac{V_{season}}{\pi H \theta}} \tag{2}$$

Where V_{season} = the total volume pumped by a well during a season, H = the well filter depth and θ = porosity of the aquifer. This equation is based on the cylindrical shape of the injected water volume: $V_{season} = \pi r_H^2 H \theta$.

In de case of $0.1 < \bar{t} \leq 1$, also a circular capture zone can be assumed, only the circle is shifted in the direction of the ambient groundwater flow. It is shifted upstream in case of an extraction well and downstream in case of an injection well. For values of $\bar{t} > 1$, the shape of the capture zones is more ellipse like. For these cases the extent of the capture zones should be calculated as described by Ceric and Haitjema [2005].

2.1.2 Energy efficiency in high density SATES system areas

The efficiency of a cluster of SATES systems is more complicated than of a single system. Wells of different systems may interfere, which affects the efficiency. The efficiency may improve if several systems of the same type interfere, but if a cold well interferes with a warm well, the efficiency may be reduced. Negative thermal interference can be prevented by a large well distance. The thermal radius r_T is described in equation (3):

$$r_T = \sqrt{\frac{c_w}{c_a}\frac{V_{season}}{\pi H}} \quad (3)$$

Where $c_w$and c_a = heat capacity of the water respectively the aquifer (both water and matrix), V_{season} = the total volume pumped by a well during a season and H = the well filter depth. The equation is based on the injection energy ($V_{season} * c_w * \Delta T$) that equals the energy in the cylinder shape of the water in the aquifer ($\pi\, r_T^2\, H\, c_a\, \Delta T$).

Sommer [2015] suggests that 2.8 – 3.3 r_T is the optimal well distance for individual doublets in the subsurface conditions of Amsterdam. However, Bloemendal *et al.* [2013] showed that theoretically a separation distance of only 1.4 times the thermal radius is sufficient to prevent negative thermal interference of the cold and warm well. A too large distance between SATES systems reduces the efficiency of the whole area, as fewer systems can be installed. Moreover, Bloemendal *et al.* [2013] suggest the present well distance is often too large, because it is based on the maximum capacity of the systems. Though generally only 60 % of the permitted well capacity is used [Bloemendal *et al.*, 2013]. A smaller well distance or a larger well discharge thus results in a potentially more optimal use of the available area.

Due to the large well distance relative to the well discharges, negative interference rarely occurs in the Netherlands. A study of SATES systems in The Hague, a Dutch city with a high SATES density, shows that negative effects of interference are negligible [De Jonge *et al.*, 2012]. The total efficiency even increased slightly when more SATES systems are simulated in the same area [MMB 7, 2012]. This is because the cold and warm wells become clustered, as a result of the required distance between cold and warm wells [Calje, 2010].

2.1.3 Common well patterns

The required well distance and prevention of negative interference results in two common well patterns: the checkerboard pattern and line pattern (Fig. 4). In the checkerboard pattern, a well distance of three times the thermal radius is advised. In the lane pattern optimal well distance between lanes should be around three times the thermal radius; between wells within a lane only half a thermal radius is optimal. There is no agreement in literature about the energetically best well pattern. Li [2014] states the checkerboard pattern is preferred above the lane pattern in regions with low groundwater velocity, because the efficiency per area is slightly higher, as the checkerboard arrangement prevents the escape of thermal bubbles. However Calje [2010] and Sommer [2015] suggest that wells in line pattern positively influence each other, while the checkerboard pattern may result in negative interference.

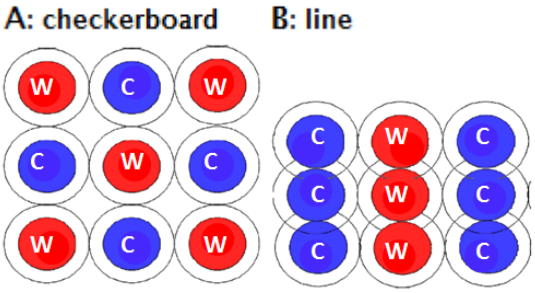

Fig. 4: The checkerboard pattern (A) and line pattern (B) [Li, 2014]. Note that the warm and cold wells become clustered in a line pattern.

2.2 The effect of SATES systems on groundwater quality

2.2.1 Groundwater quality affected by an individual SATES system

The effects of a SATES system on groundwater quality can be distinguished in two categories: temperature effects and hydrological effects.

SATES systems cause local temperature changes. As temperature has consequences for the reaction rate constant (Arrhenius equation) and equilibrium constant (Van 't Hoff equation) [MMB 3/4, 2012], chemical conditions in the aquifer are changed. Especially redox reactions can be affected in this way [Bonte, 2013]. With temperature differences larger than 20 °C or thermal imbalance, the temperature effects increase [MMB 3/4, 2012]. In addition to the impact on chemical reactions, temperature affects biodegradation. Also solubility increases and the adsorption of some contaminant species decreases with temperature, causing immobile contaminants to become more mobile [Bonte, 2013]. However these effects are minimal with the small temperature differences that SATES systems cause [Tauw, 2010], or the lifetime of SATES systems is too short for a significant change in chemical composition. Any effects in changing microbiological population cannot be measured, as the natural variation is larger than the variation due to SATES systems [MMB 3/4, 2012]. Moreover, in general temperature effects are small due to the compensating effect of the cold and warm water [Hartog *et al.*, 2013].

Hydrological effects caused by SATES systems are thought to have much more impact on the groundwater quality than thermal effects of SATES systems [MMB 3/4, 2012]. The hydrological effects can be divided in several mechanisms:

1) Groundwater mixing

SATES systems cause groundwater of different qualities to become mixed. Three different processes cause groundwater mixing.

a) Mixing in SATES wells

Groundwater has a vertical gradient in nutrients, redox conditions and salinity conditions [Bonte, 2013; MMB 3/4, 2012; MMB 9, 2012]. Also pollution and thus water quality have a gradient in the vertical direction. When a SATES system is put into operation, water is extracted, mixed and re-injected; thereby the groundwater is mixed and vertical gradients are smoothened.

b) *Due to dispersion*

At the boundary of the injected SATES water volume and the surrounding groundwater dispersion causes mixing of both water volumes [MMB 3/4, 2012]. The effect of dispersion depends on injection rates and volumes [Hartog, 2013] and the local sediment heterogeneity [Sommer, 2011].

c) *Due to ambient groundwater flow*

Natural groundwater flow causes the injected SATES water volume to become more elliptical and displaced, so the injected water is not fully recovered by the SATES system (see section 2.1.1). This way, a part of the injected water is not recovered but released to the aquifer. Also, a part of the surrounding groundwater is extracted and mixed with the SATES water volume.

2) *Increased flow*

The continuous injection and extraction of groundwater causes head changes and changes in groundwater flow pattern that can extend up to several kilometers [Bonte, 2013]. A higher hydraulic gradient accelerates groundwater flow, so advection is increased and contamination spreading increases.

3) *Transport*

Contaminants are transported by SATES system due to recirculation. Recirculation is the process of extraction and re-injection of water in another well of a SATES system. If contamination is present nearby the extraction well, it is instantly displaced and injected in the injection well.

2.2.2 Contaminant spreading in high density SATES system areas

Water mixing due to the use of several SATES systems in a relatively small area can have both positive and negative effects on a contaminated subsurface. Considering a dense non-aqueous phase liquid (DNAPL), mixing of groundwater increases dissolution [Zuurbier *et al.*, 2013], which increases the concentration and spreading of the contaminant. Considering a plume of dissolved contaminant, generally the plume becomes diluted due to spreading and increased adsorption.

Mixing can have two different effects on solute degradation. If natural degradation occurs and is sediment-limited (limited by the release of organic matter as electron donor by the sediment), contaminant spreading causes faster degradation. However if degradation is contaminant-limited, SATES systems do not increase degradation [Zuurbier *et al.*, 2013]. The amount of spreading and degradation is also dependent on local soil factors such as the geology (thickness and conductivity of layers, amount of organic matter), ambient groundwater flow and redox conditions. Also the amount and location of the contamination source and the configuration of the SATES systems are important factors affecting the spreading [Zuurbier, 2008].

MMB 9 [2012] suggests a high density of SATES systems does not necessarily lead to negative thermal interference, but it does increase the extent and rate of contaminant spreading. The effect of spreading by SATES systems is relatively highest with low ambient groundwater flow. On the other hand, net extraction by SATES systems or mixing with high quality water dilutes a contamination plume.

3. Methods

3.1 Modeling software

Both in the theoretical model and the case study model, the modeling programs MODFLOW, MT3MDS and PMPATH are used. MODFLOW is used to model groundwater flow; the wells are included in this model. Thereafter, MT3DMS or PMPATH are used. MT3DMS simulates the mass transport and PMPATH produces path lines of groundwater particles. PMWIN is used as simulation system.

3.1.1 MODFLOW

MODFLOW is used to model groundwater flow. Results are the hydraulic head distribution and water budget. In this study it is mainly used as input for the other models: MT3DMS and PMPATH.

MODFLOW is a modular three-dimensional groundwater model that is extensively used in groundwater studies [Artesia, 2015; Simcore Software, 2015; USGS, 2015]. With a finite difference approach it solves the three dimensional groundwater flow equation (4):

$$\nabla q = \nabla(k\nabla h) = S_s \frac{\partial h}{\partial t} - W \tag{4}$$

This equation describes the specific discharge q (L T^{-1}). It consists of a flux of groundwater flow on the left side, dependent on hydraulic head h (L) and hydraulic conductivity k (L T^{-1}). This equals the transient storage term $S_s \frac{\partial h}{\partial t}$ and sources and sinks W on the right hand side. The storage term is described as the head change with time, times the specific storativity $S_s = (\theta\beta + \alpha)\rho g$. The specific storativity is a measure of storage of water in the porous medium, dependent on the porosity θ, compressibility of the porous medium β, compressibility of the water α and the specific weight of the water in the aquifer ρg.

3.1.2 MT3DMS

MT3DMS stands for Modular Three-Dimensional Multispecies Transport Model. It is a further development of MT3D that works only with single-species. MT3DMS simulates solute transport using the outcome of MODFLOW [Simcore Software, 2012]. In this study it is used to simulate contaminant spreading, analyze the plume contours at different moments, analyze break through curves at several observation points and calculate travel times.

As the governing equations for heat and solute transport consist of the same terms, both can be modeled with MT3DMS [Zheng, 2010]. The research questions of this study do not require the modeling of heat transport. For completeness and understanding of the heat transport process, the equations are nevertheless discussed below.

Solute transport can be described by a formula based on the conservation of mass [Zheng, 2010], as shown in equation (5):

$$R\frac{\delta(\theta C)}{\partial t} = \left(1 + \frac{\rho_b}{\theta} K_d\right)\frac{\delta(\theta C)}{\partial t} = \nabla \cdot (\theta D_{tot} \cdot \nabla C) - \nabla \cdot (qC) + q_s C_s + \Sigma R_n \tag{5}$$

The equation solves for the solute concentration C (M L^{-3}). The left hand side consists of the transient term with a retardation factor R (–), that covers the fact that a solute might be delayed (retarded) by adsorption at the porous medium. The retardation depends on the distribution coefficient K_d (L^3 M^{-1}) representing

adsorption capacity and depending on soil composition, water temperature and pH. The right hand side of the formula has two flux terms, covers sources and sinks and at last chemical reactions.

The first flux term on the right hand side $\nabla \cdot (\theta D_{tot} \cdot \nabla C)$ reflects hydrodynamic dispersion, which consists of both diffusion and mechanical dispersion: $D_{tot} = D_{mol} + \alpha v$ ($L^2\ T^{-1}$). Diffusion is the movement of a solute from a high to low concentration following Fick's law. The diffusion coefficient is solute-dependent. Mechanical dispersion is the spreading of the solute caused by variations in flow velocity due to inhomogeneities such as flow paths through different pores and different friction. The dispersivity α is an empirical property of the porous medium.

The second flux term $\nabla \cdot (qC)$ covers advection, the travel of solute in the water due to movement of the water. Source and sink terms $q_s C_s$ can be wells, recharge, streams, contamination sources etc. At last can the solute concentration be increased or declined by occurring chemical reactions ΣR_n, such as degradation.

The equation for heat transport is based on heat conservation and consists of the same components as the solute transport equation [Zheng, 2010], as shown in equation (6):

$$R_T \frac{\delta(\theta T)}{\partial t} = \left(1 + \frac{1-\theta}{\theta} \frac{\rho_s}{\rho_w} \frac{c_s}{c_w}\right) \frac{\delta(\theta T)}{\partial t} = \nabla \cdot (\theta D_{Ttot} \cdot \nabla T) - \nabla \cdot (qT) + q_s T_s \quad (6)$$

This equation solves for temperature T. With the small temperature range of ATES systems, density and viscosity have no effect on heat transport [Sommer, 2015].

The left-side contains a thermal retardation coefficient R_T. Heat is retarded compared with fluid velocities, because heat exchange occurs with the porous medium. This is reflected in the thermal distribution coefficient $K_T = \frac{c_s}{\rho_w c_w}$ [Bakr *et al.*, 2013], which contains the ratio of the specific heat capacity of the solid (matrix) over the specific heat capacity of water.

The first flux term on the right hand side $\nabla \cdot (\theta D_{Ttot} \cdot \nabla T)$ consists of thermal dispersion which represents the heat transport by conduction and mechanical dispersion $D_{Ttot} = (D + \alpha v)$. Conduction is caused by a temperature gradient and depends on the thermal diffusion coefficient D, which is dependent on the thermal conductivity of both water κ_w and the porous medium κ_s (J m^{-1} day^{-1} $°C^{-1}$):, as shown in equation (7):

$$D = \frac{\kappa_0}{\theta \rho_w c_w} = \frac{\theta \kappa_w + (1-\theta)\kappa_s}{\theta \rho_w c_w} \quad (7)$$

Thermal dispersion consists also of a mechanical dispersion term αv, because the spreading of heat is also caused by heterogeneity's in the subsurface. This term has the same value as it has in solute transport.

Furthermore heat also travels with groundwater flow by convection as represented in the second flux term $\nabla \cdot (qT)$. This is similar to the solute transport. At last there is a source and sink term for heat $q_s T_s$.

3.1.3 PMPATH

PMPATH is the path lines model of Processing MODFLOW (PM), which uses the outcome of MODFLOW for its calculations. It uses a semi-analytical particle-tracking scheme to calculate advective transport, groundwater paths and travel times, both forward and backward, both steady-state and transient [Simcore Software, 2012]. In this study it is used to analyze flow paths and travel times, and capture zones of wells.

3.2 Setup of the theoretical model

The theoretical model is used to analyze the effect of different factors on contaminant spreading and travel time. To be able to observe the effect of individual mechanisms, a relatively simple model is set up. It consists of one layer, with hydrogeological characteristics that are comparable with the subsurface in the Utrecht area (Table 1). Solute transport takes place only by advection. To model advection, a finite difference method is used for which a Courant number needs to be specified. The Courant number reflects the portion of a cell that a solute will traverse by advection in one time step.

Table 1: Hydrogeological and transport parameters for the theoretical model [based on Deltares, 2009; MMB9, 2012; Provincie Utrecht, 2013; Tauw, 2010].

Parameter	Value	Unit
Thickness	35	m
Porosity	0.25	-
Specific storativity	0.0001	m^{-1}
Horizontal conductivity	30	m day^{-1}
Hydraulic gradient	0.001	m m^{-1}
Specific discharge	0.03	m day^{-1}
	11	m $year^{-1}$
Courant number (advection)	0.75	-

The contaminant source is modeled as a plume. The total mass of a plume does not change with time, only spreading and dilution can occur.

Several cases are run with the model. In each case, the well configuration or well discharge is changed. This way, a sensitivity analysis can be done for these factors. The exact configurations are explained in the results section 4.2.3. Then the line and checkerboard configuration are chosen, and other variables are changed. Firstly the well distance is modified and secondly the well discharge.

The model output is analyzed in two ways. Firstly, breakthrough curves of the plume are studied. The observation well lies downstream of the SATES wells, such that the effect of SATES wells will become visible in the breakthrough curves. From the breakthrough curves, the travel time can be deduced. Hence, it can be estimated to what degree SATES systems affect travel time. The peak concentration of the breakthrough curve contains information about spreading and dilution. As a second output, the plume development is observed. The total area of the plume is calculated after the plume has passed the SATES wells, such that the amount of spreading can be quantified.

3.3 Case study model setup

Before the model setup of the case study can be discussed, first the field situation in Utrecht has to be described in more detail.

3.3.1 Setting of case study Utrecht

Geology

The subsurface of Utrecht is heterogeneous and consists of an alternation of well permeable sandy aquifers and non-permeable clayey aquitards (Table 2). The upper layer is reworked due to excavations and building constructions and therefore totally mixed [Tauw, 2010]. The first (upper) aquifer consists of several horizontal layers, varying from fine sand to gravel, and has a depth from about 4 to 45 m. In the first aquifer SATES systems are placed. A 25 m thick aquitard separates the first from the second aquifer, from which drinking water companies extract groundwater. From the first aquitard downwards, faults are present, however not directly below the city center but further away in the region [Deltares, 2009].

Table 2: Simplified geology of Utrecht [after MMB 9, 2012 and Tauw, 2010].

Depth (m)	Unit	Composition	Lithostratigraphy	Comments
0 – 4	upper layer	clay with peat	Holocene (Echteld, Boxtel)	contaminated
4 – 45	aquifer 1	fine to course sand with some gravel	Kreftenheye, Urk, Sterksel	contaminated, SATES systems
45 – 70	aquitard 1	clay with peat and mud containing sand	Waalre, Peize, Strampoy	
70 – 100	aquifer 2	fine to course sand with some gravel	Peize, Waalre	Drinking water extractions
100–105	aquitard 2	clay with fine sand	Waalre, Peize	
105–160	aquifer 3	fine to course sand with some clay layers	Peize, Waalre, Maassluis	
> 160	base	clay	Oosterhout	

Hydrology

The groundwater table in the region of Utrecht varies between −0.5 and +0.9 m, which is a couple of meters below the land surface. Seven months per year there is a net surplus in precipitation; during summer there is a precipitation deficit. The total yearly net precipitation is 285 mm [KNMI, 2011], of which about 80 % flows as recharge to the groundwater [Provincie Utrecht, 2013]. A large infiltration area eastwards of Utrecht (Utrechtse Heuvelrug) and low-lying seepage areas in the west (polders) determine the groundwater flow to be westwards. The groundwater flow in the first aquifer is towards the west-northwest [Provincie Utrecht, 2013; Tauw, 2010]; in the second aquifer it is more to the west (Fig. 5). The hydraulic gradient in the second aquifer is higher, but the conductivity is lower. Hence, the groundwater velocities in both aquifers are comparable, about 10 meters per year. The head in the first aquifer is 0.5 to 1.0 m higher than in the second, inducing a small vertical head difference and thus some infiltration.

Many rivers and canals are present in and around Utrecht. Most canals have a water level of about 0.6 m, inducing infiltration from the river to the groundwater, although it amounts a small volume due to clay

layers. To the west of the city center, the south-north flowing Amsterdam-Rijnkanaal has a significant effect on the water flow, as it drains groundwater due to its low water level of -0.4 m [Tauw, 2010].

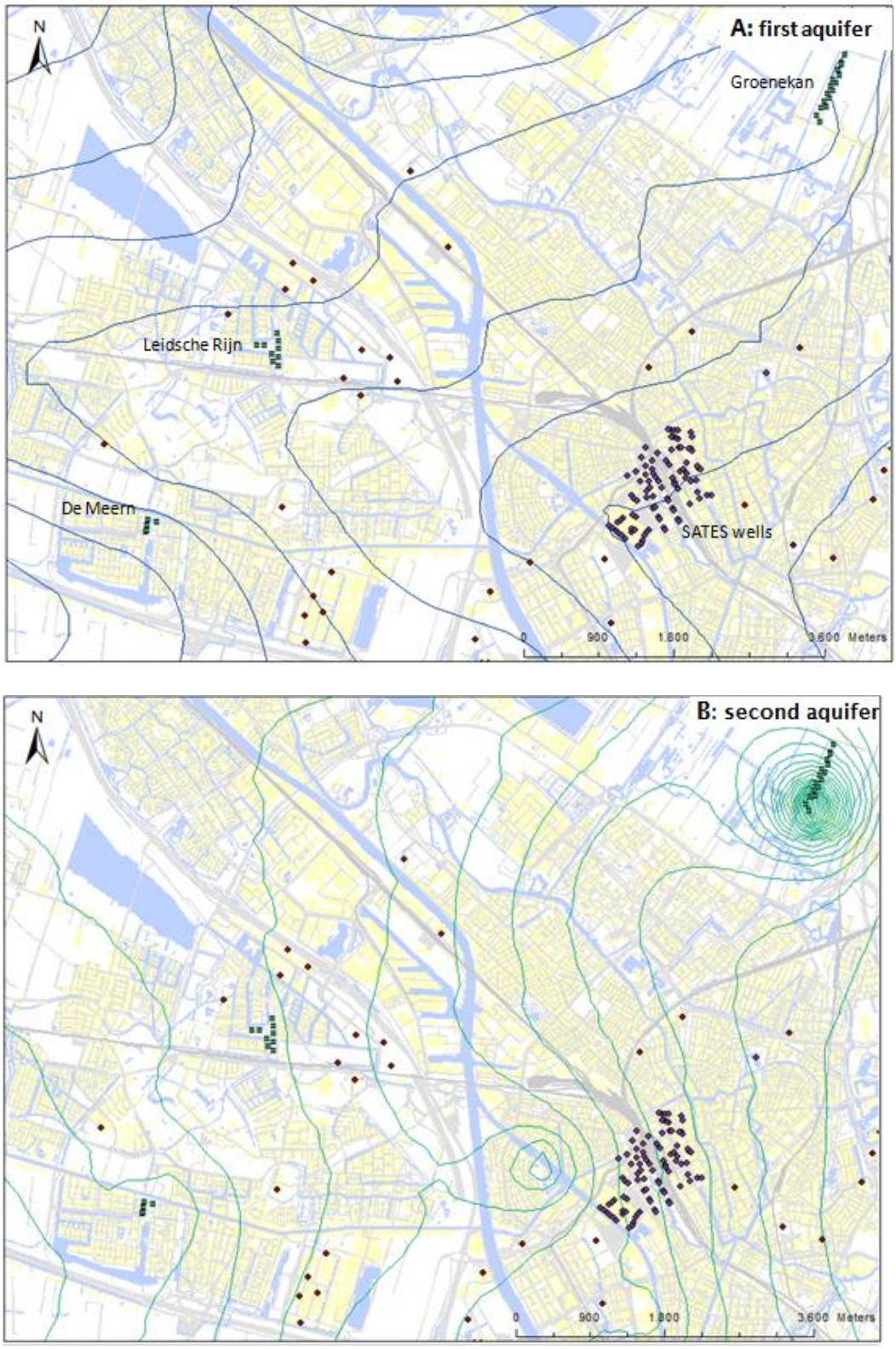

Fig. 5: 0.1 m Isohypse maps of the upper aquifer (A) and the second aquifer (B) in Utrecht. Data are from 2007 [Provincie Utrecht, 2013]. Dots indicate SATES systems in the city center (purple) and the surroundings (red). Drinking water extraction wells are indicated by green dots and labeled.

SATES systems, drinking water extractions and other wells

In the city center of Utrecht, close to the train station, 15 SATES systems are currently operational, which have a total of 91 wells. In Fig. 6 the arrangement of the systems is shown. However, also outside of the center of Utrecht more and more SATES systems are built, as shown in Fig. 7.

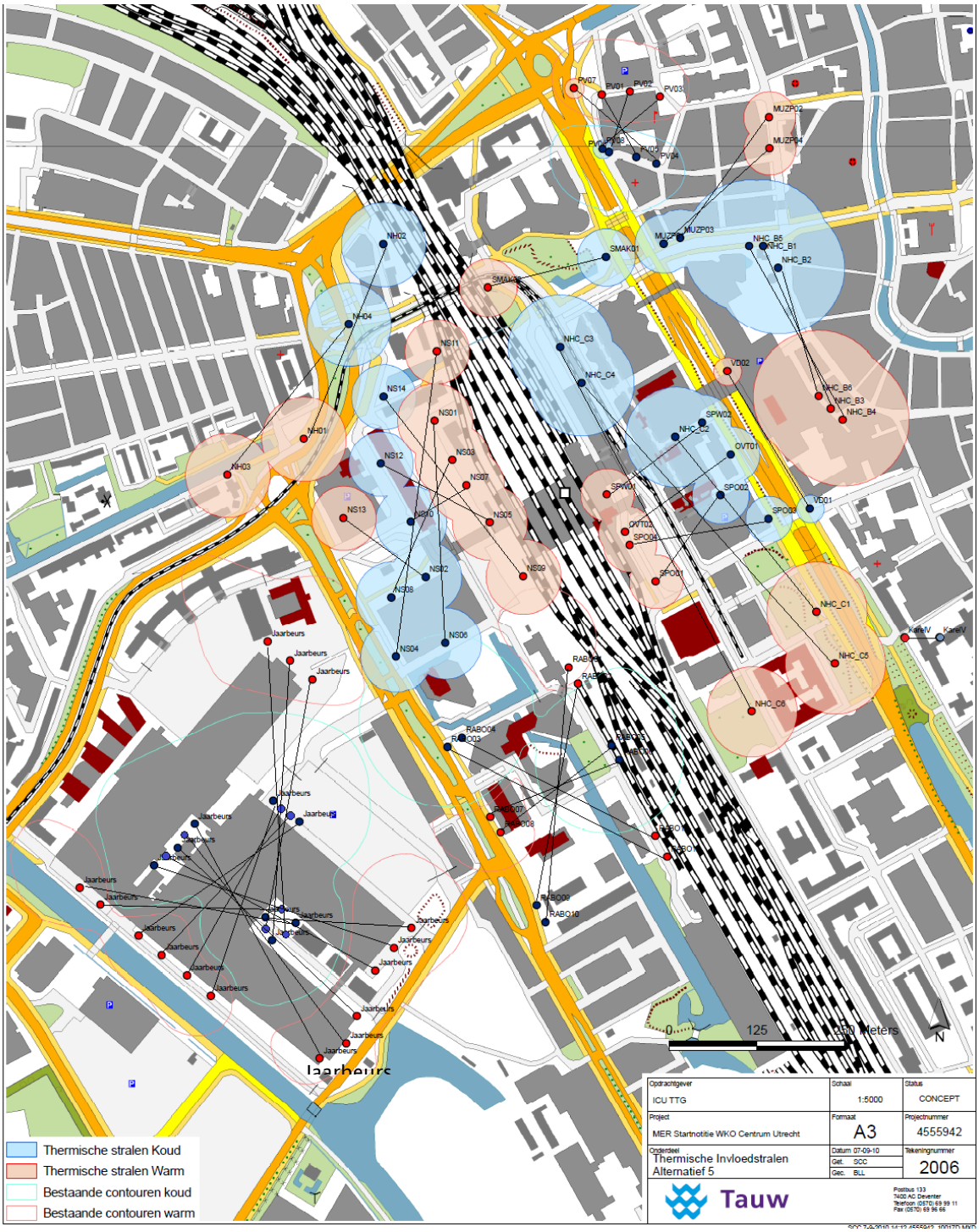

Fig. 6: SATES systems in the center of Utrecht, with warm (red) and cold (blue) wells. The circles around the wells represent the thermal radii. In the model of Utrecht, the wells are coupled as shown with the black lines.

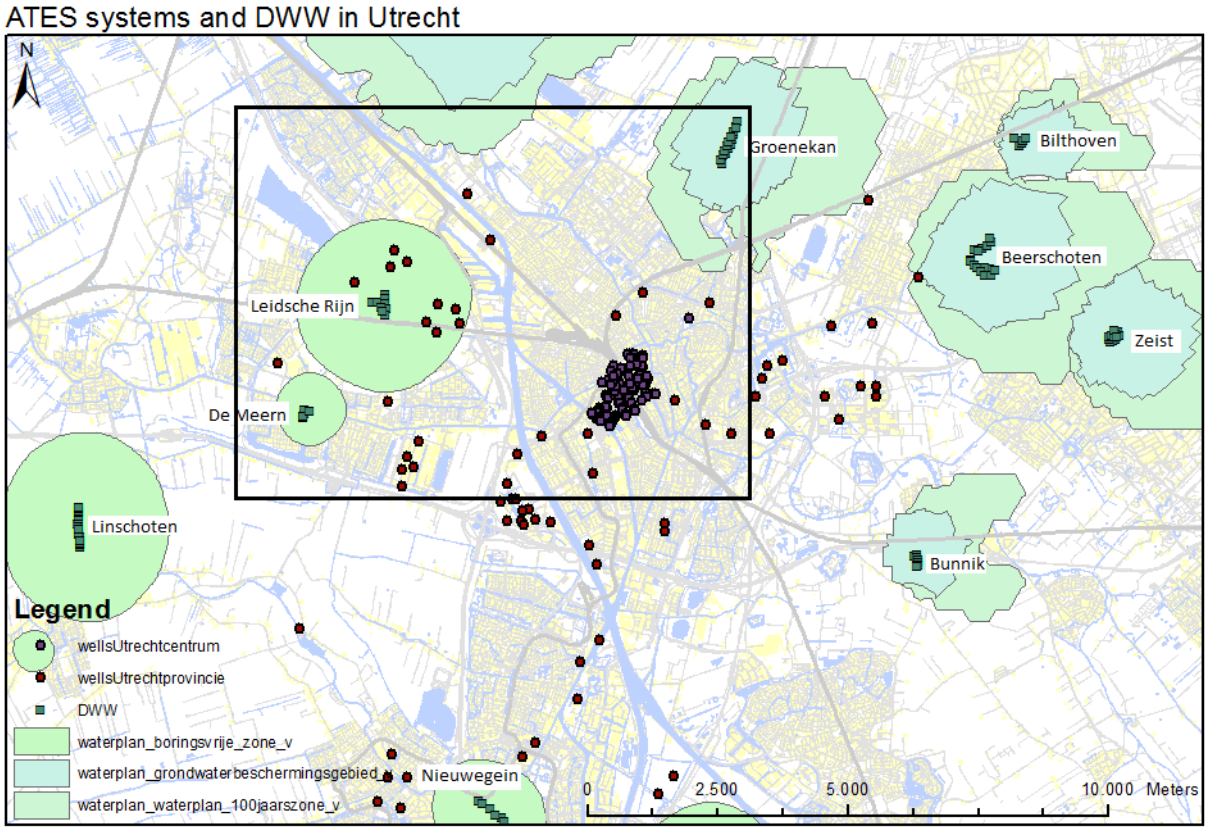

Fig. 7: SATES systems in the center of Utrecht (purple) have a much higher density than the systems in the surroundings (red). The drinking water wells lie outside of the city (green), surrounded by drilling free zones, protected areas and 100-years zones. The inner black box is the area of interest.

Nearly all the SATES systems use water of the first aquifer. About 20 million m^3 of the first aquifer is already in use, almost reaching the total volume under the center of 23 million m^3, while the demand for more systems still exists [Bloemendal *et al.*, 2013]. The SATES systems are positioned without a master plan but their locations are determined individually, causing a little energy loss due to interference [Tauw, 2010]. From 2003 to 2005, the SATES systems pumped on average at 53 % of the permitted discharge [MMB 9, 2012].

Next to the nationwide policies, there are additional requirements for SATES systems in Utrecht, according to Tauw [2010]. The systems need to be built outside of the fifty years zone of the drinking water extractions. There has to be a water balance (infiltration equals extraction) and energy balance (within 5 years the energy balance may only deviate with 15 %). Because the heat demand exceeds the cold demand, SATES systems can provide 65 % of the heat demand and 90 % of the cold demand of buildings. The temperature of the infiltrated water needs to be between 5 and 25 °C; on average the water temperature around the cold and warm wells is 8 respectively 18 °C. Earlier, the systems were only allowed in the first aquifer, but recently the province gave permission for the built of SATES systems the second aquifer in urban areas, too. However, the municipality of the city of Utrecht has not allowed this yet. They fear SATES systems in the second aquifer could increase interaction between the first and second aquifer and thus contaminate the deeper water.

Drinking water extractions in the surroundings of Utrecht are located at Leidsche Rijn, De Meern and Groenekan (Fig. 7 and Table 3). Because of the west-northwest groundwater flow, contaminants from the city center are most likely to endanger the extractions at Leidsche Rijn or De Meern.

Next to SATES wells and drinking water wells, more wells are present in the region of Utrecht [Provincie Utrecht, 2011]. These are often temporarily drainages from building excavations, remediation sites etc. As SATES systems in Utrecht have an average permitted discharge of 230 $m^3\ day^{-1}$, the discharges of other extraction wells are often significantly higher (Table 4).

Table 3: Drinking water extractions in the region of the case study, number of wells and average discharge [Vitens, 2012].

	Nr. wells	Discharge per well ($m^3\ day^{-1}$), average of last 10 years
De Meern	5	860
Groenekan	16	882
Leidsche Rijn	9	1200

Table 4: Extraction wells in Utrecht, average discharge and operational period [Deltares, 2009].

Type	Discharge ($m^3\ day^{-1}$)	Period
General	240	-
Building excavations	2400	< 6 months
Drainage for pipes and cables	1680	< 6 months
Remediation site	600	< 5 years
Test drainage	3360	< 6 months
Spray	1440	-

Contamination situation

As in many urban areas, the subsurface of Utrecht is severely polluted. Although since the seventies remediation has started, still about 50 million m^3 of Utrecht's groundwater or 180 million m^3 of subsurface is contaminated [Tauw, 2010]. Most contamination has been present for about 60 years and is labeled as serious or urgent [Arcadis, 2009]. The most common contamination plumes in Utrecht are CHC plumes. CHCs consist of the mother and daughter products tetrachloroethene (PCE), trichloroethene (TCE), dichloroethene (DCE, with a cis- or a trans-configuration) and vinyl chloride (VC). VC is most commonly present in Utrecht, and in most cases the concentration is above the intervention value [MMB 9, 2012]. Also DCEcis is present in large amounts (Table 5), also due to its low degradation rate [Arcadis, 2009].

Table 5: The mass of four contaminants at different depths in the subsurface of Utrecht [after Arcadis, 2009]

Solute	Mass [kg] -5 to -15 m	Mass [kg] -15 to -30 m	Mass [kg] -30 to -50 m	*Total [kg]*
PCE	160	5	2	*167*
TCE	67	29	4	*101*
DCEcis	120	236	2101	*2101*
VC	254	942	661	*1857*
Total	*601*	*1212*	*2768*	*4581*

Other model studies of Utrecht

In Utrecht drinking water extractions are located around the city. CityChlor [2012] analyzed a groundwater model without SATES systems. They showed that groundwater path lines in Utrecht most often end up in the drinking water wells of Leidsche Rijn and De Meern. Travel times vary between 115 years to over 1000 years; contaminants haven't reached the extraction wells within 200 years. According to the model of CityChlor, path lines originated in the city center split up. The northern part flows northwestwards and the southern part southwestwards. Further away from the city center, at the eastern side of the Amsterdam Rijnkanaal, the path lines go downwards to the second aquifer. In the second aquifer, the flow direction is towards the drinking water extractions.

The effect of groundwater mixing by SATES systems in Utrecht is currently small. According to MMB 9 [2012], the water of the first (upper) aquifer is already homogenized by the SATES systems. They state because the aquifer has overpressure and is anoxic, the effect of SATES systems on redox conditions is small, too. The temperature range is also too small to have significant effects on the chemistry and microbiology. Because of the mixed situation in the first aquifer, a couple of years ago the municipality of Utrecht decided to go for regional management of remediation for the aquifer, instead of individual approaches (also called "Biowasmachine"). Over the extent of the city area the contamination should be controlled, measured and degraded. It was thought that this could very well be combined with SATES systems, which mix the dissolved contamination, nutrients, organic matter and microbiota. Organic matter (electron donor) can react with the contaminant (electron acceptor) if the right bacteria are present. This is called anaerobic degradation. Thus the mixing by SATES systems was thought to be positive for the dissolution, containment and degradation of the contamination. Indeed model calculations of Arcadis [2009] show a decrease of contaminant concentration and total mass after 30 years with SATES systems, compared with a model run without SATES systems. The extent of the plumes stays about equal or decreases, too. The concentrations are decreased, mainly by dilution and increased adsorption. Degradation is increased, but has less effect in this model study.

However, the effect of SATES systems on remediation and especially degradation in Utrecht cannot be proven. The main reason is that the amount of organic matter is very low, reducing the possibility for anaerobe degradation. Addition of an electron donor, i.e. a carbon source, could increase degradation [MMB 11, 2012]. MMB 9 [2012] state that there is no significant aerobic degradation, because therefore oxygen is required, which is not the case in the first aquifer. Micro-aerobe degradation can possibly take place, but this is not verified. Another reason is that some SATES systems are located upstream of the contamination source, so their effect on spreading is minimal. Field research showed that the amount of SATES systems

that extracted and infiltrated contaminated groundwater was low [MMB 9, 2012]. Mixing effects were possibly only significant at the startup of the SATES systems about twenty years ago. For these reasons, MMB 11 [2012] suggests that generally SATES systems do not contribute to remediation, in contrary of earlier assumptions. Though SATES systems could contribute to controlling the plumes by for example net extraction. The extracted water could be drained, mixed with uncontaminated water or treated.

3.3.2 Case study model setup

For the second part of this study, a good calibrated subsurface model of Utrecht is required. The Hydromedah model is chosen. The Hydromedah model is developed under the authority of the water board Hoogheemraadschap De Stichtse Rijnlanden of district Utrecht. For more details of the model schematization and parameterization is referred to the report of Deltares [2009] and TNO [2004]. In this section only the main characteristics and the modifications done for this study are discussed.

The Hydromedah model covers the management area of the water board and includes a large area around it to prevent boundary effects. The Hydromedah model covers an area much larger than the area of interest for this study, which is the city of Utrecht and the drinking water wells downstream. To reduce running time, the model size is reduced. Faults are present in the original Hydromedah model, but not in the case study model, because of the smaller model extent. Constant head boundaries are set up with the heads from the Hydromedah model. To model only relevant processes and prevent longer running times, the MODFLOW packages recharge and evaporation (RCH package) and surface runoff (SOF package) are switched off. These packages contain aboveground effects, but as this study focuses on the confined aquifers 1 and 2, it is assumed the packages have minor effects on contaminant spreading.

The original Hydromedah model consists of eight layers, up to about -200 m. The more to the west, the deeper the layers lie under the subsurface. The model is a quasi-3D model with layer property flow. This implies that the aquifers are defined by a top, a bottom and a value for transmissivity. Between the aquifers no layer is defined, only a value for vertical leakage. This works well for water flow, however, solute transport with MT3DMS requires continuous layers in a full 3D model. Therefore, the model is redefined from eight to fifteen layers. Rather than transmissivity of the aquifers and leakage for the aquitards, the horizontal and vertical conductivities are defined. The values vary in the extent of the model (based on Deltares, 2009). The specific storage is set on 0.0001 m^{-1} [after Zuurbier *et al.*, 2013].

A geology of fifteen layers is more complex than the geology that is described in Table 2. This is because of the distinction of several layers with different conductivities within one aquifer. Therefore in (Table 6) the geology is related to the model layers.

Table 6: Model schematization related to the (simplified) geology. In bold the aquitards that are added to obtain a full 3D model.

Current model layer	Original Hydromedah model layer	Geology	Average depth (-m)	Comments
1	1	upper layer	+0.8 – 2.0	contaminated
2		**upper clay layer**	2.0 – 2.2	contaminated
3	2	aquifer 1	2.2 – 8.5	contaminated
4		aquifer 1	8.5 – 8.6	contaminated
5	3	aquifer 1	8.6 – 38	SATES, contaminated
6		aquifer 1	38 – 42	contaminated
7	4	aquifer 1	42 – 50	contaminated
8		**aquitard 1**	50 – 64	
9	5	aquifer 2	64 – 77.9	
10		aquifer 2	77.9 – 87.3	
11	6	aquifer 2	87.3 – 138	Drinking water extractions
12		**aquitard 2**	138 – 148	
13	7	aquifer 3	148 – 166	
14		**aquitard3**	166 – 187	
15	8	hydrological basement	187 – 260	

The time unit is days. Due to the Hydromedah standard cell size of 25x25 meter and a study area of 10,000 x 7,500 meter, the resolution of the model is 400 x 300 cells. However, to model the hydrological effects of SATES systems, cell sizes are too big, as they are 25 m whereas the average thermal radius of a SATES well is 24 m. With such a low resolution, the concentration gradient cannot be simulated well and concentration spreads faster than in reality. Therefore the cells around the SATES wells in the center are split up into cells of 12.5 x 12.5 m (Fig. 8). This results in about two cells per thermal radius, which is still quite low, as Sommer [2015] advises at least five cells per thermal radius. Due to the significantly increasing model running time when smaller cell sizes are used, nevertheless cells of 12.5 x 12.5 are chosen.

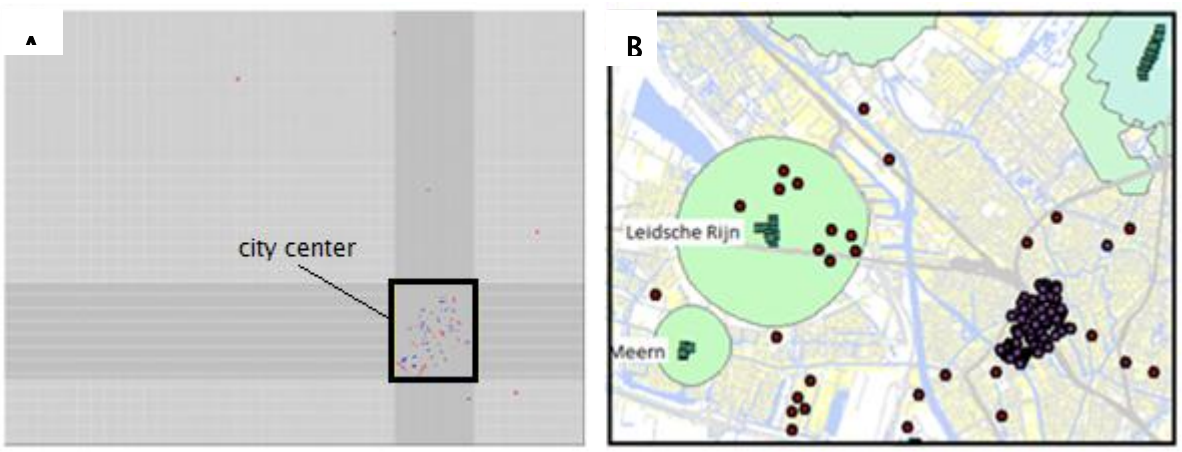

Fig. 8: (A) The fifth layer of the model containing SATES systems in the city center. The finer spatial discretization around the wells is visible. In the report, to the area containing SATES systems is further referred as the 'city center'. (B) A map of the extent of the model with SATES systems and drinking water wells.

SATES systems were initially not present in the Hydromedah model, so they were put in layer 5 of the model. The SATES systems outside the city center are not included. These systems are located at too large distances from each other, such that there is no interaction between them. In some model runs, the discharges are set on 100 % of the permitted discharge, as is the case of maximum spreading with the current configuration of SATES systems. Also model runs are done with 60 % of the permitted discharge, which is the realistic average discharge over the past years.

The drinking water wells of De Meern and Groenekan are already incorporated in the Hydromedah model, but the location of Leidsche Rijn is not. Because the same data source is desired for all drinking water extractions, all three locations are updated with data from Vitens [2012]. The well discharge is calculated based on the average extraction discharge of the period 2001-2011 as shown in Table 3.

Other extractions than SATES systems or drinking water wells in the Hydromedah model are drainages from building excavations, remediation sites etc, as shown in Table 4. Initially nothing was changed about these wells. In case of long runs where the groundwater flows from the city center towards the drinking water wells, these extractions were switched off. This was done because they had too large effects on the results, while in reality they are temporal.

As the original Hydromedah model is not used for simulating transport, all parameters had yet to be established. The values shown in Table 7 are based on values of a transport model study of a SATES system in the Uithof, Utrecht [Zuurbier *et al.*, 2013]. The porosity of the aquifer is based on Arcadis [2009]. Diffusion is negligible as it is a factor 1000 smaller than dispersion [based on Zuurbier *et al.*, 2013].

Table 7: Transport parameters in the case study model [after Arcadis, 2009 and Zuurbier *et al.*, 2013].

Parameter	Value	Unit
Porosity aquifer	0.3	–
Porosity aquitard	0.1	–
Dry bulk density aquifer	1716	kg m^{-3}.
Dry bulk density aquitard	1430	kg m^{-3}.
Courant number (advection)	0.75	–
Longitudinal dispersivity	0.1	m^2 day^{-1}
Transversal dispersivity	0.01	m^2 day^{-1}

The plumes and DNAPLs simulated with MT3DMS are predominantly theoretical contamination sources. The initial concentration of the contaminant is set on 1, representing the present concentration C over the initial concentration C_0. Hence, the value can be applied to every initial concentration C_0. Adsorption is assumed to behave like a linear isotherm with a distribution coefficient of 0.0001 m^3 kg^{-1}, which is a rough average of the four types of CHC, as PCE and TCE have a higher distribution coefficient and VC a lower [Arcadis, 2009 and Zuurbier *et al.*, 2013]. It results in a retardation factor of 1.5 (Table 8). As for the degradation rate, it is neglected such that the total mass stays equal and can be analyzed.

Table 8: Distribution coefficients, retardation factors and degradation rates used in the model [based on Arcadis, 2009]

Solute	Retardation factor aquifer (–)	Distribution coefficient (m^3 kg^{-1})	Degradation rate (day^{-1})
PCE	6	0.001	0.00038
TCE	2.4	0.0003	0.00063
DCEcis	1.5	0.0001	0.00015
VC	1.04	0.000008	0.00016

The values for solubility of the different CHCs are show in Table 9, as well as the intervention value for Dutch groundwater. Standardizing the solubility to 1, the intervention value becomes the Factor in the fourth column. It might be clear that even very small concentrations are relevant to study. Therefore, in the results the concentration contour of 1E-06 is highlighted, as representing an indication for the value where the intervention value is exceeded, if the contamination source equals solubility.

Table 9: Solubility value and intervention value [SKB, 2007], and the factor of intervention value divided by solubility.

Solute	Solubility (g/L)	Intervention value (µg/L)	Factor (-)
PCE	0.15	40	2.7E-04
TCE	1.1	500	4.5E-04
DCEcis	0.8	20	2.5E-05
VC	1.1	5	4.5E-06

In one model run, a real DCEcis plume in Utrecht is modeled. The initial size and concentration of the plumes of the CHCs are based on Arcadis [2009]. Adsorption and degradation rates are shown in Table 8. Arcadis [2009] based the retardation factors on literature. These are comparable with Zuurbier *et al*. [2013]. The distribution coefficients are calculated based on the retardation factors and used in a linear sorption isotherm. The degradation rates are based on the half-lives from Arcadis [2009], assuming first-order degradation. They calibrated the values with measurements of the city of Utrecht. The degradation rates again have the same order of magnitude as those of Zuurbier *et al.* [2013], based on literature.

The model output is analyzed in several ways. The development of plume contours is studied, to determine the effect of overlapping capture zones and recirculation. The sizes of the contaminant plumes are calculated, as a measure for spreading. Also the mass added by the DNAPL can be calculated this way. The average concentration in the plumes is used as a measure for dilution. The propagation of the plumes is also a measure for travel time. Besides, breakthrough curves are used to determine travel times and dilution. The water budget is used to determine increased water flow caused by SATES systems. PMPATH is used to determine flow paths and travel times.

4. Contaminant spreading mechanisms of SATES systems

As explained in section 2.2.1, four mechanisms cause contaminant spreading by SATES systems. In this chapter these four mechanisms are further studied. When possible, the method is described analytically, so the variables that affect spreading could be derived. In the second part of this chapter, a theoretical model is used to study the effects of these variables on spreading and verify the importance of each variable and mechanism.

4.1 Qualifying mechanisms and variables: the analytical approach

The different hydrological effects of SATES systems on contaminant spreading are discussed in the same order as in section 2.2.1.

4.1.1 Mixing effects

Mixing in SATES wells

Due to mixing within a SATES well, vertical gradients are smoothened (Fig. 9). Especially at the startup of a SATES system, this has effect on the water quality. When a contamination source is present, its mass becomes spread over the cylindrical shape of the injected water volume around the SATES system. A larger injection volume increases the effect of this mechanism. Because in MODFLOW the SATES wells are modeled as one cell, it is not possible to study vertical gradients. Therefore this mechanism is not included in this study.

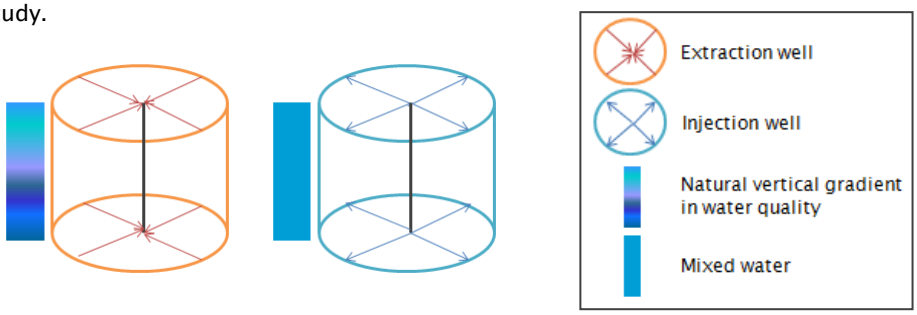

Fig. 9: Groundwater mixing and smoothening of vertical gradients at the startup of a SATES system.

Due to dispersion

Dispersion causes mixing at the boundary of the injected SATES water volume. If contaminants enter the injected cylindrical water volume due to dispersion, it is mixed with the rest of the SATES water during extraction. A higher pumping rate and a larger water volume, hence a larger well discharge, increases the dispersion mixing effect.

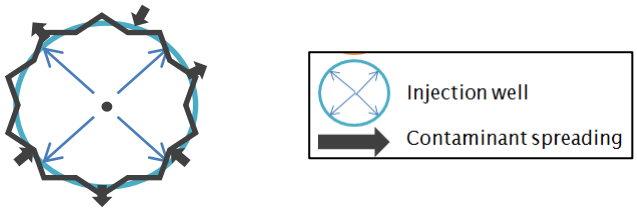

Fig. 10: Groundwater mixing due to dispersion at the boundary of the injected water volume.

Due to ambient groundwater flow

The last mixing mechanism is caused by ambient groundwater flow. Natural groundwater flow causes the injected SATES water volume to become more elliptical and displaced, so the injected water is not fully recovered by the SATES system (see section 2.1.1). This way, every pumping cycle a part of the contaminant is released to the aquifer and spread. Also, natural groundwater will be extracted by the SATES well and become mixed. This way, new contaminants can reach the SATES system (Fig. 11).

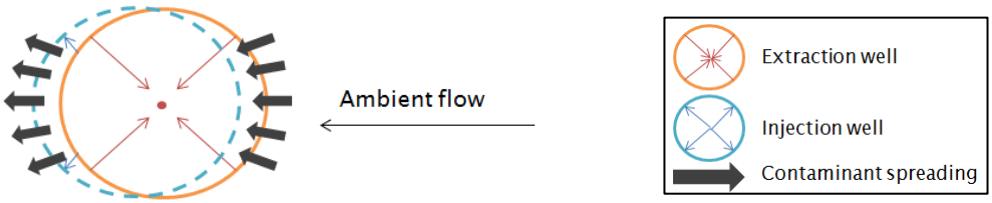

Fig. 11: Contaminant release to the aquifer.

The amount of contaminated water that is released to the aquifer depends on the recovery of the SATES well, hence, the recovery ratio. Assuming a concentration C_0 in the well, the mass that is released M_{rel} can be described as shown in equation (8):

$$M_{rel} = C_0 \cdot V_{ex} \cdot (1 - RR) \quad (8)$$

Where V_{ex} = extracted water volume, RR = recovery ratio. The term $(1 - RR)$ is the dilution term.

If the well is instantaneously contaminated and thereafter only pure groundwater reaches the SATES well, the total mass released by the well to the aquifer after n years can be described as shown in equation (9):

$$M_{rel} = C_0 \cdot V_{ex} \cdot (1 - RR^n) \quad (9)$$

This is not a realistic scenario, but it contributes to the understanding of the spreading mechanism of a SATES system.

The recovery ratio predominantly depends on the ambient groundwater flow relative to the well discharge and pumping duration (see also section 2.1.1). A higher well discharge relative to the ambient groundwater flow, results in a more circular capture zone, a higher recovery ratio and consequently a higher contaminant recovery. This results in a lower concentration in the ambient groundwater flow in the aquifer, and hence, more spreading and dilution.

Overlapping of capture zones of different SATES systems

As not all injected water is recovered by the same well, it is possible that water injected by a well is extracted by a nearby well. The time scale for this process can be several years, depending on the distance between the two wells and the ambient groundwater flow. If however the capture zones of two wells overlap, it might happen within one year. Hence, contaminants present in the water might spread from one SATES system to another within one year (Fig. 12).

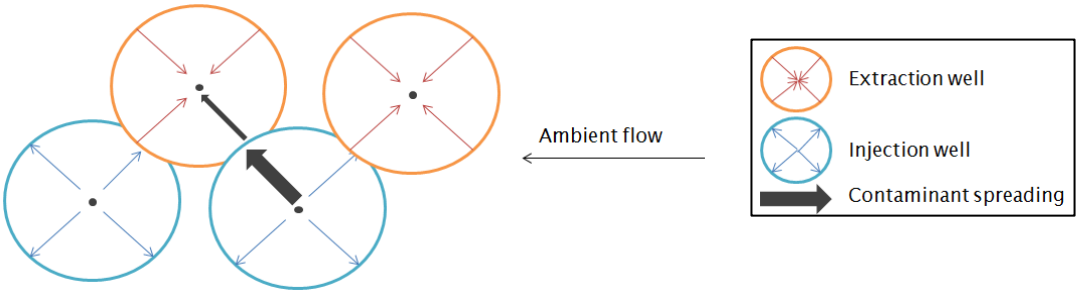

Fig. 12: Overlapping of capture zones might cause contamination to be carried over from one SATES system to another.

Whether or not two capture zones are overlapping, depends on the extent of the capture zones and the distance between the wells. Assuming circular capture zones, two capture zones overlap if the distance between two wells of different SATES systems is smaller than two times the hydraulic radius r_H. The current Dutch guideline for well distance is three times the thermal radius r_T, which results in the following expression:

$$2 \cdot r_H \geq 3 \cdot r_T$$

$$r_H \geq 1.5 \cdot r_T$$

Hence, capture zones overlap is the hydraulic radius is larger than 1.5 times the thermal radius. So to verify whether overlapping of capture zones is the case, the ratio of the hydraulic radius over the thermal radius has to be calculated. This ratio is called x in the following expression.

$$r_H = x \cdot r_T$$

In reality, the hydraulic radius is always larger than the thermal radius because of the thermal retardation process (see section 3.1.2). The hydraulic radius r_H and the thermal radius r_T of a well can respectively be calculated according to equations (2) and (3). This results in equation (10) for x:

$$\sqrt{\frac{V_{season}}{\pi\, H\, \theta}} = x \cdot \sqrt{\frac{c_w}{c_a}\frac{V_{season}}{\pi\, H}}$$

$$\frac{V_{season}}{\pi\, H\, \theta} = x^2 \cdot \frac{c_w}{c_a}\frac{V_{season}}{\pi\, H}$$

$$\frac{1}{\theta} = x^2 \cdot \frac{c_w}{c_a}$$

$$x = \sqrt{\frac{c_a}{c_w}\frac{1}{\theta}} \qquad (10)$$

Where $x > 1.5$ results in overlapping capture zones. The factor x (dimensionless) only depends on the ratio of the heat capacity of the aquifer over the heat capacity of water, and the inverse of the porosity. The heat capacity of the aquifer c_a is the combined heat capacity of the solid matrix and the water. The value depends on the type of soil and is about 2.6 MJ m^{-3} °C^{-1}; the heat capacity of water c_w is 4.2 MJ m^{-3} °C^{-1} [Sommer, 2015]. With an aquifer porosity of 0.27, the factor x becomes 1.5. With a smaller porosity or a higher heat capacity of the aquifer, the hydraulic radius becomes larger compared to the thermal radius and the capture

zones will overlap, resulting in contaminant transfer from one SATES system to another. In Fig. 6 the thermal radii of the SATES wells in Utrecht are shown and it can clearly be observed that hydraulic radii of the wells, that will be 1.5 times larger, will cause overlapping.

If capture zones do not overlap, it is still possible for contamination to spread from one SATES system to another, only it takes longer than a year. The ambient groundwater flow, accelerated by SATES induced head changes, will take the contamination downstream.

Effect contamination transfer on travel time

Contaminants that are carried over from one system to another shorten contaminant travel times significantly. The maximum effect can be determined analytically. Assuming conservative transport, the travel time without SATES systems amounts: $t = \frac{y}{q}$, where y is the total distance and q the ambient groundwater flow. However, in the worst case scenario, SATES systems would be present over the whole distance, and they would be built in such a way that contaminants can be carried over from one system to another once a year. Then they travel the maximum well distance of 3 times the thermal radius r_T per year. Assuming each SATES system has the same hydraulic radius, the travel time becomes as shown in equation (11):

$$t = \frac{y}{3\, r_T} \tag{11}$$

With SATES systems, the contaminants thus travel $\frac{3\, r_T}{q}$ times faster than without. In the study case of Utrecht the average permitted SATES well discharge of 230 m^3 day^{-1} results in a hydraulic radius of 25 m and a 6.8 times shorter travel time. For a distance of 4500 m from the city center towards drinking water extraction Leidsche Rijn, the travel time would be reduced from 413 years to 61 years.

4.1.2 Increased flow

Head changes caused by the pumping of SATES systems reach much further than the hydraulic radius [Bonte, 2013]. The most important effect of head changes is a higher hydraulic gradient, which results in groundwater flow accelerations. Another important consequence is the extra dissolution of nearby DNAPLs. A well position close to the contamination source and a high discharge significantly increase contaminant dissolution, as shown by Zuurbier *et al.* [2013].

Another consequence of head changes is that the advection process is increased, and thus travel times are shortened and spreading is increased. In a line pattern the head changes are relatively large, whereas in a checkerboard they are leveled out, so it is expected SATES wells in a line pattern result in more spreading and shorter travel times than SATES systems in a checkerboard configuration.

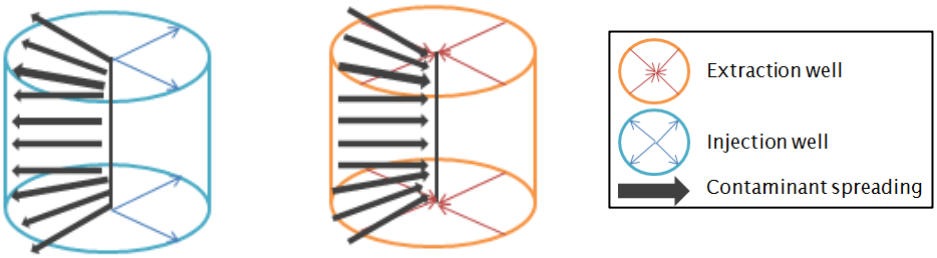

Fig. 13: The effect of SATES induced change in hydraulic head.

The effect of horizontal travel time from a certain distance r_0 towards an extraction well r_w can analytically be estimated by equation (12) after Fitts [2002]:

$$t = \int_{r\_0}^{r\_w} \frac{1}{v} dr = \frac{-2\pi\,\theta\,D}{Q} \int_{r\_0}^{r\_w} r = \frac{-\pi\,\theta\,D}{Q} (r_w^2 - r_0^2) \quad (12)$$

Where t = travel time (T), r_w = well radius (L), v = groundwater velocity (L T^{-1}), r = distance (L), θ = porosity (–), D = aquifer depth (L) and Q = well discharge (L^3 T^{-1}).

The effect of SATES systems on the travel time is represented in the well discharge. The equation shows the well discharge and travel time are inversely related. An increase of well discharge with a factor 2 will decrease the travel time with a factor 2, relatively to the ambient groundwater flow. Using the representative values for Utrecht (Table 1), with a well discharge of 230 m^3 day^{-1}, the travel time over a distance of 30 m decreases from 990 days to 107 days. When a SATES well injects water, the effect is the same, only contaminants are accelerated to flow away from the well.

Head changes are not limited to the horizontal plane. Increased flow is even the only mechanism that increases vertical flow and thus vertical transport and spreading. Vertical spreading is important to study, as in Utrecht drinking water wells extract water from deeper aquifers, whereas SATES systems are placed in the upper aquifer. Hence, the head changes caused by pumping of SATES systems might result in transport downwards through an aquitard towards a deeper aquifer.

Formula and model analyses show that:

- An injection well and an extraction well with the same well discharge result in the same vertical head difference;

- Assuming no natural vertical flow:
  $$Q \sim \frac{dh}{dz} \sim q_z \quad (13)$$
  Hence, if the well discharge Q is doubled, the vertical head difference $\frac{dh}{dz}$ and thus the amount of vertical flow q_z are doubled too, provided that no initial vertical head difference was present;

- $\frac{1}{T_a} = \frac{1}{k_a D_a} \sim \frac{dh}{dz} \sim q_z$
  Hence, if the transmissivity T_a (the horizontal hydraulic conductivity k_a times the aquifer depth D_a of the aquifer containing the well is doubled, the head difference and the vertical flow are halved;

- $L = \frac{1}{c} = \frac{k_z}{D_z} \sim q_z$
  Hence, if the leakance L of the aquitard (the inverse of the vertical resistance c, or the vertical hydraulic conductivity k_z divided by the aquitard depth D_z) is doubled, the vertical flow is doubled too;

- Combined:
  $$\frac{1}{\lambda^2} = \frac{k_z}{k_a D_a D_z} \sim q_z \quad (14)$$
  λ is the so-called leakage factor;

- Time through clay layer: $t \geq \frac{D_z}{q_z} = \frac{-D_z}{k_z}\frac{dz}{dh}$

  Hence, contamination passes the clay layer and reaches the underlying aquifer after time t has passed. If the duration of the injection period is smaller, then the contamination has only partly penetrated the clay layer and will retreat during extraction time.
  The thicker the clay layer, the longer the contamination is present in the clay layer. The time is inversely related with the vertical conductivity and the vertical hydraulic gradient. As shown above, the vertical hydraulic gradient is linearly dependent on the well discharge.

Above analysis shows that vertical leakage through an aquitard between two aquifers is dependent on SATES wells by the well discharge. When the well injection discharge is doubled, the vertical head difference is doubled, too and the vertical travel time is halved. The same principal holds for an extraction well, only that results in upward flow. During extraction, not all downward transported contaminants are recovered by the well, because some contaminants are displaced by horizontal ambient groundwater flow and dispersion effects. Therefore, there is net vertical contaminant transport due to the alternation of injection and extraction. The amount of contaminants that are transported vertically is dependent on well discharge.

In short, the mechanism of increased flow causes increased DNAPL dissolution, increased contaminant spreading and reduced travel times. The effect is directly dependent on the SATES well discharge.

4.1.3 Transport by recirculation

Recirculation is the process of extraction and re-injection of water in another well of a SATES system. When contamination is present nearby the extraction well, it is instantly displaced and injected in the injection well (Fig. 14A). In case of more than two wells in a SATES system, contaminant is extracted, mixed with water from other extraction wells and re-injected in all the injection wells (Fig. 14B). Hence, the more wells within a SATES system, the more spreading and dilution the system causes. Also the further the extraction well is located from the injection well, the more spreading and the more travel times are shortened.

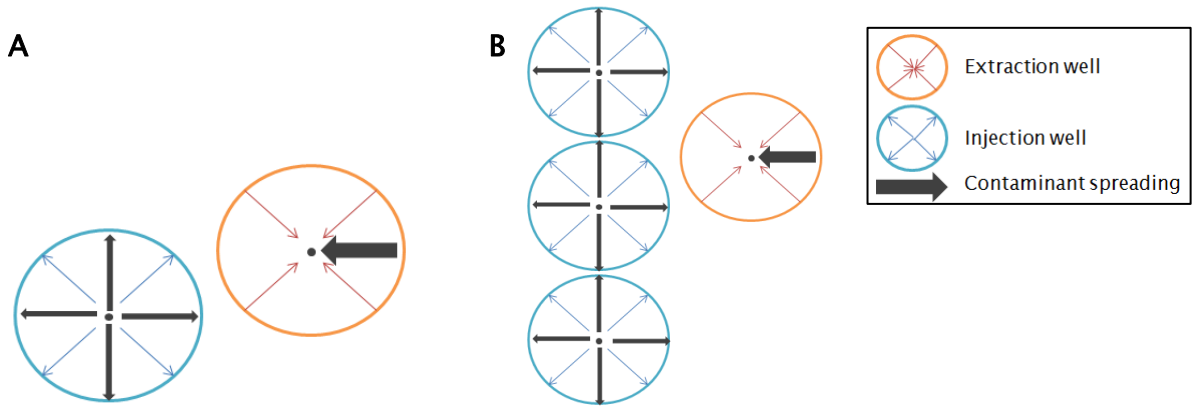

Fig. 14: The recirculation mechanism. (A) Extraction of contamination in one well and re-injection in the other well. (B) Extraction of contamination in one well and re-injection in several other wells.

4.2 Qualifying mechanisms and variables using a theoretical model

Before a sensitivity analysis can be executed, first two model settings have to be analyzed. The first one considers the seasonal variability of the SATES well discharge, which should be simplified. The second consideration is about modeling the process of recirculation. Then the sensitivity analysis is done. The effect of the recovery ratio is not tested, although it contributes to the degree of spreading. In reality, however, it is always attempted to get the highest possible recovery ratio, to get the best performance of the SATES system. It is thus not a variable that will be used to manage contaminant spreading.

4.2.1 Modeling well discharge

The wells of a SATES system do not always pump at a constant rate. The heating and cooling demand mirrors the injection and extraction discharges of the corresponding wells. In the Netherlands, during winter there generally is a large demand for heat, but for a relatively short time span. During summer, cold is demanded for a longer period, but less is needed. This has consequences for the SATES well discharge distribution over the year, as shown in Fig. 15.

When modeling effects of SATES systems on a long timescale, it is not possible to express fluctuating well discharge in such detail, as it prolongs the running time of a model significantly. Especially when modeling large areas, the running time would become unfeasibly long. Therefore, the discharge distribution of a SATES well over the year should be simplified to one injection stage and one extraction stage per well. In some model studies an injection period of six months is assumed, as well as an extraction period of six months, assuming a water balance over the year [e.g. Arcadis, 2009; Tauw, 2010]. However, it is not the most representative simplification of the seasonality described in the previous paragraph. In SATES system De Uithof the injection period of the cold well lasts for only four months, whereas extraction takes place during eight months. Therefore the well discharge can be better simplified with a 4/8 month distribution rather than a 6/6 month distribution (Fig. 15).

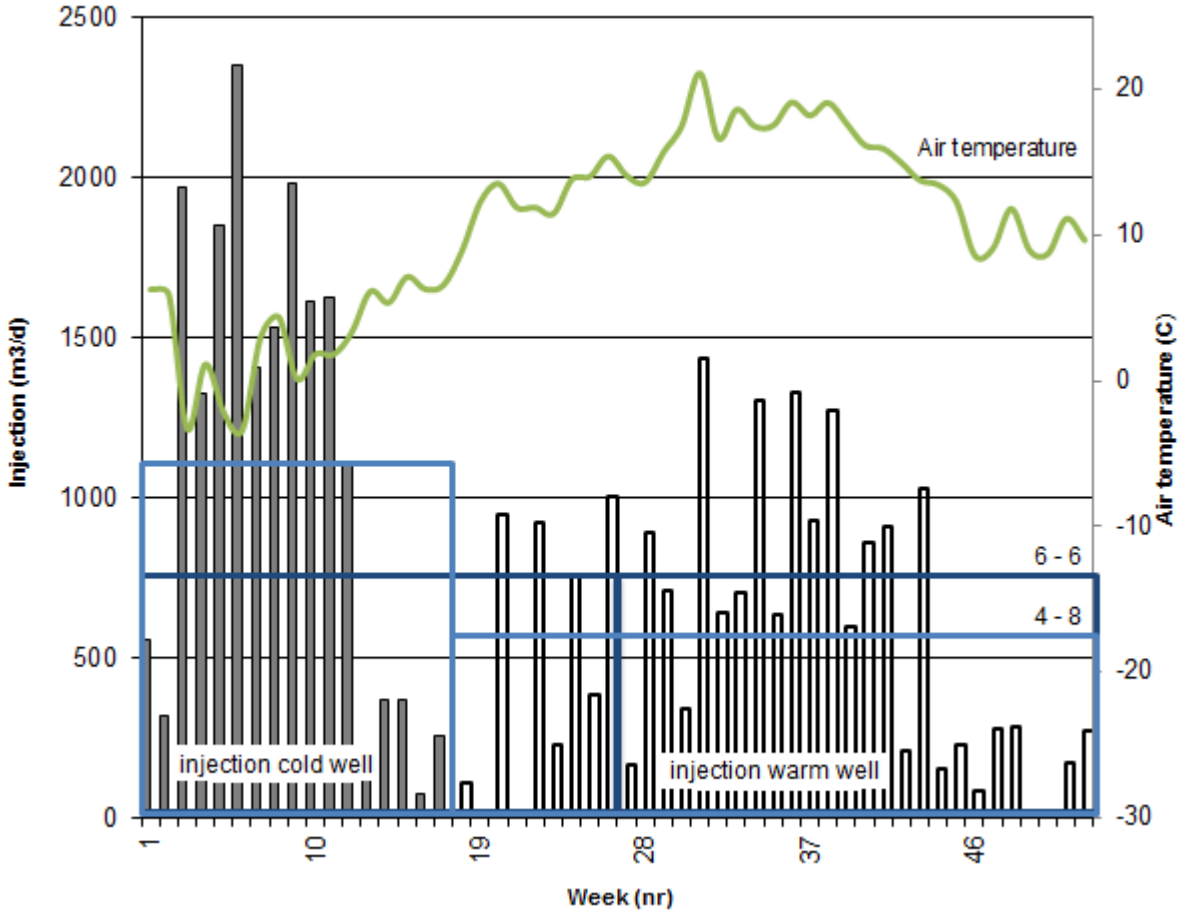

Fig. 15: The air temperature at De Bilt and the corresponding weekly cumulative injection discharge in SATES system 'De Uithof' in Utrecht [after MMB11, 2012; Zuurbier *et al.*, 2013]. The blue boxes represent the simplified discharge, with dark blue a 6/6 month distribution and light blue 4/8 months. Note that the injection period of the warm well is twice as large as the injection stage of the cold well, and that the 4/8 month distribution represents this behavior better.

The difference between the real discharge and the simplified discharge can be calculated for each day and added up for the whole year. Comparing the 4/8 month assumption to the 6/6 month assumption, the error is reduced by 24 %. Also, the hydraulic radius of the 4/8 month assumption and the radius of the well with variable discharge are calculated. The hydraulic radius of the well with simplified 4/8 distributed discharge is 1.3 % larger than the well with real variable discharge.

Because of above two reasons, the 4/8 month distribution will be used to simulate well discharge in the case study of Utrecht. This will be done for all wells, as (1) SATES system the Uithof is located very close to the study area so it is probably representative, (2) the data from the Uithof is very detailed, and (3) the function of the Uithof building is comparable with the buildings of the SATES systems in the city center of Utrecht, so the heat demand is probably similar.

Because injection discharge and duration differ for warm and cold wells, the recovery ratios differ, too. Since the cold well typically has a lower extraction discharge, it has a lower recovery ratio than the warm well, as shown in Appendix I.

4.2.2 Modeling recirculation

Recirculation is not standard included in MT3DMS and should therefore manually be incorporated. For a doublet, the contaminant concentration of an injection well of a doublet should be equal to the extracted concentration. This can be modeled with the source/sink package of MT3DMS. Using this package, one can assign a certain concentration to an injection well. A second option is to refer to the concentration of another cell, using the reference number of the cell. To make clear it is not a concentration but a reference, a minus sign is put in front. In case of a doublet, the injection well will get the right concentration using the negative reference number of the extraction well. The reference number RN can be calculated with the formula (15) [Zheng, 2010]:

$$RN = NrCol \cdot NrRow \cdot (K-1) + NrCol \cdot (I-1) + J \quad (15)$$

In this formula $NrCol$ and $NrRow$ are the total number of columns and rows of the model. K, I and J are respectively layer number, row number and column number of the reference cell (the extraction well). For each period, the right negative reference number has to be assigned to each injection well in the source/sink file of MT3DMS.

In practice many SATES systems consist of more than two wells. Hence, if water of one extraction well is contaminated, the contamination is diluted and ends up in several injection wells. In MODFLOW or MT3DMS, there is no direct way to model this effect. Therefore it was explored how this could be best modeled to represent reality. Three options were compared:

1. *Linear coupling*
   Recirculation is modeled using reference numbers as described above. SATES wells are linearly coupled (Fig. 16B).

2. *Cross coupling*
   Recirculation is modeled using reference numbers as described above. SATES wells are linearly coupled (Fig. 16C).

3. *Multinode well package*
   Another option is to use the MODFLOW multinode well (MNW) package, which is originally designed for wells in multiple layers. One assigns one total discharge, and MODFLOW calculates the amount of water that is extracted per layer, based on the hydraulic head and conductivity. These amounts all add up to the total well discharge. The MNW package can also be applied horizontally to combine multiple wells of one SATES system.

A theoretical model is run to estimate the most realistic simulation of recirculation by SATES systems. The model contains a SATES system of five cold wells and five warm wells in a line pattern. Four cases are compared to examine which one generates the most realistic output: a case without SATES system, a case with an SATES system with linear well coupling, a case with an SATES system with cross well coupling, and a case with SATES systems with the MNW package, as shown in Fig. 16.

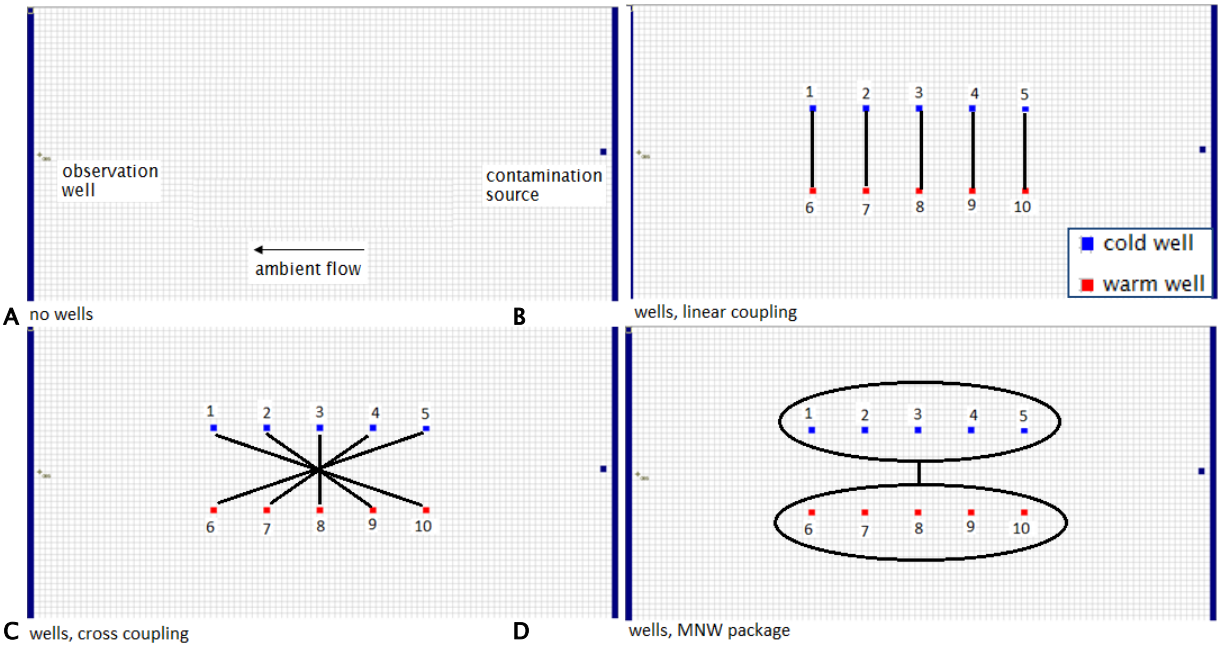

Fig. 16: The four cases to model solute transport by a SATES system.

The four cases are compared for two scenarios: a plume (modeled as an initial concentration in a plume of 7x7 cells and total concentration of $C/C_0 = 1$), and a DNAPL (modeled as a constant head cell with a constant concentration of 1). The plume and DNAPL are introduced upstream (on the right side of the wells), while ambient groundwater flow is from right to left, so that the contamination should flow through the capture zones of the wells. On the left side of the model is an observation well in line with the concentration source. The output is compared in two ways: the breakthrough curve of the observation well and the development of the concentration contours.

The development of the plumes of the different cases is shown in Fig. 17. Contamination that reaches the first MNW extraction well, is injected in all five injection wells. Also the working of the linear and the cross coupling are clear. The propagation of the plume is the fastest in the MNW case, secondly comes the case of cross coupling and at last linear coupling. The cases cross and linear coupling do not taken into account the effect of mixing with all five wells extraction, thus resulting in too less dilution.

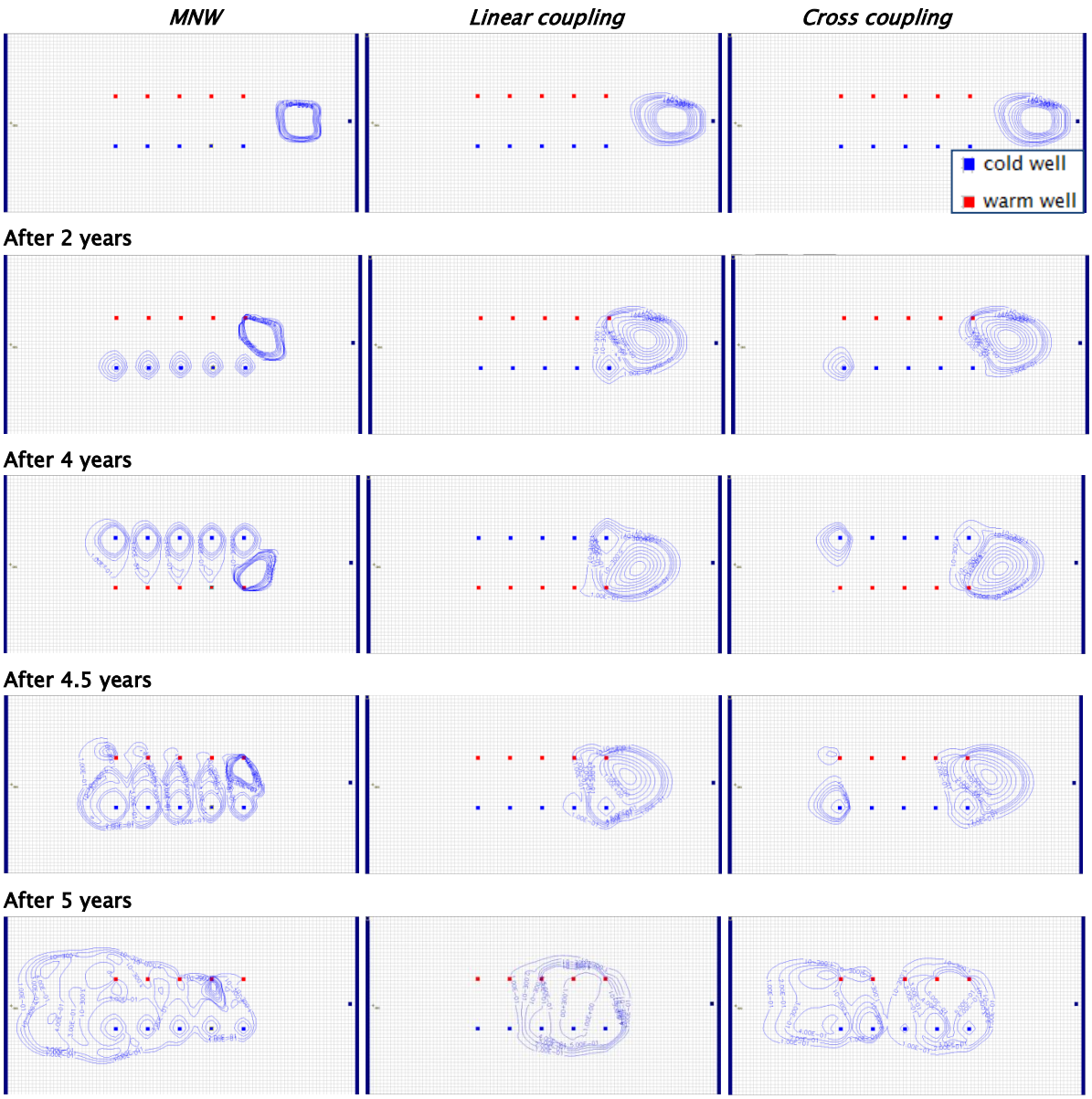

Fig. 17: Plume contours for three different cases at several time steps.

The breakthrough curves of the plume show the concentration peak arrives early in the MNW case and the cross coupling case (Fig. 18A, C). Probably this is because the contaminated water at upstream well 10 is (also) injected in downstream well 1. The peak concentration of the cases MNW and cross coupling are comparable. The peak concentration without any wells is significantly higher and later, because no wells were present to spread the plume. Cross coupling results in an early peak with a long tail. The early peak probably is too high, because contamination from upstream is directly injected in a well downstream, while actually it should be injected in all five injection wells.

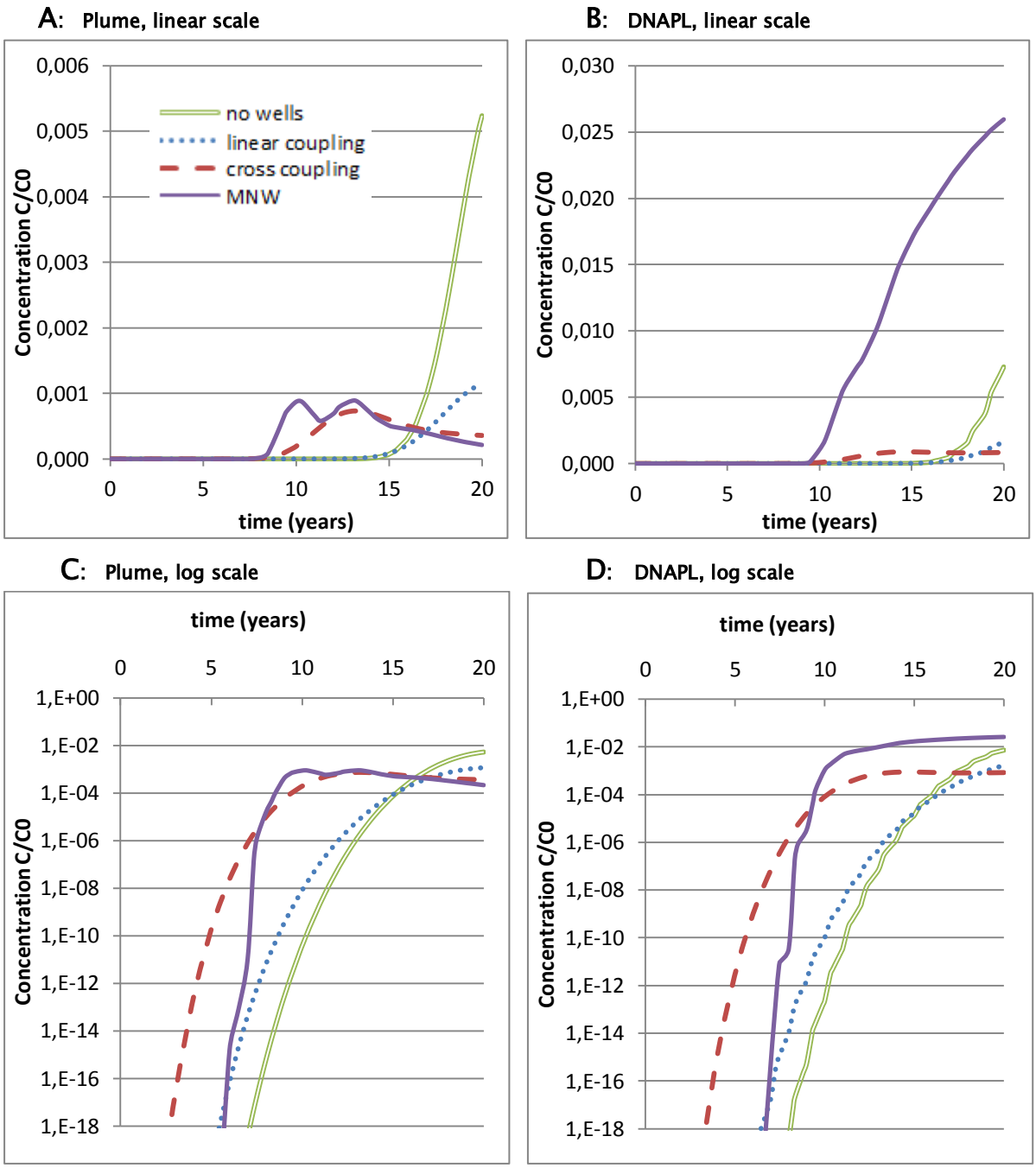

Fig. 18: Breakthrough curves at observation well. Curves are for a scenario with DNAPL and a scenario with a plume. Output is shown in both linear scale and log scale. Based on the ratio of solubility and intervention value, the concentrations from 1E-6 and higher are relevant.

Observing the breakthrough curves of the DNAPL, it is not the case without wells that has the highest concentration, but the MNW case. Probably this has not to do with little spreading in the MNW case, but because extra mass is added to the model. Wells cause the head difference around the DNAPL (constant head cell) to become larger, resulting in more contaminant dissolution. The same amount of wells is present in the MNW case, the case with linear coupling and the case with cross coupling. However, analysis showed that the total mass in the case of cross coupled wells is increased to 1.4 after five years, whereas it is 23 for the case with MNW. The cause for the high amount of mass in the MNW case is probably the discharge

distribution of the MNW wells, which is shown in Table 10. The discharge differs per well, because only a total discharge for all warm wells and a total for all cold wells is specified. The model calculates the individual well discharges based on the local head. Because upstream, close to the contamination source, the head is higher, the extraction discharge is high and the injection discharge low. The high extraction discharge causes the head difference at the constant head cell to increase, such that more mass is diluted.

Table 10: Well discharges of the five cold wells of the SATES system in line pattern. In cases without MNW (linear coupling or cross coupling), the discharge is equally distributed over the five wells. However, in the MNW case the individual well discharge diverges significantly. Upstream (well 5) there is high extraction and low injection. The same applies for the warm well.

		Injection during winter		Extraction during summer	
Well nr. (Fig. 16)		**Discharge (m^3) with MNW**	**Discharge (m^3) without MNW**	**Discharge (m^3) with MNW**	**Discharge (m^3) without MNW**
C	**1**	954	750	-256	-375
C	**2**	772	750	-305	-375
C	**3**	702	750	-351	-375
C	**4**	663	750	-413	-375
C	**5**	659	750	-550	-375
		3750	*3750*	*-1875*	*-1875*

The discharge distribution of the wells in the MNW case has two other disadvantages. Firstly, the discharge distribution is not realistic, because in practice injection and extraction volume are about equal to maintain optimal recovery. Secondly, the contaminant spreading is not modeled realistically. Because upstream there is net extraction and downstream net injection, there is a net transport of water of 140 $m^3\,day^{-1}$ from the upstream well to the downstream well, resulting in too much spreading. Additionally, the multinode well package requires a long running time. Because of these reasons, it is advised not to use the MNW package when modeling contaminant spreading by SATES systems.

The choice remains between linear coupling and cross coupling. Cross coupling results in shorter travel times, more dilution and thus a lower and longer concentration peak. This is thought to be the most realistic option to model recirculation by SATES systems with more than two wells.

Cross coupling is thus applied in the case study model. In the center of Utrecht there are six doublets, which could simply be coupled. There are nine systems with more than two wells. The wells of these systems are cross coupled, as shown in Fig. 6. The Jaarbeurs SATES system is a special case, because it has a different number of cold and warm wells: 8 cold and 15 warm. If the 8 cold wells would be coupled with 8 warm wells, the mass extracted in the other 7 wells would not be recirculated and the mass would be lost. Also the discharge of the extraction and injection well should be equal to ensure no mass is lost or produced. To solve for these problems in the model, 7 cold wells are added to the Jaarbeurs SATES system. These wells are placed in between other cold wells, to minimize thermal consequences and hydraulic head changes. In Fig. 6, the light blue cold wells in between the other cold wells are manually added to the model. All wells are assigned the same discharge. Thereafter each cold well is cross-coupled with a warm well.

4.2.3 Sensitivity analysis on the mechanisms

In section 4.1, the different hydrological mechanisms by which SATES systems cause contaminant spreading, are theoretically analyzed. Thereby the well variables important for the amount of spreading were estimated: the well discharge and the SATES configuration (number of wells, well pattern and well distance). In this section, a sensitivity analysis is done on these variables.

Actually section 4.2.2 describes the first part of the sensitivity analysis. The breakthrough curves and plume sizes show that recirculation results in a significant decrease of travel time, as contamination extracted upstream is partly injected downstream. Also, spreading is increased, as the peak concentration becomes lower and the plume size becomes larger. If the well distance would be higher or the well number of the SATES system would be increased, the effect on contaminant spreading would increase.

The effect of well pattern on flow path and travel times

In this section firstly flow paths are studied, as they visualize the effect of SATES systems on flow, so it could be useful to explain observed spreading effects. In Fig. 19 the flow paths caused by different SATES well configurations are shown. When two wells are in line with the ambient groundwater flow and injection takes place upstream, the injection well causes flow lines to flow around the well. This causes the capture zone of the drinking water well to be enlarged around the two SATES wells. However, in the other cases the wells are placed perpendicular to the groundwater flow, which is more common to reduce the probability of thermal interference. In those cases the capture zone is enlarged further upstream, too.

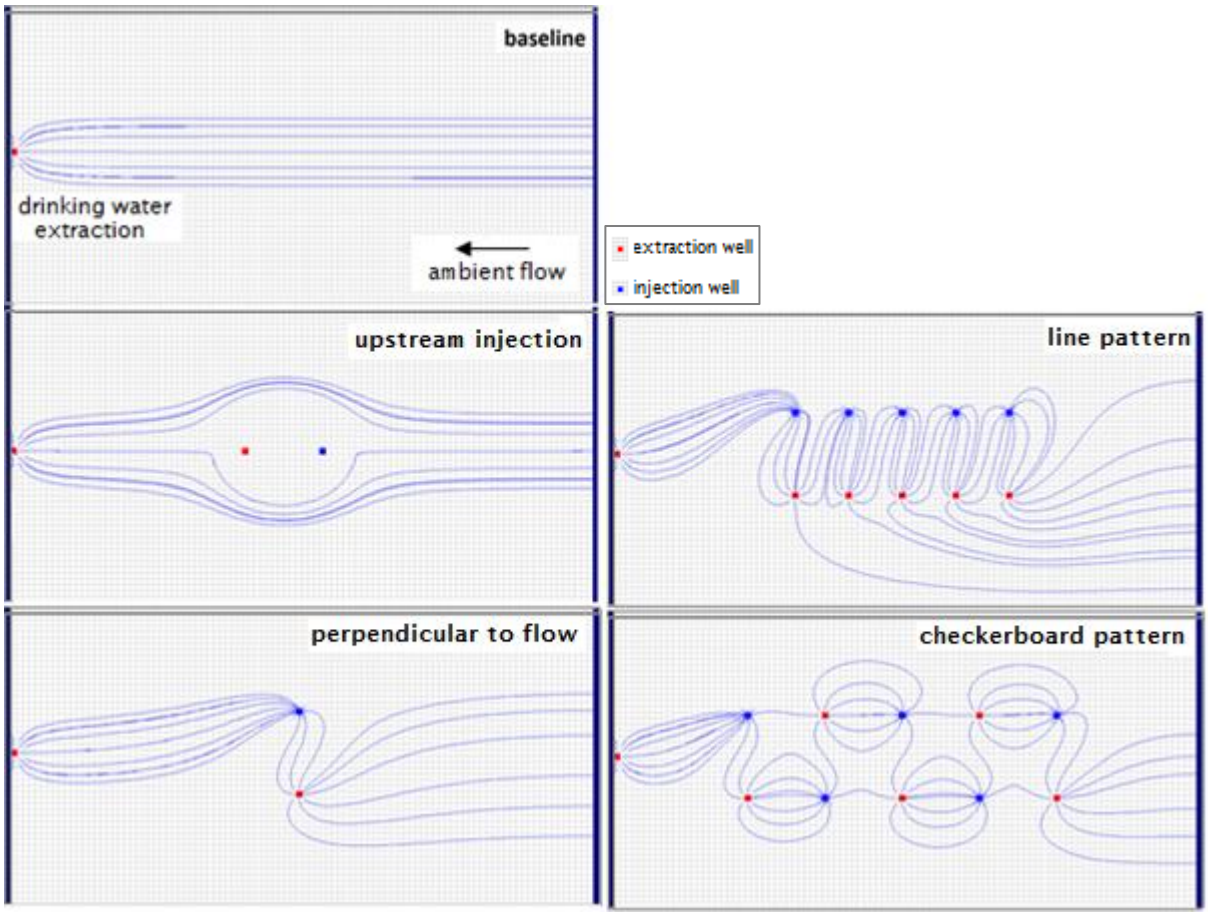

Fig. 19: Flow paths towards the drinking water well at the left end. In the different cases different SATES system arrangements are modeled. The flow paths reverse from season to season as a result of alternating injection and extraction, with opposite effects.

Breakthrough curves of the observation well at the end of the model give information about concentration and travel time, shown in Fig. 20. In the case of extraction upstream and injection downstream, the peak occurs the earliest and the travel time is decreased the most. This is because flow is accelerated towards the extraction well, extracted and re-injected in the injection well, where it is accelerated downstream. Hence, travel time is decreased by SATES induced head differences and recirculation. With the opposite configuration, the injection well upstream, the flow is decelerated significantly. Combining the two in a doublet with seasonal alternation of injection and extraction, the accelerating effects predominate and the travel time is decreased with approximately 13 %. In all three cases in which the wells are placed in line with the groundwater flow, the concentration of the peak is reduced to about a tenth of the concentration without SATES systems. Probably this dilution is caused by spreading by the injection well. However, with a doublet perpendicular to the flow, the breakthrough curve shows a much higher peak than the case without SATES wells. Probably the continuously pumping between the two wells prevents the contamination to escape from the well influence, so the contamination accumulates.

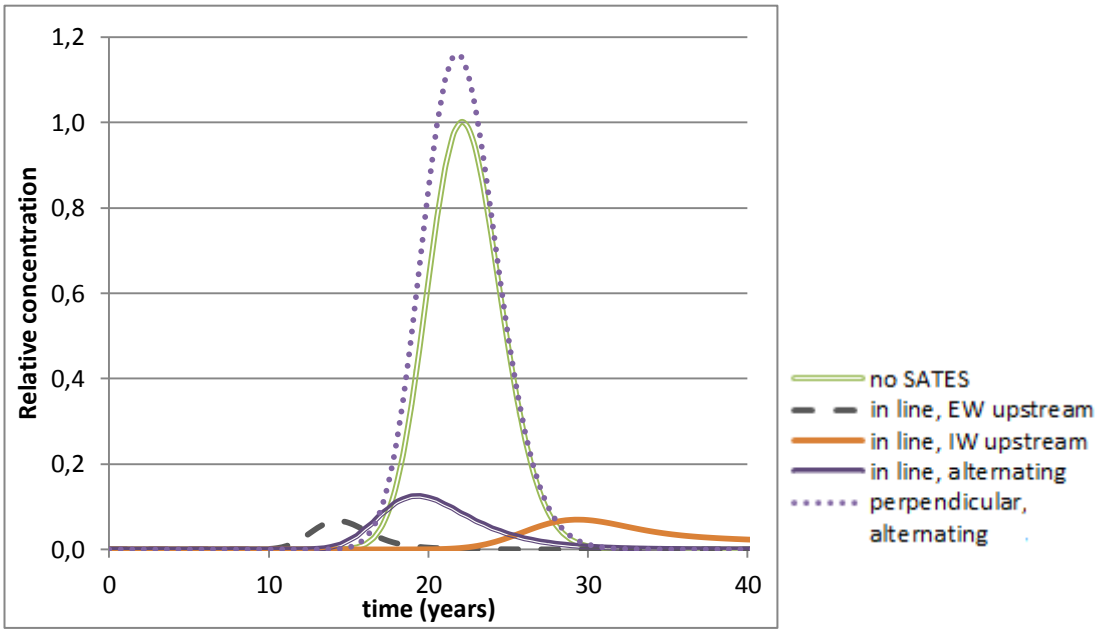

Fig. 20: The breakthrough curves of a case without SATES wells and four cases with a doublet (in line or perpendicular to groundwater flow, EW = extraction well, IW = injection well). The concentrations are relative to the case without SATES systems.

The effect of well pattern, well discharge and well distance on travel time and spreading

After an analysis of SATES doublets, the sensitivity analysis is upscaled to more than two wells. Ten wells are placed in line pattern, after which the well discharge and well distance in line with the groundwater flow are modified one-by-one to observe their effect on spreading and travel times. The same is done for the checkerboard pattern.

Firstly the effect on travel time is analyzed using breakthrough curves of all scenarios (Fig. 21). In this part of the sensitivity analysis, the SATES wells are linearly coupled such that the effect of recirculation on travel time is minimized and the effect of the other well variables could be estimated clearly. As the contamination peak arrives after 22 years in the model without SATES systems (Fig. 20), it becomes clear that SATES systems have little effect on travel time if recirculation is not included properly (i.e. with cross coupling, see section 4.2.2).

The sensitivity analysis for well distance also contains information about the effect of overlapping capture zones. With a small well distance ("well distance 60 %"), the capture zones of the SATES wells are overlapping, whereas in the other cases the capture zones do not overlap. As shown in Fig. 21, the difference in travel time is negligible.

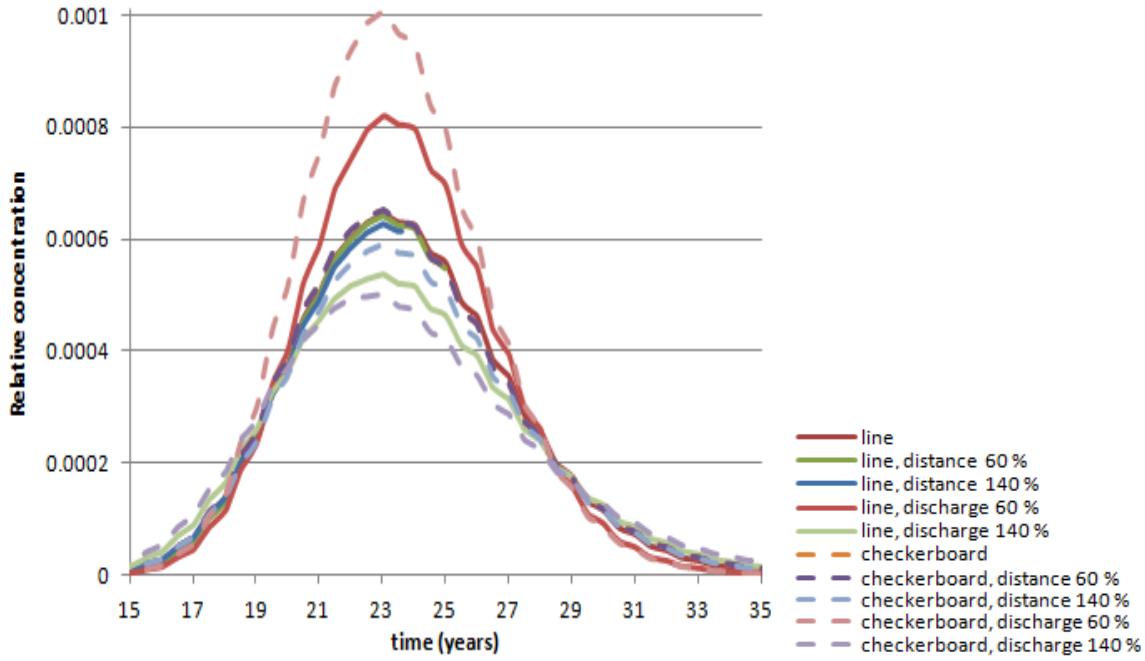

Fig. 21: The breakthrough curves of the cases in line pattern and checkerboard pattern result in a slightly shorter travel time as the case without SATES systems that is shown in Fig. 20. The differences in travel time between the ten cases are very small.

Although the travel times of the different scenarios are very similar, the different peak concentrations show that spreading differs significantly per scenario. The amount of spreading is further analyzed by observing the plume development. The plume development of the line and checkerboard pattern is shown in Fig. 22. The line pattern results in a little more spreading; after ten years the plume is about 12 % larger than the plume of the checkerboard pattern. Probably this is caused by the larger head difference between the two lines that are mutually reinforcing. However, after twenty years, the difference in plume size is negligible.

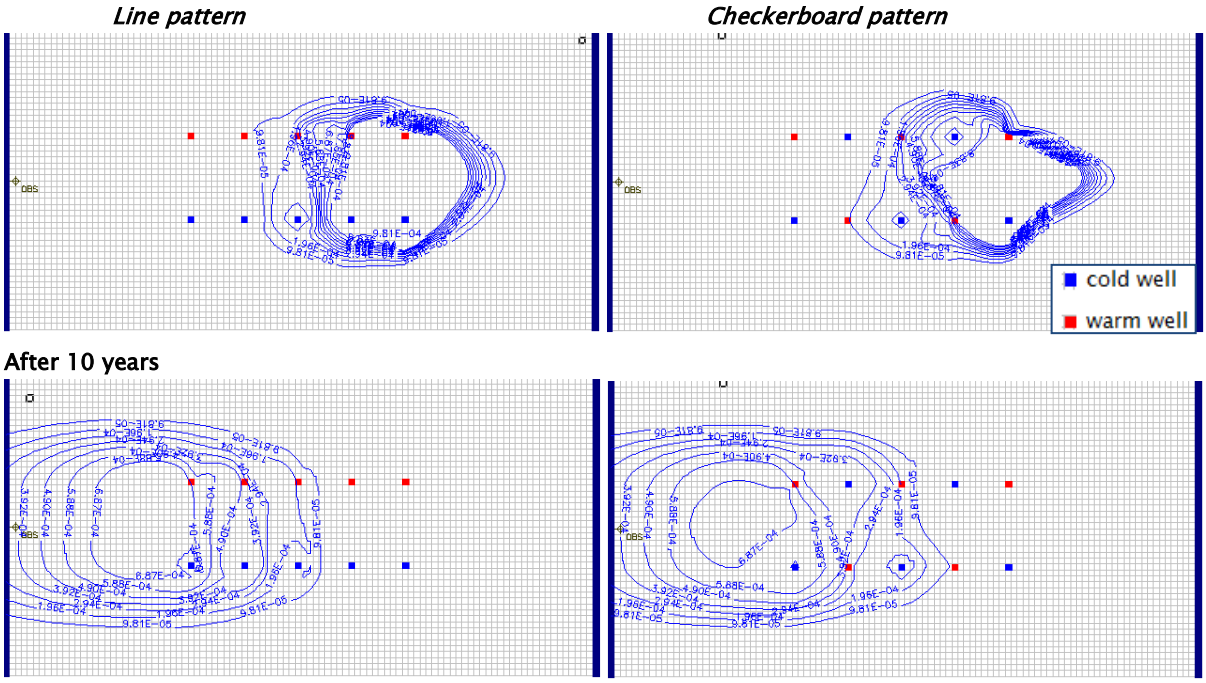

Fig. 22: The extent of the plume in line pattern and checkerboard pattern after 10 and 20 years. The travel time is about equal for both cases. The plume size after 10 years is about 12 % larger for the line pattern. After 20 years, the difference in plume size is negligible.

The relative plume size of all modeled cases is shown in Table 11. The table shows that with a line pattern, the well distance has a very small impact on spreading. Probably this is because the line pattern results mainly in lateral spreading and the head difference between the two lines stay equal, so the amount of spreading is not affected by well distance between the wells in one line. For the checkerboard pattern a larger well distance significantly increases the plume area. The head gradient for the checkerboard is in all directions, so flow and spreading occurs not only laterally. Furthermore the extra well distance implies the wells lie further away from each other and thus cover a larger part of the area, so head changes have effect on a larger part of the area.

For the well discharge, the line and checkerboard pattern show the same effect. A higher well discharge results in a significantly larger plume.

Table 11: The plume size after ten years relative to the 100 % case, for both the line and checkerboard pattern. Firstly the well distance is modified between the wells in line with the groundwater. A well distance of 60 % implies overlapping capture zones, a well distance of 100 % and 140 % do not. Thereafter the well discharge is changed.

		line pattern	checkerboard pattern
well distance	60%	1.00	0.89
	100%	1	1
	140%	0.99	1.14
well discharge	60%	0.84	0.87
	100%	1	1
	140%	1.10	1.09

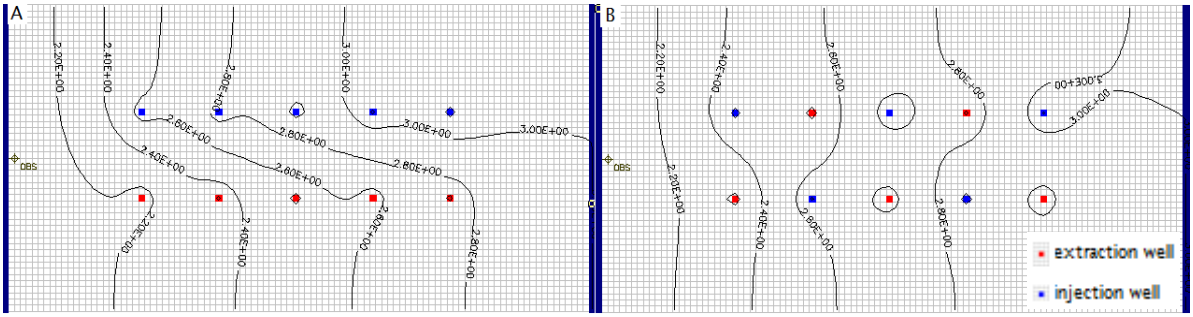

Fig. 23: The hydraulic head distributions of the line pattern (A) and checkerboard pattern (B), in the cases with 140 % well distance.

5. SATES systems spreading effects in a case study: Utrecht, the Netherlands

In the previous chapter, the most important spreading mechanisms are clarified. Results of the theoretical model showed that SATES systems cause contamination plumes to spread significantly in a horizontal plane. However, in the theoretical model the SATES systems were placed in a line and checkerboard pattern, whereas in practice the configuration of SATES systems is more complex. The next step is to zoom out and simulate contaminant spreading in realistic SATES model, the case study of Utrecht. Firstly a cluster of SATES systems is studied: the city center of Utrecht. Contaminant spreading is described and where possible quantified. Subsequently the spreading is studied on a regional scale and effects are placed in a regional perspective.

5.1 Spreading in a high density SATES systems area

Firstly, a hypothetical plume and DNAPL are simulated (see Fig. 24 for the initial setup). The DNAPL is located in between SATES systems, such that the effects of SATES systems on the dissolution of contamination can also be studied. Both model cases are run for a simulation period of fifty years. A series of snapshots of contaminant spreading in the first twenty years is presented in Fig. 25. In the first season, the contamination reaches a couple of extraction wells. Note new plumes are created at corresponding injection wells due to recirculation. After ten years the plume covers half of the SATES system area. When recirculation is not included in the model, no new plumes are created at injection wells and spreading is much less, as shown in Fig. 26.

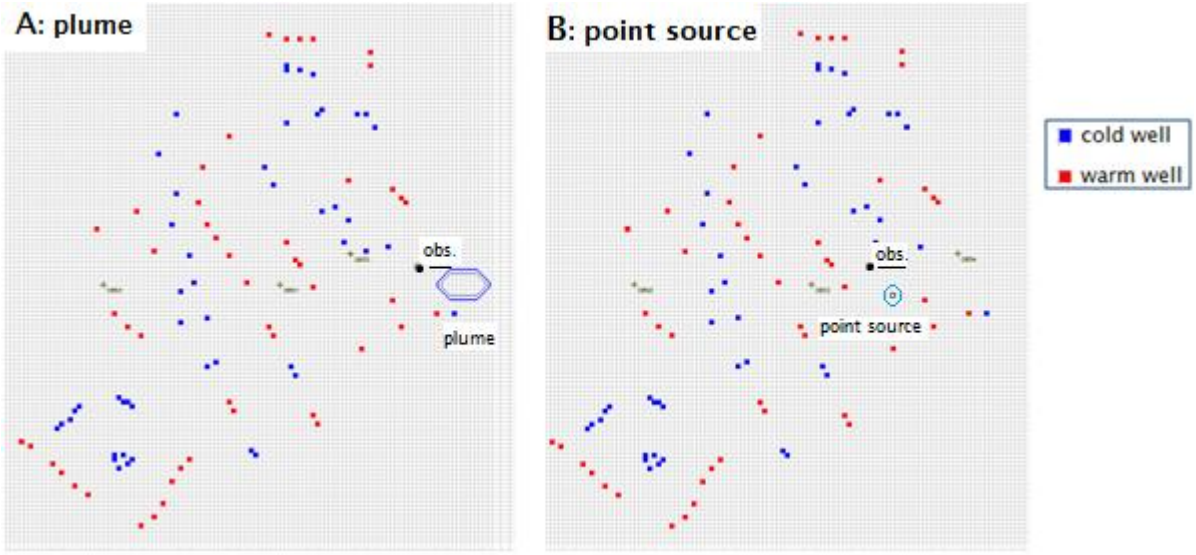

Fig. 24: Overview of SATES systems (see Fig. 6) with initial conditions for the model runs: a hypothetical plume (A) and a hypothetical DNAPL in the circle (B). Underlined the analyzed observation wells.

Fig. 25: Contaminant spreading caused by the modeled DNAPL. The contamination contours are logarithmically scaled.

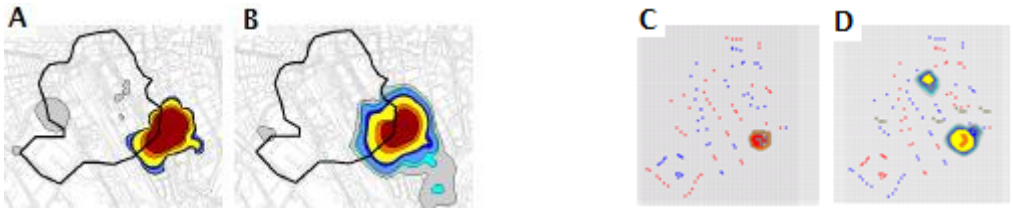

Fig. 26: The effect of recirculation in contaminant spreading. (A) Initial DCEcis plume in Arcadis [2009]. (B) Plume after 15 years according to Arcadis [2009]. In the model SATES wells pump at 82.5 % for 6-6 months and recirculation is not incorporated. (C) Initial plume in Hydromedah model. (D) Plume after 2 years in Hydromedah model. Note that already a new plume is present where Arcadis [2009] shows after 15 years no contamination. The contamination is transported over a large distance, because the contamination is extracted by a SATES system of which the cold and warm wells are located far from each other (see Fig. 6, NHC-system). In the model SATES wells pump at 60 % for 4-8 months and recirculation is incorporated.

Breakthrough curves of the plume and DNAPL measured at the observation wells (Fig. 24) are shown in Fig. 27. These are analyzed for a scenario without SATES systems, a scenario with SATES systems at 60 % of their permitted discharge, which is the average discharge in practice, and a scenario with SATES systems at 100 % of their permitted discharge. The breakthrough curve of the plume (A) shows that when SATES systems are present, the contamination peak breaks through earlier, but the peak is much lower than the situation without SATES systems. With a discharge capacity of the SATES wells of 60 % and 100 %, the travel time is reduced by 18 % and 26 % and the concentration is reduced by 72 % and 76 %, respectively, compared with a situation without SATES systems. The observation well lies relatively close to the contamination source, so even more spreading might occur further away, which would result in even earlier and lower concentration peaks.

The breakthrough curve of the DNAPL shows a different behavior. Here the concentration peak of the case with SATES systems with maximum discharge is even higher than the peak of the case without SATES systems. This is because of the extra dissolution caused by the SATES systems. The seasonality of the SATES systems is visible in the alternation of concentration increase and decrease.

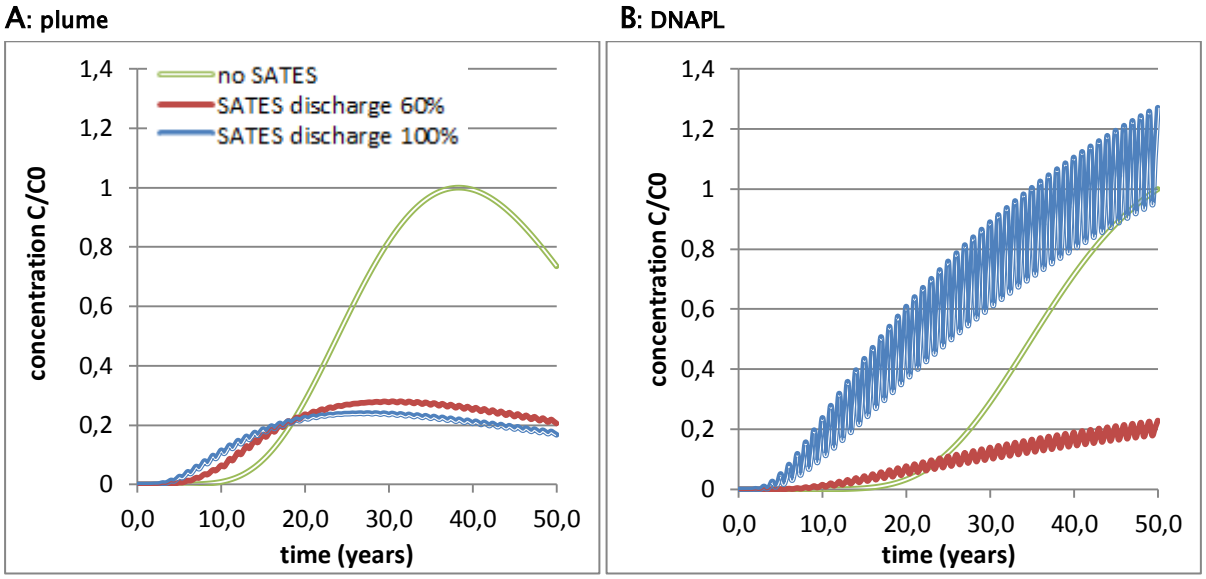

Fig. 27: Breakthrough curves at observation wells shown in Fig. 24. The breakthrough curves are shown for the plume (A) and DNAPL (B). Both cases show results for the normalized situation without SATES systems. Also the relative concentrations are shown from the situations with SATES systems at 60 % and 100 % of the discharge.

After 50 years, the differences in plume extent between the cases with SATES systems at a discharge of 60 % and 100 % are relatively small, because in both cases the whole SATES area is covered by the plume and extra spreading depends mainly on ambient groundwater flow. In both cases the plume extent is significantly larger than is the case without SATES systems (Fig. 28).

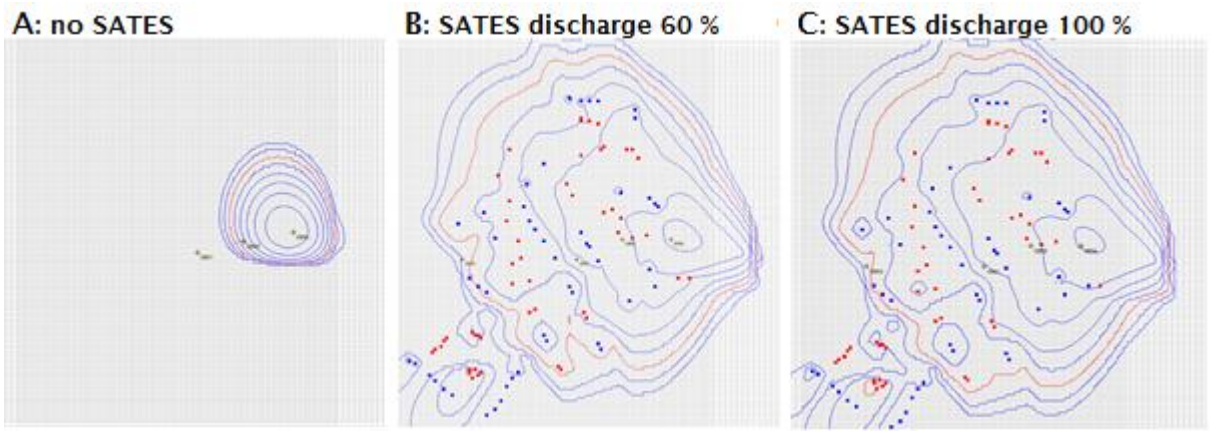

Fig. 28: The spreading of the hypothetical plume after 50 years, for a situation without SATES (A) and with SATES with discharge on 60 % of the maximum (B) and at 100 % of the maximum (C). Concentration contours are scaled logarithmically in steps of a factor 10; the red line corresponds with 1E-06.

The total area and average concentration of the plume after 50 years is calculated as the total number of cells that is covered by the plume. The case without SATES systems is normalized to 1 (Table 12). With SATES systems at 60 % discharge, the extent of the plume is 7.9 times larger than without SATES systems. Dilution is even higher, 9.7 times larger. The fact that the relative dilution is higher than the relative horizontal spreading implies also vertical spreading has taken place. The same effect is visible in the case with SATES systems at 100 % discharge. Considering DNAPL, the relative spreading is higher than the relative dilution. It is presumably that transport is also in vertical direction to other model layers, but that the lower dilution is caused by the addition of extra mass, which increases the average concentration.

Table 12: Relative spreading and dilution of a plume and DNAPL. The horizontal spreading is based on the plume area and normalized to the situation without SATES systems. The dilution is based on the average concentration of the plume: If the average concentration is 0.5 compared with the situation without SATES systems, the dilution is twice as high.

		No SATES	SATES discharge 60 %	SATES discharge 100 %
plume	relative horizontal spreading	1	7.9	8.4
	relative dilution	1	9.7	10.9
DNAPL	relative horizontal spreading	1	11.8	17.7
	relative dilution	1	6.3	2.2

Vertical flow and transport is studied as well. After 50 years of model simulation, the total mass in layers 3 to 7 is analyzed and compared with the first aquifer (layer 5) that contained the contamination source (Table 13). When no SATES systems are present, less than 1 % of the total contaminant mass is transported to other layers. If there are SATES systems present, the well pumping causes vertical head differences and mass transport upwards and downwards. In case of the plume, the situations with 60 % and 100 % SATES discharge result in an increase of vertical mass transport. The total mass that is transported vertically

becomes 10 % and 12 %, respectively, which implies 50 and 60 times more vertical mass transport than without SATES systems. Vertical transport is higher in case of a DNAPL than in case of a plume, which is probably caused by the initial location of the contamination source in between SATES wells.

Table 13: The percentage of mass that is transported upward and downward with regard to the layer with SATES systems (layer 5), based on the total mass in layers 3-7 after 50 years model simulation.

		no SATES	SATES discharge 60 %	SATES discharge 100 %
plume	% upward	0.03	7.3	8.9
	% downward	0.2	2.8	3.4
	% mass transported vertically (total)	*0.2*	*10.1*	*12.3*
DNAPL	% upward	0.3	14.9	16.9
	% downward	0.07	3.5	4.6
	% mass transported vertically (total)	*0.4*	*18.4*	*21.5*

Mass transported upwards is in each scenario about three times as high as the total mass transported downwards. This is probably caused by the hydraulic conductivities and thickness of layers 4 and 6, as well as the initial vertical hydraulic gradient (see equation 9 and 10). Both the horizontal and vertical hydraulic conductivity of layer 4 are a factor 5 higher than of layer 6, but the thickness is much smaller and the initial vertical hydraulic gradient was downwards, resulting in a factor 3 more transport upwards than downwards.

This effect becomes also clear when the MODFLOW water balance is studied. A subregion is defined in layer 5 containing the cluster of SATES systems. The flow in and out of the subregion is shown in Fig. 29. Again it is clear that the introduction of SATES systems and the increase of the well discharge results in increased interaction, both horizontally and vertically. Keep in mind that this is the interaction at the boundary of the subregion; inside the region the horizontal interaction probably is higher because of the SATES systems. Flow downwards is increased with 33 % in the case of maximum well discharge. The total interaction, both horizontally and vertically, is increased with a factor 3.0 in the case of 60 % well discharge and a factor 4.5 in the case of 100 % well discharge.

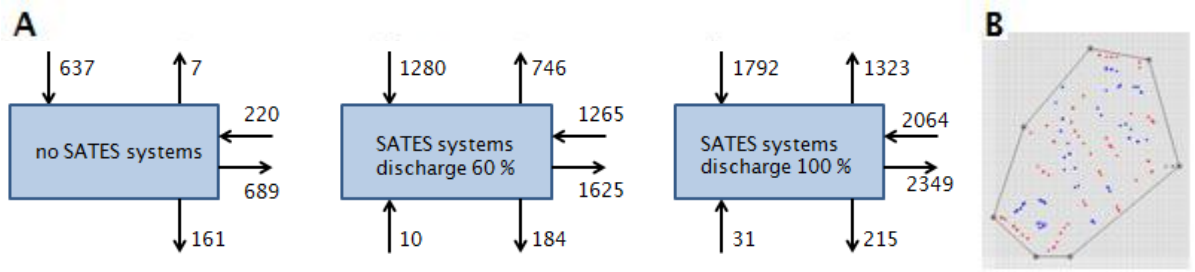

Fig. 29: (A) Flow in and out of the subregion in layer 5 containing SATES systems. Fluxes (m^3 day^{-1}) represent interaction with layer 4, layer 6 and the surrounding region of the subregion in layer 5. These are the fluxes of model period 1, which are representative for the whole simulation period, as the difference with fluxes of other periods is negligible, because the total of the whole area is calculated. (B) The defined subregion.

Testing overlapping capture zones in Utrecht

During the model simulations that were executed to produce the above results, another analysis has been done. In section 4.1.1, it is explained that it is likely that contamination is carried over from one SATES system to another within one year, if the capture zones of the wells overlap. Overlapping of capture zones can be predicted using the hydraulic radii of the SATES models and compare it with the well distance. This hypothesis is validated using the model of Utrecht. Firstly, it is predicted whether or not contamination would be carried over to the next system. Then the model simulations are used to validate whether the prediction was right. In 13 of the 15 cases, the analytical formula resulted in a right prediction. In two cases the hydraulic radii of the wells did not overlap, so it was predicted contamination would not be carried over from one system to another, but it did in the model.

5.2 Spreading by SATES systems in a regional perspective

In previous chapter the spreading effects are studied within a cluster of SATES systems. However on a larger scale the importance of the effects can be different. The case study model of Utrecht is used to study the effect of SATES systems on regional contaminant spreading and the implications for drinking water wells in the surroundings of the city. Therefore the flow paths of particles from the city center towards the downstream drinking water wells in the region are studied. Then three methods are used to estimate the travel time: one of them includes the effect of SATES systems and the two other methods do not. Finally, the relative importance of SATES systems on groundwater quality is reviewed and compared with other extraction wells.

5.2.1 Spreading effects on a regional scale

PMPATH is used to analyze the flow path from the city center towards the drinking water wells. Using PMPATH it is not possible to analyze flow paths starting in the city center, as they end up in one of the SATES wells, so the particles are introduced at the western boundary of the city center. Flow paths in the first aquifer split up, as the northern part flows northwards and the southern part south-westwards (Fig. 30). Further away from the city center, at the eastern side of the Amsterdam Rijnkanaal, the water flows downwards to the second aquifer (Fig. 31). In the second aquifer, the flow is directed towards the drinking water extractions. The path lines are predominantly directed towards drinking water extraction Leidsche

Rijn. Some others reach drinking water extraction De Meern, but no groundwater from the city center will end up in Groenekan.

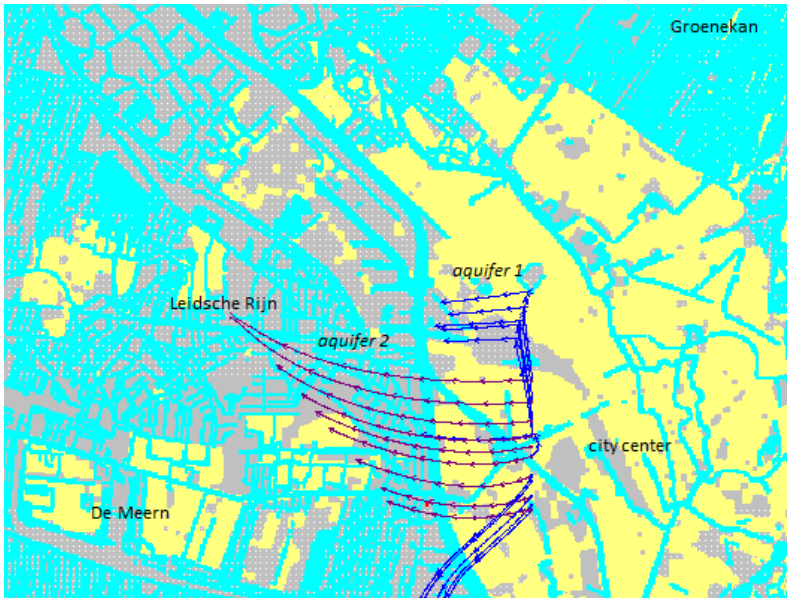

Fig. 30: Flow paths for the first and second aquifer, starting at the western side of the city center. Time mark interval is 50 years.

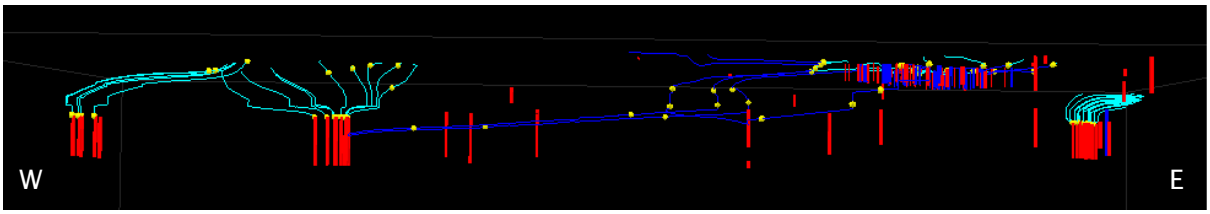

Fig. 31: 3D visualization of the model. Flow lines starting at the city center flow firstly westwards and then to the deeper aquifer. Also flow lines towards the drinking water extractions are shown.

A calculation is done for the travel time of groundwater following the described path from the city center towards drinking water extraction Leidsche Rijn. Using a distance of 4500 m and a specific discharge of 11 m year^{-1}, the horizontal travel time through the aquifer is 413 years. Then the vertical travel time through the clay layers should be added. The vertical structure of the model is shown in Fig. 32. The average vertical conductivity, vertical head differences and thickness of the layers between can be used to calculate vertical travel time from layer 5 with SATES systems to layer 11 with drinking water extractions. This results in a vertical travel time of 178 years. The total travel time from SATES systems towards Leidsche Rijn would thus amount about 600 years.

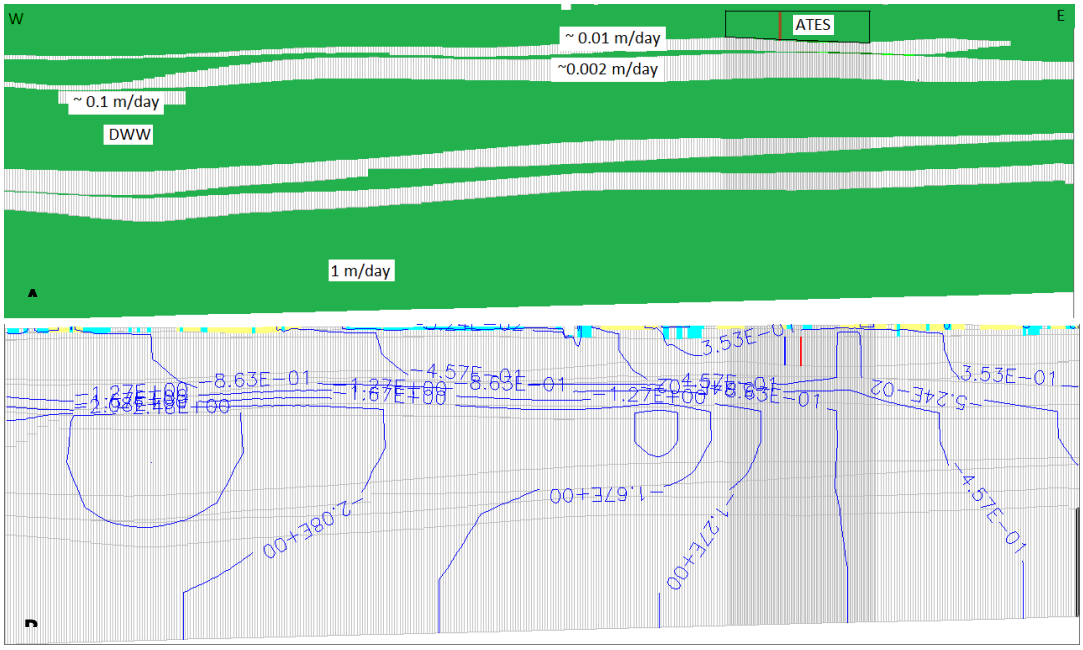

Fig. 32: Two east-west model cross sections (row 262). In (A) the vertical conductivity of the clayey layers is shown. The green layers represent sand with an average vertical conductivity of 1 m day^{-1}. In (B) the hydraulic head is shown for the same cross section. Note the east to west decline of heads and the effect of the drinking water extractions.

Travel times towards the drinking water extractions can also be analyzed with PMPATH, using time marks on the path. Particles starting in the first aquifer at the western side of the city center, have a travel time ranging from 400 to 700 years. The travel time of particles starting in the second aquifer is on average about 200 years shorter (Fig. 30). Hence, if there is already contamination present in the second aquifer, it would still take 200 to 500 years to reach the drinking water extractions.

However, the calculation with PMPATH does not include SATES systems, recirculation, dispersion and retardation. These effects are included by modeling contaminant spreading with MT3DMS. To model worst case scenario, a DNAPL is introduced in the city center. The contaminant spreading over 1000 years for the first aquifer, the aquitard and the second aquifer is shown in Fig. 33. Because a DNAPL is modeled, the mass increases during the model run and the contamination plume covers the SATES system area the whole simulation period.

The plume contours suggest the contamination starting at the city center flows by other paths than PMPATH suggests. The downward flow is not located westwards from the city center, but in the city center, as after 100 years a plume is visible in the second aquifer around the city center. This is probably caused by the injection wells of the SATES systems, which cause the vertical head difference to become larger. This effect could not be visualized with PMPATH, as flow paths end up in the wells and are not re-injected. Spreading occurs fast within the city center, but also outside of the city center. The time scale is long enough for dispersion processes to influence the plume. Another cause for the spreading outside of the city center is probably the flow that is split up and flows partly northwards and partly southwards as shown in Fig. 30.

Layer 5 (SATES) *Layer 8 (clay)* *Layer 11 (Drinking water extraction)*

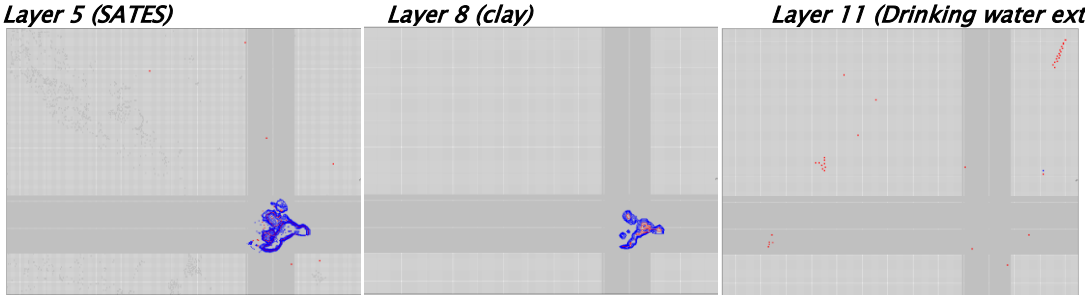

After 1 year

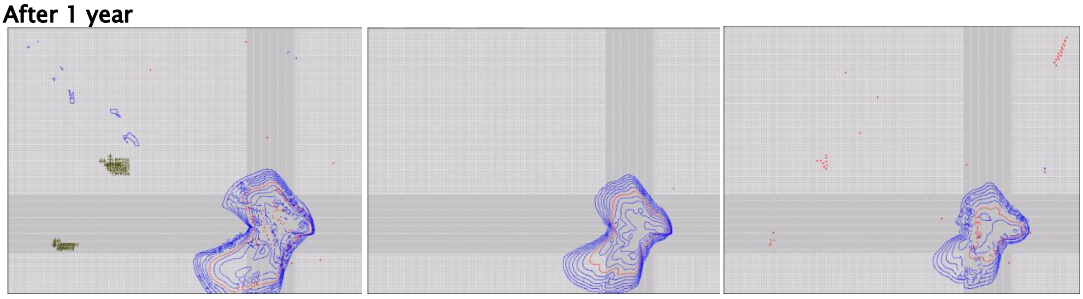

After 100 years

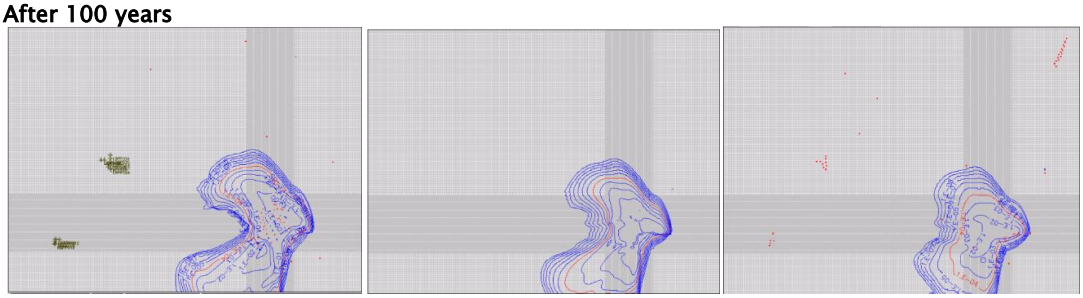

After 200 years

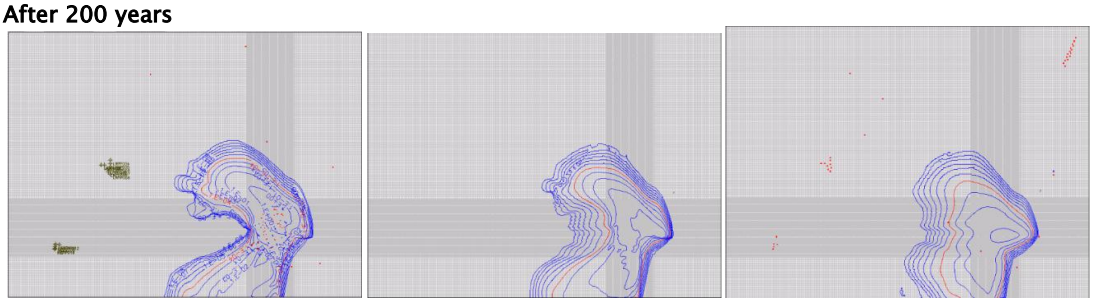

After 300 years

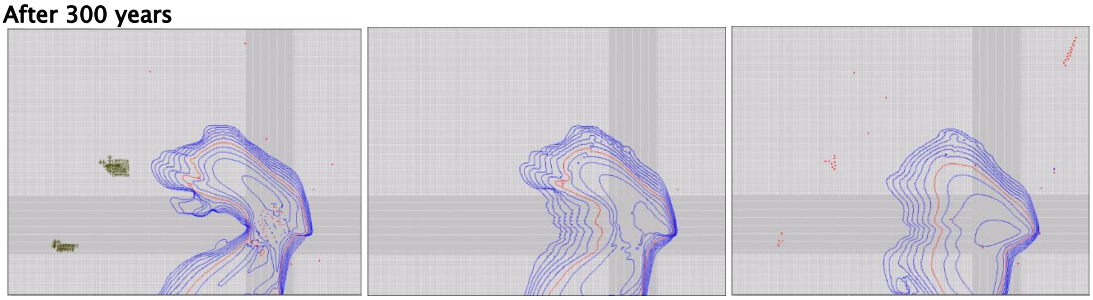

After 400 years

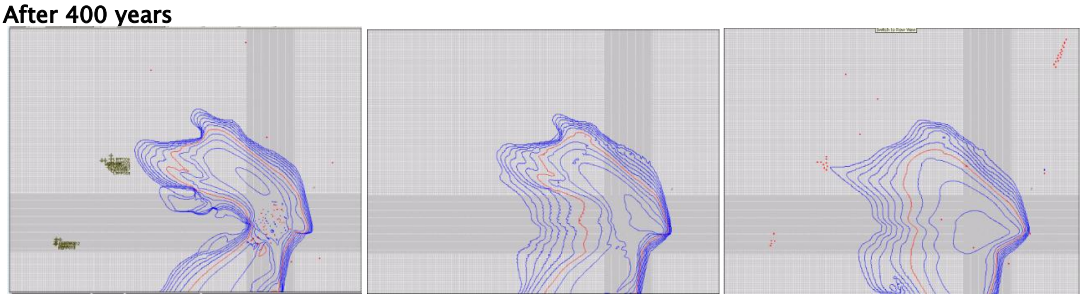

After 500 years

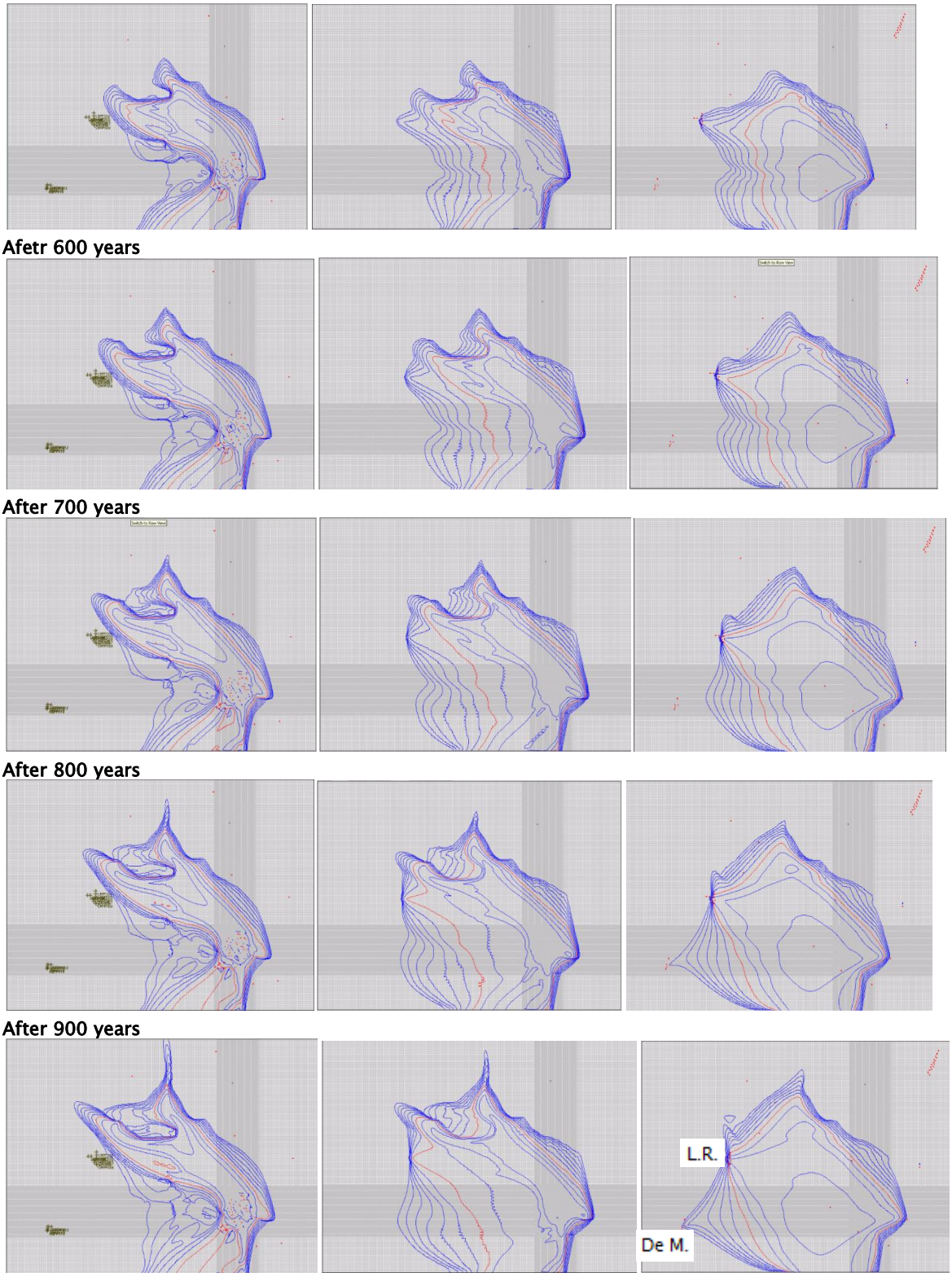

Fig. 33: 1000 years of plume development in Utrecht for the first aquifer, the aquitard and the second aquifer. Plume contours are on logarithmic scale starting at 1E-10. Because a DNAPL is modeled, the total mass increases during the model run. SATES wells pump at 60 % of their permitted discharge.

Another observation that can be made is that a large part of the plume in the first aquifer passes drinking water extraction Leidsche Rijn. Apparently the effect of the extraction in the second aquifer does not reach the first aquifer. Contamination in the second aquifer ends up in both Leidsche Rijn and De Meern. Again drinking water extraction Groenekan is not reached. Plume contours in the aquitard are directed to Leidsche Rijn. However, the specific discharge in the aquitard is very low and mainly vertical, as also shown by the hydraulic heads in Fig. 32 and the flow paths. Therefore it is assumed that the progression of the plume in layer 8 is caused by vertical flow from the overlying and underlying layers.

The first plume contour (1E-10) arrives after 500 years in Leidsche Rijn and after 900 years in De Meern. However, this is a very low concentration, as the average initial concentration of the plume in the city center was 100. Breakthrough curves of each drinking water well show after 700 years a more significant amount of contamination reaches Leidsche Rijn (Fig. 34). After 1000 years the concentration in De Meern is still negligible (Fig. 35).

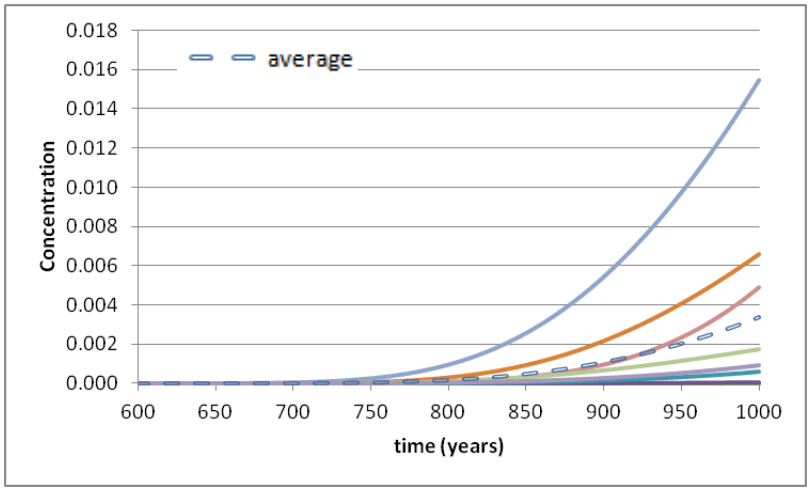

Fig. 34: Breakthrough curves of the plume at the seven drinking water extraction wells of Leidsche Rijn and the average.

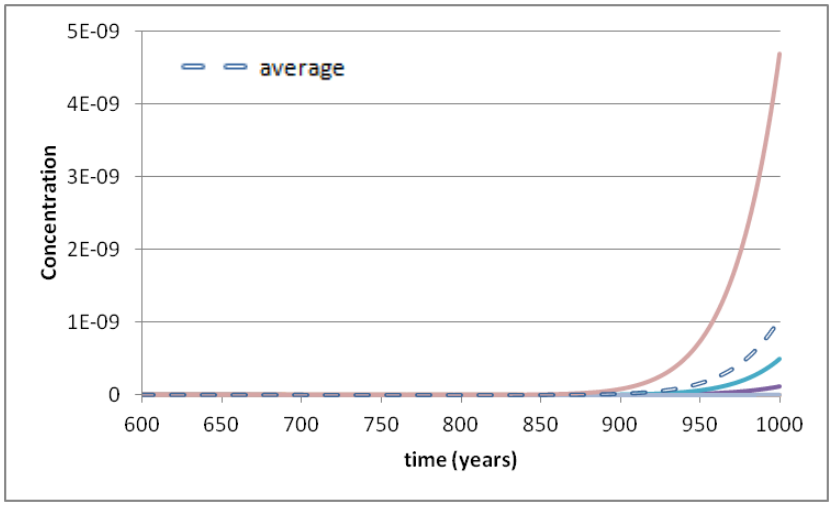

Fig. 35: Breakthrough curves of plume at the four drinking water extraction wells of De Meern and the average.

5.2.2 The effect of other extraction wells

Not only drinking water extractions and SATES systems are present in the Hydromedah model of Utrecht, but also other extractions. The majority of these drainages is temporarily (Table 4). In the following examples the effect of the wells is shown. The purpose of the wells is determined using data of Provincie Utrecht [2011].

In Fig. 36, the majority of the flow paths passing the city center end up in a large temporarily extraction well. This would reduce the threat of contamination in the city center for the drinking water extraction wells significantly. If this well is switched off in the model, the effect of another extraction well, just outside of the model area becomes visible (Fig. 37). When modeling a contamination source in the city center, most of the contamination flows northwards towards a building site related extraction (Fig. 38). On a regional scale, other extraction wells have thus significant effect on the groundwater quality.

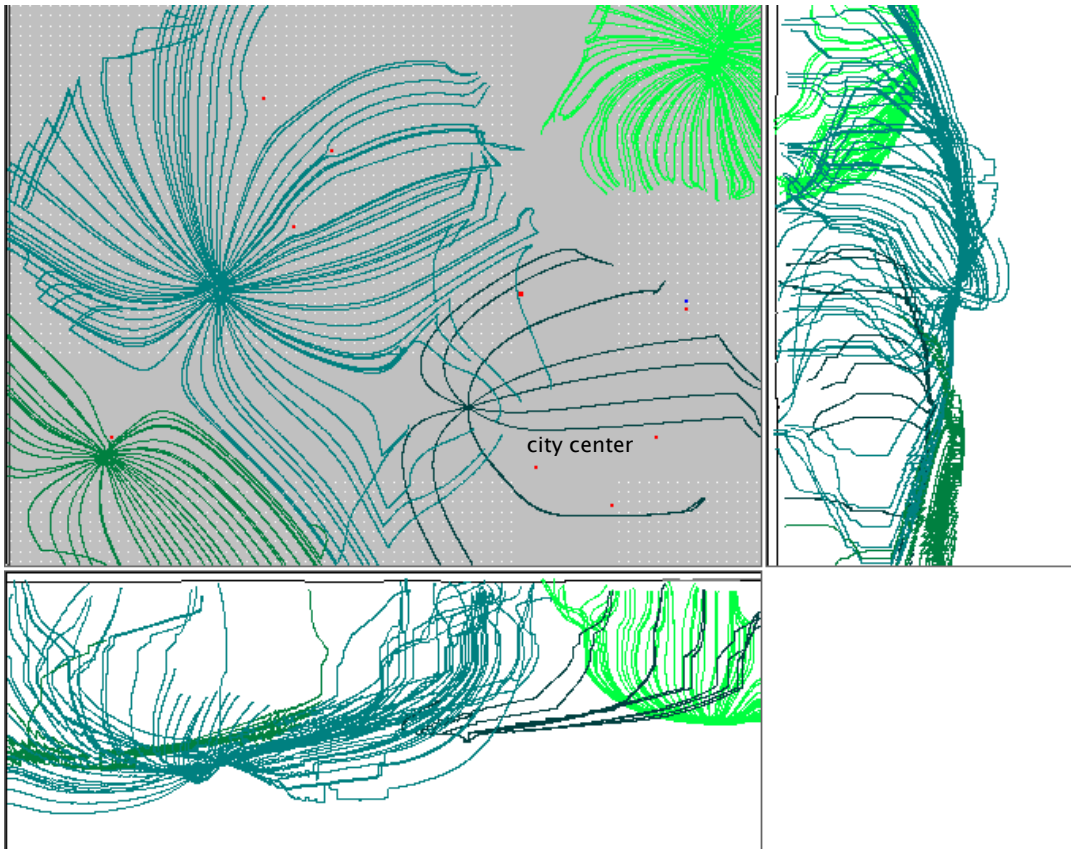

Fig. 36: Large temporarily extraction well in dark blue (the Cereol Benelux B.V. Factory). Flow lines towards the well come from the whole city center and vertical flow downwards is increased. The other three extractions are the drinking water wells.

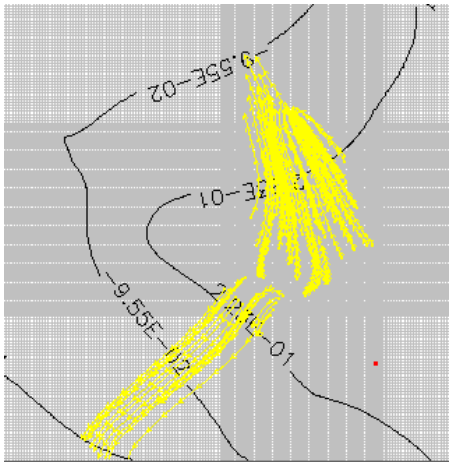

Fig. 37: Flow lines originated in the city center. The south-westwards flow direction is probably caused by an extraction well belonging to a parking lot (Papendorp, Utrecht).

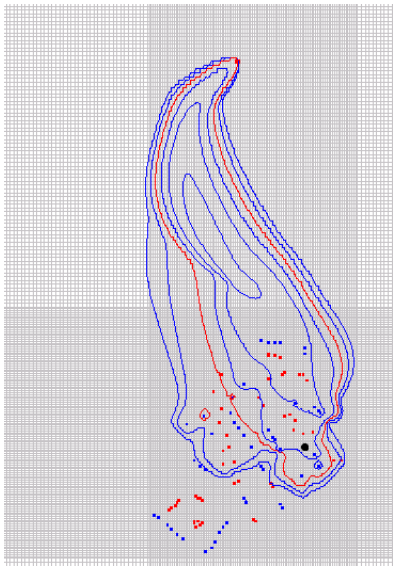

Fig. 38: Concentration contours after 200 years. The contamination flows from the city center towards an extraction well related to a building site, with the peak arriving after 130 years (Zandpad, Utrecht). The contamination source is modeled as a DNAPL at the black spot.

6. Discussion

The discussion is divided in three sections. In the first section, the spreading mechanisms described and qualified in chapter 4 are related to the effect that a cluster of SATES systems has on contaminant spreading, which is discussed in section 5.1. In the second part, the effects of contaminant spreading on a regional scale are discussed, and the resulting implications for regional planning. For each subject, uncertainties are mentioned and their effects are discussed. This chapter is concluded with recommendations for further research.

6.1 SATES system induced contaminant spreading

Model simulations show that the effect of SATES systems on spreading is significant. SATES systems increase the plume size with approximately a factor 10 (Fig. 28, Table 12). Vertical transport in Utrecht is even increased with a factor 50 (Table 13).

An implication of spreading is the involved dilution, which could be positive. As a small plume becomes spread over a SATES system area, the concentration might reduce to permitted values. The resulting water quality is dependent on the size of the area and the total contaminant mass. The effect of spreading and dilution on degradation rates is not taken into account in this study. The large dilution might have positive effects on degradation, which is positive for the water quality as well.

Studying different spreading mechanisms and variables, the spreading effect can be better understood.

6.1.1 Recirculation is most important contaminant spreading mechanism of an individual SATES system

A single SATES system contributes to spreading by groundwater mixing and recirculation. Groundwater mixing happens at the startup of a SATES system, due to dispersion and due to ambient groundwater flow. Theoretically, a higher pumping rate and a large water volume increase the effect of these mechanisms to spreading. Regarding groundwater mixing by ambient groundwater flow, the recovery ratio is identified to be the determining factor for spreading and dilution (equation 8).

In this research groundwater mixing is not studied extensively, as its contribution to hydrological interaction between different SATES systems is relatively small and it has less effect on a larger scale. Also, other studies cover these spreading effects (e.g. Bonte [2013], MMB 3/4 [2012], Zuurbier [2008], Zuurbier *et al.* [2013]).

Previous studies (e.g. MMB 9 [2012]) suggested that the contribution of recirculation to the amount of contamination spreading is relatively low. However, theoretically, recirculation has a large impact on spreading, as contamination extracted by a SATES well is injected in another well and thereby travels instantaneously a certain distance. The distance between the extraction and injection well is thus important for the travel time. This is in agreement with the model simulations of section 4.2.2. Injection far away from the extraction well (cross coupling) results in significantly shorter travel times than injection nearby (linear coupling) (Fig. 18). This effect is especially important, because other variables do not affect travel time significantly, according to the model results of the sensitivity analysis. Also the simulation of spreading in Utrecht confirms the importance of recirculation for both travel time and plume size (Fig. 25).

In other model studies [Arcadis, 2009; Tauw, 2010] recirculation is not taken into account and only hydrological mixing effects of SATES systems are modeled, which results in significantly less spreading (Fig.

26). This might affect the degradation rates of Arcadis [2009], who calibrated their values with measurements of contamination concentration in Utrecht. When underestimating spreading and dilution rates, the low contaminant concentrations could be explained by degradation rates, which they thus estimated to be higher than those of Zuurbier *et al.* [2013] based on literature.

Uncertainties regarding recirculation

If a system consists of more than two wells, the number of locations in which the contaminant is injected is increased, which increases spreading and dilution. Unfortunately MODFLOW and MT3DMS do not provide a method to model re-injection in multiple wells. Cross coupling is the best option, but because injection is only in one well, dilution is not fully taken into account. This results in a breakthrough curve with a high peak and a long tail (Fig. 18), whereas the curve probably should have a lower and later peak. The injected contamination concentrations are thus probably too high at the downstream boundaries of the plume in the model of Utrecht. For this reason, the plume sizes are calculated as a measure for spreading. One should keep in mind that the size of the plume contains no information about the concentration distribution.

Furthermore, one should be careful with modeling recirculation using equation 15. If a reference cell is wrongly determined, mass will be added or removed from the model and the mass balance and model results are incorrect.

6.1.2 Overlapping of capture zones is causes hydrological interaction between SATES systems and increases contaminant spreading

Hydrological interaction between SATES systems is caused by overlapping of capture zones. Contamination can this way be carried over from one SATES system to another within a year. This may decrease travel time significantly (equation 11).

In section 4.1.1, the capture zones are represented by circles with a hydraulic radius. When the hydraulic radii of two SATES wells are overlapping, contamination would be carried over. Thereafter, in the sensitivity analysis, the effect of overlapping capture zones was tested by changing the well distance. However, the difference in travel time between the case with and without overlapping capture zone is negligible (Fig. 21). A circle with a hydraulic radius describes a capture zone thus not correctly. When SATES systems are located close to each other, the change in hydraulic head is large. The effect of increased groundwater flow reaches further than the hydraulic radius. Thereby, the capture zones are transformed and enlarged. This might cause contamination to be carried over to the next system, even when the hydraulic radii are not overlapping.

For a line pattern, the spreading by a case with overlapping capture zones (well distance 60 %) is similar to the case without overlapping capture zones (well distance 100 %) (Table 11). In a checkerboard pattern a higher well distance results in more spreading. Presumably, this is because the total area affected by SATES wells is larger.

The analytical approach of overlapping hydraulic radii was also tested in the Utrecht model. Based on the hydraulic radius and the well distance, analytically a prediction can be made for overlapping capture zones (using equation 10). The analytical prediction was tested in the model of Utrecht. Two times the analytical solution predicted no contaminant transfer, whereas the model simulations showed contamination was carried over from one system to the other (see section 5.1, page 52). This might also be the effect of a large change in hydraulic head and increased groundwater flow, which results in larger capture zones of SATES wells. However, also the ambient groundwater flow can contribute to this effect, as shown in the study of Ceric and Haitjema [2005]. In Utrecht the value of $\bar{t}$ is approximately 0.3 (see section 2.1.1 for an

explanation of $\bar{t}$). This implies that well capture zones in Utrecht are not exactly a circle that can be described by the hydraulic radius. Instead, the ambient groundwater flow is such that a circular capture zone applies; only it is shifted along the direction of the ambient groundwater flow. The stretched capture zone might thus explain the contaminant transfer from system to system in the model, whereas it was not predicted using the hydraulic radius. Probably better results are obtained if not the hydraulic radius is used for predictions, but other methods as described by Ceric and Haitjema [2005].

Uncertainties regarding interaction of SATES systems

As is explained in section 3.3.2, the current discretization of the Utrecht model is such that a thermal radius covers about two grid cells. However, Sommer [2015] advises at least five cells per thermal radius. Due to the significantly increasing model running time when smaller cell sizes are used, nevertheless cells of 12.5 x 12.5 are chosen. Because of this inaccuracy, contaminants travel instantly one cell distance, which might result in overestimation of contaminant spreading. However, presumably this overestimation is small, because for the purpose of this study the thermal radius was not important, but the larger hydraulic radius. Also, the effects were studied on a much larger scale than Sommer [2015] did.

6.1.3 A higher well discharge causes increased groundwater flow and contaminant spreading

The importance of increased flow on interaction between SATES systems is described in the previous section. But increased flow has more consequences for contaminant spreading. Well discharge is clearly the most important factor in this mechanism.

Analytical solutions show that groundwater travel time in the horizontal plane (equation 12) is directly related to the discharge of SATES wells. Though head changes can both accelerate and decelerate water. The sensitivity analysis shows these effects level each other out for a large part. An increase of well discharge results in a small decrease of travel time (Fig. 21).

The analytical solutions thus showed that well discharge has a large impact on groundwater flow (equation 12 and 13). Increased groundwater flow implies increased contaminant spreading. This is confirmed by the sensitivity analysis. An increase in well discharge of 40 % results in an approximately 10 % larger plume (Table 11). Assigning different discharges in the case study model results in an increase of spreading of the same order of magnitude (Table 12). Increasing well discharge results also in significant dilution. A change in well discharge has significantly larger effect on the amount of spreading than well distance (Table 11). Also the well pattern (line or checkerboard) is of less importance for the degree of spreading. A line pattern results in little more spreading than a checkerboard pattern, because of the reinforcing effect of the wells on the hydraulic head, which causes lateral spreading (Fig. 22).

Head changes are not only important for spreading, but also for the contaminant dissolution of a DNAPL. The location of the DNAPL with regard to SATES wells is important, as was already stated by Zuurbier *et al.* [2013]. The smaller the distance between the contamination source and the SATES well, the larger the effects on the hydraulic head are, so more contamination is dissolved. The case study of Utrecht shows that indeed well discharge is a determining factor for the amount of contaminant dissolution (Fig. 27, Table 12). Hence, when considering a DNAPL, well discharge has even more impact on spreading than when considering a contaminant plume.

In Hydromedah, model layers in the aquifer are up to tens of meters thick. In practice a DNAPL is located at the bottom of an aquifer. However, in MT3DMS it is modeled as a cell with a constant concentration. Because this cell is about 35 meters high, the amount of water that passes the DNAPL is overrated. The results of the

dissolution of contaminants by a DNAPL might thus be overestimated, too (compare with e.g. Zuurbier *et al.*, 2013).

The model run of a thousand years (Fig. 33) shows that vertical transport takes place in the city center, where the SATES systems are present. Without SATES systems, almost no contamination is transported vertically, whereas with SATES systems the vertical transport is increased to about 10 % of the total mass present in the model (Table 13). Not only the relative amount, but also the total amount of vertical transport increases. Water budget analysis shows that the total interaction of the SATES system area with its surroundings is increased with a factor 3.0 with a 60 % well discharge and a factor 4.5 with a 100 % well discharge. The model simulations thus confirm the analytical approach, which showed that a higher well discharge, results in a larger vertical hydraulic gradient and more vertical transport (equation 13).

Next to spreading, dilution and the reduction of travel time, the interaction between SATES systems also has the consequence that the capture zone of a drinking water well is increased (Fig. 19). If the SATES systems cover a larger area, flow paths from a larger area are directed into drinking water extractions. Hence, the probability for contamination to end up in the drinking water extraction increases.

Uncertainties regarding well discharge

Although the discharge of a SATES well for contaminant spreading has proven to be very important, in both the theoretical and case study model the variability in well discharge over a year has been simplified to two periods with a constant discharge. In section 4.2.1 is explained that the hydraulic radius of the simplified well is 1.3 % larger than the hydraulic radius of the well with variable discharge. The difference is low, presumably because the hydraulic radius is based on the total seasonal volume injected. The total volume of the simplified well discharge is overestimated, because the alternation of injection and extraction in mid-seasons is not taken into account. However this overestimation is relatively small, because the discharge during autumn and spring is low compared to the discharge in other seasons. The difference in hydraulic head is small, which suggests that the difference in contaminant spreading is small, too. Probably on a short time scale, the variability in discharge results in variability of head changes and little more spreading. However, on a longer time scale, this effect probably is negligible. Using the 4/8 month simplification, spreading by an individual well is underestimated, due to the neglecting of the alternation of injection and extraction. On the other hand, spreading by multiple wells is overestimated slightly due to the overestimation of the hydraulic radius. This combination shows the 4/8 month distribution has little consequences studying contaminant spreading on a longer timescale. In fact, using the 4/8 month well discharge simplification has a large advantage compared to the 6/6 simplification which has been used in previous studies, as is shown by the reduction in the well discharge error of 24 % (section 4.2.1).

6.1.4 Combining mechanisms: total spreading effect

Above discussion shows that recirculation and head changes are the mechanisms that contribute the most to contaminant spreading in a cluster of SATES systems. The variables that have most impact on contaminant spreading and travel times are the following, ordered from most important to least important:

- *well discharge*: a higher well discharge results in larger head changes, more hydrological interaction of SATES systems and more contaminant spreading; also the dissolution of contamination is increased;
- *SATES distance to DNAPLs*: the smaller the distance, the more mass is dissolved;
- *total size of SATES system area*: the larger the total area, the larger the contamination plume will become; also the capture zone of a drinking water well becomes larger;

- *number of wells in a system*: the more wells a SATES system contains, the more important the contribution of recirculation;
- *well distance*: the larger the well distance between wells in a SATES system, the more important the contribution of recirculation; also a larger well distance indirectly contributes to a larger total size of the SATES system area. However, if the distance between two SATES systems is really large, there is no hydrological interaction, which results in a lower rate of contaminant spreading;
- *well pattern*: a line pattern results in more spreading than a checkerboard pattern, because of the reinforcing head changes.

6.2 SATES system induced spreading in a regional perspective

6.2.1 Spreading effects on a regional scale

Vertical and horizontal travel times are shortened by SATES systems. However, when contamination leaves the SATES system area horizontally or vertically, also the effect of head changes will diminish. The travel time between the SATES system area and drinking water wells is dependent on the ambient groundwater flow.

Analysis with PMPATH results in flow paths that are similar to the ones described in CityChlor [2012]. Travel times determined with these flow paths exclude diffusion and dispersion. PMPATH has the disadvantage that flow paths end up in SATES wells and are not re-injected. Therefore a location westwards of the city center was chosen as the starting point of the particles. The travel times range from 400 to 700 years. Calculation by hand results in a travel time of 600 years. In both cases vertical transport occurs westwards of the city center and the vertical travel time is estimated on approximately 200 years. The model MT3DMS includes transport parameters and simulated a plume starting in the city center. The outcome is of the same order of magnitude as the other outcomes: about 750 years. One should keep in mind that this is modeled with a retardation factor of 1.5. For example, VC has a negligible retardation factor, so this would result in a travel time of about 500 years. Hence, the contamination in the city center spreads at such a high rate, that on a regional scale the travel time within the city center can be neglected. Probably the vertical transport time is reduced due to the vertical head difference caused by SATES wells, which causes vertical transport to take place within the city area. Better results would have been obtained if two model runs with MT3DMS were done, comparing a situation with SATES systems with a situation without. However, the long running time of MT3DMS this was impossible.

The buffer zone between the SATES systems and the drinking water extractions is thus really large. During the time contamination flows through the buffer, the plume disperses even more. This results in lower concentrations and relatively less impact of the spreading by SATES systems.

The relative effect of SATES systems on a regional scale is also decreased because other extractions have a relatively large impact on regional flow. Injection and extraction is alternated in the case of SATES systems, reducing the hydrological effect, while the other drainages are purely extracting. Moreover, the drainage wells extract often from the second aquifer, enhancing vertical flow downwards through confining layers. Also their discharge is often higher (Table 4). On the other hand can travel times be prolonged by other extractions, as the drainage wells can also pull the contamination against the regional groundwater flow. Besides, the contaminated water can be extracted by one of these wells before it reaches drinking water extractions; this would certainly be a positive effect for the water quality. Overall, the most important effect of the extraction wells probably would be extra spreading and shortening of travel times. However, because most extractions are temporarily, the effect is hard to quantify. Dependent on their location, the effect on

travel time is more important than the effect of SATES systems, due to their net extraction and their larger discharge. SATES systems probably have more effect on spreading and dilution because of their number and position close to each other and their location close to contamination sources.

6.2.2 Implications for planning

Based on the research results, some suggestions for SATES system planning can be made, which are also applicable to other locations with a high density of SATES systems:

- In Utrecht SATES systems cause spreading to increase with a factor ten. Hence, spreading is accelerated in such a high degree that the whole SATES system area is contaminated within a relatively short period, compared with travel times to drinking water wells. Therefore the area can be considered as one large contamination plume.

- SATES systems contribute significantly to contaminant dissolution from DNAPLs. Therefore it is suggested that before placing SATES systems or increasing well discharge, research is done on the location of DNAPLs.

- A high well discharge has shown to affect spreading significantly. On the other hand, a high well discharge is positive for the energy efficiency. One way to increase the efficiency and at the same time not increase contaminant spreading, is inducing a larger temperature difference by the SATES systems.

- Model simulations have shown that the interaction between SATES systems occurs even with a large well distance. Because a large well distance does not necessarily prevent spreading, and a higher density of SATES systems will increase the efficiency of the area, a small well distance is advised, where the minimum well distance should be determined by thermal interference. A smaller total area results automatically in a larger buffer zone.

- When the buffer zone is covered with SATES systems, contaminants reach drinking water wells within a short period. Therefore new SATES systems should be built in the buffer zone only in a limited amount. Upstream of the contamination source SATES systems can increase contaminant spreading only if they interact with other SATES systems.

- In Utrecht, the large buffer zone between the drinking water extractions and the city center with contamination sources and SATES systems results in long travel times and dilution, this is positive for the groundwater quality. Hence, a large distance and a small ambient groundwater flow create an effective buffer between the contamination in the SATES system area and drinking water wells. Observation wells could be placed to monitor groundwater travelling towards drinking water wells downstream of the SATES system area.

- If the buffer zone is smaller than in Utrecht, SATES systems are a threat for the drinking water quality. Some measures can be taken to reduce the negative effect of SATES systems on contaminant spreading. One possibility is to reduce the well discharge of SATES system at the downstream end of the SATES system cluster. Another option to control the contamination, is increasing the recovery ratio of wells at the downstream end of high density SATES system areas. Increasing the recovery ratio reduces the amount of contamination that escapes from the area and lowers the concentration. One way to increase the recovery of contaminants is net extraction by

SATES systems. Net extraction wells can remove contaminants from the groundwater. The extracted water can be drained aboveground, treated or mixed with high quality water. Another option is to install other extraction wells that remove contaminants from the groundwater. Net extraction is also a possibility to apply nearby DNAPLs.

- As the demand for SATES systems is still increasing, it is expected more SATES systems will be built in future. When new SATES systems are built nearby the existing systems, it can be assumed the contamination will spread to that system quickly. This might be positive, as it will be diluted. The probability that contamination spreads upstream is less than downstream, so building SATES systems upstream from the contamination source results in a smaller threat for the water quality. Placing new SATES systems in deeper aquifers, vertical transport probably will be increased in the same way that is increased by current SATES wells. A large buffer zone can reduce the risk.

Applicability of the case study in other locations

Above implications for planning can be used for SATES system areas on other locations than Utrecht. Considering the threat for drinking water wells, the extent of the buffer zone as well as natural groundwater flow should be studied.

A part of the results of this study is based on the case study of Utrecht. Although SATES systems are generally built in thick permeable aquifers with a low hydraulic gradient, the hydrogeological characteristics in other SATES system areas might be different from the field situation in Utrecht. The most important external factor is probably the ambient groundwater flow. A larger ambient groundwater flow decreases the relative effect of well discharge and thus the effect of SATES induced head changes. Also the recovery ratio of SATES wells declines with a larger ambient groundwater flow. The mechanism of recirculation stays the same. Generally, it is expected that a larger ambient groundwater results in less lateral spreading and more spreading downstream.

6.3 Further research

For future research regarding contaminant spreading in a high density SATES system area, the following recommendations are made:

- The mechanisms behind spreading and the implications for planning are applicable in other locations. Further research should quantify the effect of hydrogeological factors, such as the ambient groundwater flow. To do this, a sensitivity analysis could be performed.

- Recirculation has shown to be an important spreading mechanism. Modeling recirculation by cross coupling is the most realistic option presently available for the used model software. However, results will be improved when re-injection in multiple wells are modeled. For example, the MODFLOW multinode well package could be modified such that a discharge per cell can be defined. Furthermore, the importance of recirculation can be verified by monitoring contaminant concentrations in SATES wells.

- Overlapping of capture zones of SATES wells causes contamination to be carried over from one SATES system to another. This study showed that it is not possible to predict overlapping of capture zones using the hydraulic radius of SATES wells. Future research should determine how the

overlapping of capture zones can be predicted.

- The effect of increased well discharge on contaminant spreading is studied by injecting and extracting a larger water volume during a pumping season. However, the discharge was equal during the whole season. Future research should study contaminant spreading with a well discharge varying with time.

- The effect of recirculation is increased by a higher number of wells and the effect of increased flow by a higher well discharge. Further research should determine to what extent a system of two wells with a high discharge results in less contaminant spreading than a system of multiple wells with a lower discharge.

- The degree of spreading and dilution presented in this study is higher than shown by other studies. Therefore previous studies may have overestimated degradation rates based on modeled concentrations. This should be addressed through further study.

- The effect of the well recovery ratio on spreading should be studied further, to fully understand the possibilities of net extraction as a measure to control contamination at the downstream end of a high density SATES system area.

7. Conclusions

In this study, analytical solutions, a theoretical model and a case study model of Utrecht are used to describe, quantify and explain contaminant spreading in a high density SATES system area and place it in a regional perspective.

After 50 years model simulation of Utrecht, SATES systems have increased spreading with a magnitude of factor 10. Model results show that vertical mass transport is even a factor 50 larger due to SATES systems. Thus SATES systems contribute significantly to contaminant spreading. In case of a plume, SATES systems have probably a positive effect due to this large dilution effect. In case of a DNAPL, SATES systems cause dissolution of contamination into the groundwater, which is negative for the groundwater quality.

Model simulations show that recirculation is a very important factor for contaminant spreading and travel times. Furthermore, both the theoretical model and case study model show that including recirculation in a transport model is essential when modeling realistic SATES system induced contaminant spreading. Implementing recirculation results in more spreading than previous model studies in this field have shown [i.e. Arcadis, 2009]. As a second spreading mechanism, SATES induced head changes are responsible for accelerating flow and enhancing contaminant spreading significantly. Thereby, it is the only mechanism that increases vertical spreading. The most important variables for these mechanisms are well discharge, well location and the number of wells per system.

Interaction of SATES systems causes fast contaminant spreading in a SATES system cluster. Interaction takes place when capture zones of SATES wells overlap. However, it is not always possible to determine the size of a capture zone of a SATES well correctly using the hydraulic radius. This is because the capture zone becomes larger and stretched by SATES induced head changes and ambient groundwater flow.

The Utrecht model shows that spreading is increased in such degree, that on a timescale of decades, which is typical for groundwater flow, the contamination in a high density SATES system area can be considered one large plume. The travel times within a high density SATES system area are very small, but in the case of Utrecht a large buffer zone is present between the contaminated area with SATES systems and drinking water wells, which reduces the threat for the drinking water quality. In a regional perspective, other extraction wells have probably more effect the water quality than SATES systems. In general though, when extraction of groundwater for drinking water purposes occurs in the proximity of a contamination in an area with high density SATES systems, SATES systems are a threat for the drinking water quality because contaminant travel times are shortened significantly.

This study shows how contaminant spreading is significantly increased in a high density SATES system area. Future research could further analyze recirculation and overlapping capture zones and focus on how this knowledge can be applied in regional subsurface planning.

Acknowledgements

I'd like to thank the following people for their contribution to this study:

- **Martin Bloemendal** and **Niels Hartog**; who motivated me with their enthusiasm, kept me focused, and gave me good feedback during the whole process;
- **Willem-Jan Zaadnoordijk**; who helped me with the modification of the Hydromedah model;
- **Koen Zuurbier**; who helped me with the multinode well package;
- The KWR staff from geohydrology and ecohydrology; who gave me a great internship and invited me on their trip to the Ardennen;
- **Albert de Vries, Inge Rosenthal** and **Sjoerd Rijpkema** who gave me insight in the perspective of a drinking water company and the municipality of Utrecht;
- **Majid Hassanizadeh**; who is always willing to think along with me and knows how to get most out of his students;
- **Huub Zwart**; who helped me in the writing process and kept motivating me.

References

Arcadis (2009). Dols. *Saneringsplan ondergrond Utrecht, Gefaseerde gebiedsgerichte aanpak*.

Artesia (2015). *MODFLOW.* http://www.artesia-water.nl/software/MODFLOW/ Consulted at 23-01-2015.

Bakr, M.; Van Oostrom, N.; Sommer, W. (2013). *Efficiency of and interference among multiple Aquifer Thermal Energy Storage systems; A Dutch case study.* Renewable energy Vol. 60 p. 53-62. doi: 10.1016/j.renene.2013.04.004

Bear, J.; Jacobs, M. (1965). *On the movement of water bodies injected into aquifers.* Journal of Hydrology Vol. 3, p. 37-57.

Bloemendal, M.; Olsthoorn, T.; Boons, F. (2013). *How to achieve optimal and sustainable use of the subsurface for Aquifer Thermal Energy Storage.* Energy policy. Doi: 10.1016/j.enpol.2013.11.034i.

Bonte, M. (2013). *Impacts of shallow geothermal energy on groundwater quality. A hydrochemical and geomicrobal study of the effects of ground source heat pumps and aquifer thermal energy storage.* PhD thesis, Vrije Universiteit Amsterdam, Amsterdam, the Netherlands.

Bonte, M.; Van den Berg, G.; Van Wezel, A. (2008). *Bodemenergiesystemen in relatie tot grondwaterbescherming.* Bodem 5 p. 22-26.

Calje, R.J. (2010). *Future use of Aquifer Thermal Energy Storage below the historic centre of Amsterdam.* MSc thesis, Technische Universiteit Delft, Delft, the Netherlands.

CBS Centraal Bureau voor de Statistiek (2013). *Hernieuwbare energie in Nederland 2013.*

Ceric, A.; Haitjema, H. (2005). *On using simple time-of-travel capture zone delineation methods.* Groundwater Vol. 43, No. 3, p. 408-412.

CityChlor (2013). *Geohydrological modelling - Predictions for an area-oriented approach for groundwater contamination in the City of Utrecht.*

De Jonge, H.; Koenders, M.; De Zwart, B. (2012). *Bodemenergiesystemen kunnen dichter bij elkaar.*

Deltares (2009). Borren, W.; Berendrecht, W.; Heijkers, J.; Snepvangers, J.; Veldhuizen, A. *Ontwikkeling HDSR hydrologisch modelinstrumentarium - HYDROMEDAH. Deelrapport 1: Beschrijving MODFLOW model.*

DWA installatie- en energieadvies and IF Technology (2012). *Onderzoek criteria energiebalans WKO.* Eindrapportage in opdracht van skb.

Fitts, C.R. (2002) *Groundwater science.* Academic press, Elsevier Science. ISBN 0-12-257855-4.

Haehnlein, S.; Bayer, P.; Blum, P. (2010). *International legal status of the use of shallow geothermal energy.* Renewable and Sustainable Energy Reviews Vol. 14 p. 2611-2625.

Hartog, N.; Drijver, B.; Dinkla, I.; Bonte, M. (2013). *Field assessment of the impacts of Aquifer Thermal Energy Storage (ATES) systems on chemical and microbial groundwater composition.* European Geothermal Congres 2013.

KNMI (2011). *Klimaatatlas.* http://www.klimaatatlas.nl/klimaatatlas.php. Consulted at 15-10-2014.

Li, Q. (2014). *Optimal use of the subsurface for SATES systems in busy areas. Towards more robust master plans using a two-stage assessment method.* MSc Thesis, Technische Universiteit Delft, Delft, the Netherlands.

Ma, R. and Zheng, C. (2010). *Effects of density and viscosity in modeling heat as a groundwater tracer.* Ground water Vol. 48 No. 3 p.380-389.

Meer Met Bodemenergie rapport 3/4. Bioclear, Deltares, IF Technology and Wageningen Universiteit (2012). *Effecten op de ondergrond. Effecten van bodemenergiesystemen op de geochemie en biologie in de praktijk. Resultaat metingen op pilotlocaties en labtesten*.

Meer met Bodemenergie rapport 7. Bioclear, Deltares, IF Technology and Wageningen Universiteit (2012). *Interferentie. Effecten van bodemenergiesystemen op hun omgeving – modellering grootschalige inpassing in stedelijke gebieden.*

Meer met Bodemenergie rapport 9. Bioclear, Deltares, IF Technology and Wageningen Universiteit (2012). *Effecten op sanering. Effecten van bodemenergiesystemen bij inzet bodemsanering – resultaat metingen op pilotlocaties en in labtesten.*

Meer met Bodemenergie rapport 11. Bioclear, Deltares, IF Technology and Wageningen Universiteit (2012). *Gebiedsgericht grondwaterbeheer Inpassing van bodemenergie in bodemgericht grondwaterbeheer – kansen en aandachtspunten.*

Nederlandse Vereniging voor Ondergrondse Energieopslagsystemen (2006). *Werkwijze en richtlijnen ondergrondse energieopslag.*

Provincie Utrecht (2013). *Bodemloket.* https://www.provincie-utrecht.nl/loket/kaarten/geo/bodemloket-0/ Consulted at 15-10-2014.

Provincie Utrecht (2011). Grondwater register uittreksel 2009-2010, 2010-2011.

Schepers, B.L. and Aarnink, S.J. (2014). Kansen voor warmte. Het technisch potentieel voor warmtebesparing en hernieuwbare warmte. Update van 200-200 in 2020. CE Delft.

Simcore Software (2012). Processing MODFLOW. An Integrated Modeling Environment for the Simulation of Groundwater Flow, Transport and Reactive Processes.

Simcore Software (2015). *Processing MODFLOW 8.042.* http://www.simcore.com/ Consulted at 23-01-2015.

SKB (2007). Nipshagen, A.; Praamstra, T. *Vluchtige chloorkoolwaterstoffen (VOCl) in bodem.* Cahier van skb duurzame ontwikkeling ondergrond.

SKB (2013). Bloemendal, M.; Mathijsen, H. *Bodemenergie warm aanbevolen.* Cahier van skb duurzame ontwikkeling ondergrond.

Sommer, W.; Valstar, J.; Leusbrock, I.; Grotenhuis, T.; Rijnaarts, H. (2015). *Optimization and spatial pattern of large-scale aquifer thermal energy storage.* Applied Energy Vol. 137

Taskforce WKO (2009). *Groen licht voor bodemenergie*.

Tauw bv (2010). Bloemendal, M.; Boerefijn, M.; Blonk, A.; Hoekstra, J.; Winters, G. *M.e.r. Koude-Warmteopslag Stationsgebied Utrecht*.

TNO (2004). Gunnink, J.L .; Veldkamp, J.G.; Dam, D.; Weerts, H.J.T.; Van der Linden, W. *Deklaagmodel en geohydrologische parametrisatie voor het beheersgebied van het Hoogheemraadschap "De Stichtse Rijnlanden".*

USGS (2015). *MODFLOW and related programs*. http://water.usgs.gov/ogw/MODFLOW/ Consulted at 23-01-2015.

Vitens (2012). *Info winningen Utrecht. Lokatie en jaarlijkse debieten drinkwaterwinningen in en om Utrecht.*

Zheng, C. (2010). *MT3DMSv.5 Supplemental User's Guide*.

Zuurbier, K.G. (2008). *Effecten Warmte-Koude Opslag-systemen (WKO) op met gechloreerde koolwaterstoffen verontreinigde grondwatersystemen.* MSc Thesis, Deltares and University of Utrecht, the Netherlands.

Zuurbier, K.G.; Hartog, N.; Valstar, J.; Post, V.E.A.; Van Breukelen, B.M. (2013). *The impact of low-temperature seasonal aquifer thermal energy storage (SATES) systems on chlorinated solvent contaminated groundwater: Modeling of spreading and degradation.* Journal of Contaminant Hydrology. Vol. 147 p. 1-13. doi: 10.1016/j.jconhyd.2013.01.002

List of symbols and units

Description	Symbol	Unit
Time	t	day
Distance	y	m
Hydraulic head	h	m
Transmissivity	T	$m^2\ day^{-1}$
Hydraulic conductivity	k	$m\ day^{-1}$
Layer depth	D	m
Leakance of aquitard	L	day^{-1}
Vertical resistance	c	day
Specific discharge	q	$m\ day^{-1}$
Leakage factor	λ	m
Specific storativity	S_s	-
Sources and sinks term	W	$m\ day^{-1}$
Discharge	Q	$m^3\ day^{-1}$
Well filter length	H	m
Concentration	C	$kg\ m^3$
Porosity	θ	$m^3\ m^{-3}$
Retardation factor	R	-
Distribution coefficient	K_d	$m^3\ kg^{-1}$
Hydrodynamic dispersion coefficient	D_{tot}	$m^2\ day^{-1}$
Molecular diffusion coefficient	D_{mol}	$m^2\ day^{-1}$
Dispersivity	α	m
Groundwater velocity	v	$m\ day^{-1}$
Reaction term	R_n	$kg\ m^{-2}\ day^{-1}$

Temperature	T	°C
Thermal retardation factor	R_T	–
Thermal distribution coefficient	K_T	$m^3\ kg^{-1}$
Thermal dispersion coefficient	D_{Ttot}	$m^2\ day^{-1}$
Density	ρ	kg/m^3
Volumetric heat capacity	c	$J\ m^{-3}\ °C^{-1}$
Thermal conductivity	κ	$J\ m^{-1}\ day^{-1}\ °C^{-1}$
Recovery ratio	RR	–
Parameter determining shape of capture zone	$\bar{t}$	–
Ratio of extraction over injection discharge	β	–

List of figures

Fig. 1: The working of a SATES system [Bonte, 2013]. 7
Fig. 2: The increase of SATES systems in the utilities sector in the Netherlands [Sommer, 2015]. 8
Fig. 3: (A) The length of the capture zone (x-axis) vs. the elongation as parameter t (y-axis). (B) The view from above of the shapes of the pumping (extraction) and injection capture zones. Again the length of the capture zone is projected on the x-axis. Larger circles represent more elongated capture zones (larger t values) [after Bear and Jacob, 1965]. 11
Fig. 4: The checkerboard pattern (A) and line pattern (B) [Li, 2014]. Note that the warm and cold wells become clustered in a line pattern. 13
Fig. 5: 0.1 m Isohypse maps of the upper aquifer (A) and the second aquifer (B) in Utrecht. Data are from 2007 [Provincie Utrecht, 2013]. Dots indicate SATES systems in the city center (purple) and the surroundings (red). Drinking water extraction wells are indicated by green dots and labeled. 19
Fig. 6: SATES systems in the center of Utrecht, with warm (red) and cold (blue) wells. The circles around the wells represent the thermal radii. In the model of Utrecht, the wells are coupled as shown with the black lines. 20
Fig. 7: SATES systems in the center of Utrecht (purple) have a much higher density than the systems in the surroundings (red). The drinking water wells lie outside of the city (green), surrounded by drilling free zones, protected areas and 100-years zones. The inner black box is the area of interest. 21
Fig. 8: (A) The fifth layer of the model containing SATES systems in the city center. The finer spatial discretization around the wells is visible. In the report, to the area containing SATES systems is further referred as the 'city center'. (B) A map of the extent of the model with SATES systems and drinking water wells. 26
Fig. 9: Groundwater mixing and smoothening of vertical gradients at the startup of a SATES system. 29
Fig. 10: Groundwater mixing due to dispersion at the boundary of the injected water volume. 29
Fig. 11: Contaminant release to the aquifer. 30
Fig. 12: Overlapping of capture zones might cause contamination to be carried over from one SATES system to another. 31
Fig. 13: The effect of SATES induced change in hydraulic head. 32
Fig. 14: The recirculation mechanism. (A) Extraction of contamination in one well and re-injection in the other well. (B) Extraction of contamination in one well and re-injection in several other wells. 34
Fig. 15: The air temperature at De Bilt and the corresponding weekly cumulative injection discharge in SATES system 'De Uithof' in Utrecht [after MMB11, 2012; Zuurbier *et al.*, 2013]. The blue boxes represent the simplified discharge, with dark blue a 6/6 month distribution and light blue 4/8 months. Note that the injection period of the warm well is twice as large as the injection stage of the cold well, and that the 4/8 month distribution represents this behavior better. 36
Fig. 16: The four cases to model solute transport by a SATES system. 38
Fig. 17: Plume contours for three different cases at several time steps. 39
Fig. 18: Breakthrough curves at observation well. Curves are for a scenario with DNAPL and a scenario with a plume. Output is shown in both linear scale and log scale. Based on the ratio of solubility and intervention value, the concentrations from 1E-6 and higher are relevant. 40
Fig. 19: Flow paths towards the drinking water well at the left end. In the different cases different SATES system arrangements are modeled. The flow paths reverse from season to season as a result of alternating injection and extraction, with opposite effects. 42

Fig. 20: The breakthrough curves of a case without SATES wells and four cases with a doublet (in line or perpendicular to groundwater flow, EW = extraction well, IW = injection well). The concentrations are relative to the case without SATES systems. 43
Fig. 21: The breakthrough curves of the cases in line pattern and checkerboard pattern result in a slightly shorter travel time as the case without SATES systems that is shown in Fig. 20. The differences in travel time between the ten cases are very small. 44
Fig. 22: The extent of the plume in line pattern and checkerboard pattern after 10 and 20 years. The travel time is about equal for both cases. The plume size after 10 years is about 12 % larger for the line pattern. After 20 years, the difference in plume size is negligible. 45
Fig. 23: The hydraulic head distributions of the line pattern (A) and checkerboard pattern (B), in the cases with 140 % well distance. 46
Fig. 24: Overview of SATES systems (see Fig. 6) with initial conditions for the model runs: a hypothetical plume (A) and a hypothetical DNAPL in the circle (B). Underlined the analyzed observation wells. 47
Fig. 25: Contaminant spreading caused by the modeled DNAPL. The contamination contours are logarithmically scaled. 48
Fig. 26: The effect of recirculation in contaminant spreading. (A) Initial DCEcis plume in Arcadis [2009]. (B) Plume after 15 years according to Arcadis [2009]. In the model SATES wells pump at 82.5 % for 6-6 months and recirculation is not incorporated. (C) Initial plume in Hydromedah model. (D) Plume after 2 years in Hydromedah model. Note that already a new plume is present where Arcadis [2009] shows after 15 years no contamination. The contamination is transported over a large distance, because the contamination is extracted by a SATES system of which the cold and warm wells are located far from each other (see Fig. 6, NHC-system). In the model SATES wells pump at 60 % for 4-8 months and recirculation is incorporated. ... 48
Fig. 27: Breakthrough curves at observation wells shown in Fig. 24. The breakthrough curves are shown for the plume (A) and DNAPL (B). Both cases show results for the normalized situation without SATES systems. Also the relative concentrations are shown from the situations with SATES systems at 60 % and 100 % of the discharge. 49
Fig. 28: The spreading of the hypothetical plume after 50 years, for a situation without SATES (A) and with SATES with discharge on 60 % of the maximum (B) and at 100 % of the maximum (C). Concentration contours are scaled logarithmically in steps of a factor 10; the red line corresponds with 1E-06. 50
Fig. 29: (A) Flow in and out of the subregion in layer 5 containing SATES systems. Fluxes (m^3 day^{-1}) represent interaction with layer 4, layer 6 and the surrounding region of the subregion in layer 5. These are the fluxes of model period 1, which are representative for the whole simulation period, as the difference with fluxes of other periods is negligible, because the total of the whole area is calculated. (B) The defined subregion. 52
Fig. 30: Flow paths for the first and second aquifer, starting at the western side of the city center. Time mark interval is 50 years. 53
Fig. 31: 3D visualization of the model. Flow lines starting at the city center flow firstly westwards and then to the deeper aquifer. Also flow lines towards the drinking water extractions are shown. 53
Fig. 32: Two east-west model cross sections (row 262). In (A) the vertical conductivity of the clayey layers is shown. The green layers represent sand with an average vertical conductivity of 1 m day^{-1}. In (B) the hydraulic head is shown for the same cross section. Note the east to west decline of heads and the effect of the drinking water extractions. 54
Fig. 33: 1000 years of plume development in Utrecht for the first aquifer, the aquitard and the second aquifer. Plume contours are on logarithmic scale starting at 1E-10. Because a DNAPL is modeled, the total mass increases during the model run. SATES wells pump at 60 % of their permitted discharge. 56

Fig. 34: Breakthrough curves of the plume at the seven drinking water extraction wells of Leidsche Rijn and the average. 57
Fig. 35: Breakthrough curves of plume at the four drinking water extraction wells of De Meern and the average. 57
Fig. 36: Large temporarily extraction well in dark blue (the Cereol Benelux B.V. Factory). Flow lines towards the well come from the whole city center and vertical flow downwards is increased. The other three extractions are the drinking water wells. 58
Fig. 37: Flow lines originated in the city center. The south-westwards flow direction is probably caused by an extraction well belonging to a parking lot (Papendorp, Utrecht). 59
Fig. 38: Concentration contours after 200 years. The contamination flows from the city center towards an extraction well related to a building site, with the peak arriving after 130 years (Zandpad, Utrecht). The contamination source is modeled as a DNAPL at the black spot. 59
Fig. 39: Efficiencies of a cold and warm well with a 4-8 month discharge distribution for the first year. In theory the extracted water of the warm well is 18°C, however in reality there are losses. During four months of extraction of the warm well, 66.8% of the theoretical temperature is recovered. During the eight months of extraction of the cold well, 63.8% of the theoretical temperature is recovered, which is a little smaller efficiency than the warm well. If the well discharge distribution was 6-6 months, the efficiencies of both wells would be 65.4%. 83
Fig. 40: Temperature-time curve showing the stabilization of temperature after 10 years (520 weeks). 84

List of tables

Table 1: Hydrogeological and transport parameters for the theoretical model [based on Deltares, 2009; MMB9, 2012; Provincie Utrecht, 2013; Tauw, 2010]. 17
Table 2: Simplified geology of Utrecht [after MMB 9, 2012 and Tauw, 2010]. 18
Table 3: Drinking water extractions in the region of the case study, number of wells and average discharge [Vitens, 2012]. 22
Table 4: Extraction wells in Utrecht, average discharge and operational period [Deltares, 2009]. 22
Table 5: The mass of four contaminants at different depths in the subsurface of Utrecht [after Arcadis, 2009] 23
Table 6: Model schematization related to the (simplified) geology. In bold the aquitards that are added to obtain a full 3D model. 25
Table 7: Transport parameters in the case study model [after Arcadis, 2009 and Zuurbier *et al.*, 2013]. 27
Table 8: Distribution coefficients, retardation factors and degradation rates used in the model [based on Arcadis, 2009] 27
Table 9: Solubility value and intervention value [SKB, 2007], and the factor of intervention value divided by solubility. 28
Table 10: Well discharges of the five cold wells of the SATES system in line pattern. In cases without MNW (linear coupling or cross coupling), the discharge is equally distributed over the five wells. However, in the MNW case the individual well discharge diverges significantly. Upstream (well 5) there is high extraction and low injection. The same applies for the warm well. 41
Table 11: The plume size after ten years relative to the 100 % case, for both the line and checkerboard pattern. Firstly the well distance is modified between the wells in line with the groundwater. A well distance of 60 % implies overlapping capture zones, a well distance of 100 % and 140 % do not. Thereafter the well discharge is changed. 46
Table 12: Relative spreading and dilution of a plume and DNAPL. The horizontal spreading is based on the plume area and normalized to the situation without SATES systems. The dilution is based on the average concentration of the plume: If the average concentration is 0.5 compared with the situation without SATES systems, the dilution is twice as high. 50
Table 13: The percentage of mass that is transported upward and downward with regard to the layer with SATES systems (layer 5), based on the total mass in layers 3-7 after 50 years model simulation. 51
Table 14: Values for injection and extraction of cold and warm well at the Uithof, Utrecht [after Zuurbier *et al.*, 2013]. The analysis is done for a 6-6 month distribution of injection and extraction, and a 4-8 month distribution. The recovery ratio is estimated based on figures from Bear and Jacobs [1965]. 79
Table 15: Recoveries for the cold and warm well in three cases: the recovery of water (R = 1), injected temperature (R = 1.6) and the solute VC (R = 1.1). This is the model output from the first year and the tenth year (stabilized). 84

Appendix I: Recovery ratio of the warm and cold well

The demand for heat and cold is not equally spread throughout the year (see section 4.2.1). This has consequences for the recovery ratio as determined by Bear and Jacobs [1965] (see section 2.1.1). As heat is extracted in 4 months during winter and the same volume of water is extracted during summer by the cold well in 8 months, the factors β and $\bar{t}_{inj}$ and $\bar{t}_{ex}$ and thus the recovery ratio are different for the cold and warm well. To study this effect, the factors are calculated for the discharges of the wells in the Uithof case (same case as used in section 4.2.1**Fout! Verwijzingsbron niet gevonden.**).

The results of the calculations are shown in Table 14. In case of the warm well, β is approximately 2, as the extraction discharge is approximately two times as large as the injection discharge due to the peak in heat demand during winter. On the contrary, the value for β is 0.5 of the cold well. This suggests a higher efficiency for the warm well than for the cold well. On the other hand, the durations of injection and extraction differ, which results in other values for $\bar{t}$. For the warm well, the extraction time is short. This results in a smaller $\bar{t}_{ex}$ relative to $\bar{t}_{inj}$, being negative for the recovery ratio. For the cold well the opposite applies. Using the figures of Bear and Jacobs [1965], the recovery ratios of the warm and cold well are estimated. The warm well has a recovery ratio of about 0.7, whereas the cold well only has a recovery ratio of 0.6. Hence, for the warm well the recovery ratio is higher due to the relative high extraction discharge; the shorter extraction time has less influence.

Table 14: Values for injection and extraction of cold and warm well at the Uithof, Utrecht [after Zuurbier *et al.*, 2013]. The analysis is done for a 6-6 month distribution of injection and extraction, and a 4-8 month distribution. The recovery ratio is estimated based on figures from Bear and Jacobs [1965].

	6-6 months		4-8 months	
	Warm well	**Cold well**	**Warm well**	**Cold well**
Q inj (m^3 $month^{-1}$)	23704	23704	17874	35226
Q ext (m^3 $month^{-1}$)	23704	23704	35226	17874
t_inj (months)	6.0	6.0	8.0	4.0
t_ex (months)	6.0	6.0	4.0	8.0
$\beta = Q_{ext}/Q_{inj}$	1.0	1.0	1.97	0.51
$\bar{t}$_inj	0.19	0.19	0.33	0.09
$\bar{t}$_ext	0.19	0.19	0.09	0.33
estimated recovery ratio	0.7	0.7	0.7	0.6

To validate the theory that a warm well has a higher recovery ratio than the cold well, a model is set up. In a first run, the cold well is modeled with 4 months injection and 8 months extraction. In a second model the warm well is simulated. Again the discharge values are based on the Uithof case. In the pumping well an observation point is placed, which monitored the temperature or solute concentration per time. This results in Fig. 39.

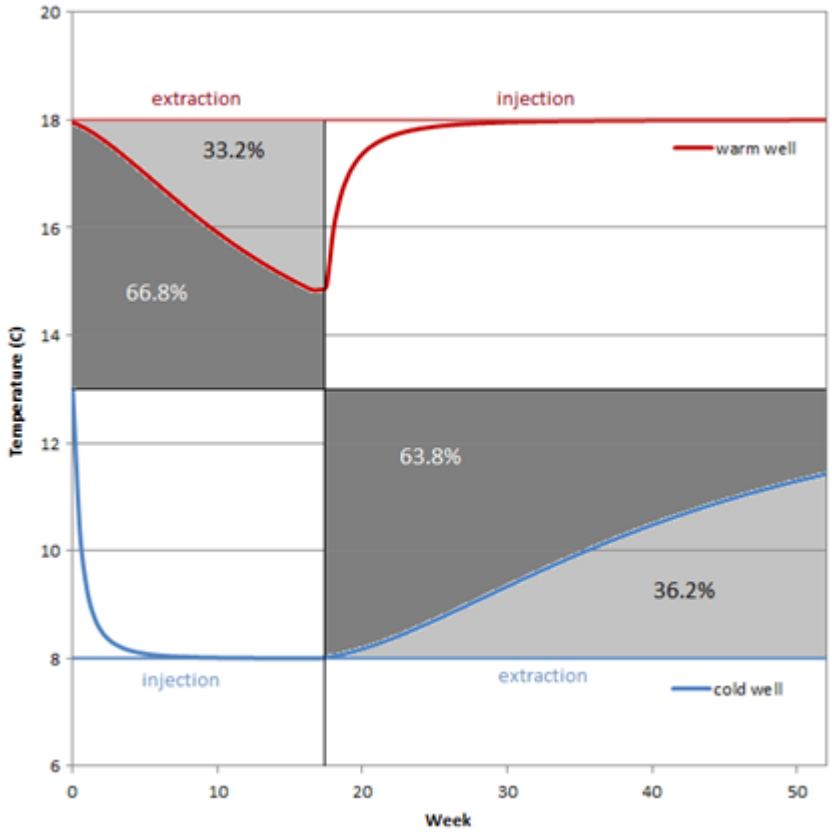

Fig. 39: Efficiencies of a cold and warm well with a 4-8 month discharge distribution for the first year. In theory the extracted water of the warm well is 18°C, however in reality there are losses. During four months of extraction of the warm well, 66.8% of the theoretical temperature is recovered. During the eight months of extraction of the cold well, 63.8% of the theoretical temperature is recovered, which is a little smaller efficiency than the warm well. If the well discharge distribution was 6-6 months, the efficiencies of both wells would be 65.4%.

From the observation data, the recovery ratio can be calculated. For temperature, the following equation is used [Sommer, 2015]:

$$RR = \frac{real\ recovery}{theoretical\ recovery} = \frac{\int (T_{ex} - T_{sur})\ c_w\ Q\ dt}{\Delta T\ c_w\ Q\ dt} = \frac{\int (T_{ex} - T_{sur}) dt}{\Delta T\ \ dt}$$

Where T_{ex} = temperature of extracted water (°C), T_{sur} = the surrounding temperature of 13 °C, c_w = heat capacity of water (J m^{-3} °C^{-1})), Q = well discharge (m^3 week^{-1}) and t = time (week).

Calculating the recovery ratio is done for the first year, in which the efficiency of ATES systems is lower, because the surroundings are not yet heated up or cooled down. It is also calculated for the tenth year, as a stabilized situation with a representative recovery ratio (Fig. 40).

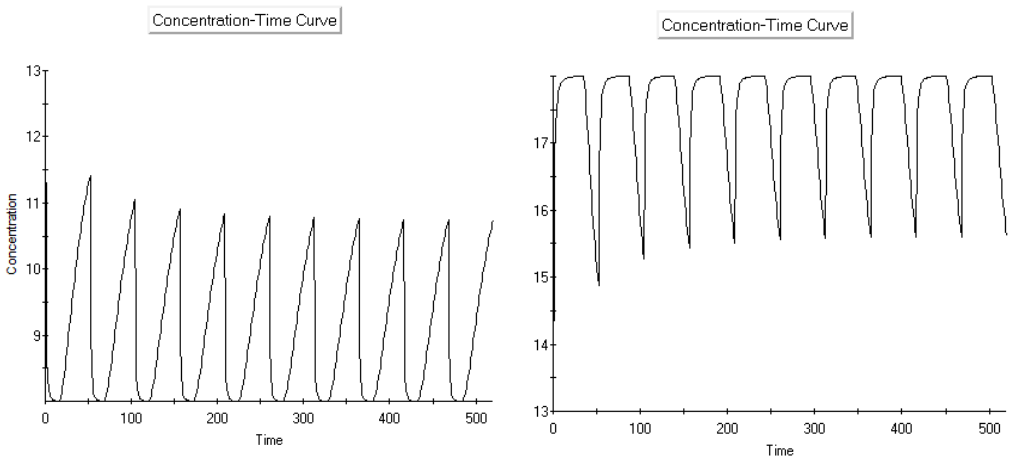

Fig. 40: Temperature-time curve showing the stabilization of temperature after 10 years (520 weeks).

Table 15: Recoveries for the cold and warm well in three cases: the recovery of water (R = 1), injected temperature (R = 1.6) and the solute VC (R = 1.1). This is the model output from the first year and the tenth year (stabilized).

Scenario		Recovery cold well (%)	Recovery warm well (%)
Water	1st year	62.7	64.9
	stabilized	64.9	67.3
VC	1st year	62.3	64.5
	stabilized	65.3	67.6
Temperature	1st year	63.8	66.8
	stabilized	71.4	74.8

Three different cases are analyzed: the recovery of water (without retardation, so retardation factor R = 1), the recovery of solute VC (R = 1.1, with dispersion) and the recovery of injected temperature (R = 1.6, with diffusion and dispersion). The results are shown in Table 15. A first observation from the table is that the efficiencies are higher after 10 year than after 1 year. Possibly this is caused by the fact that the surrounding water, that mixes with the injected water, becomes 'contaminated' with the injected water, VC or temperature. Secondly it is clear that for all scenarios, the efficiency of the warm well is higher than of the cold well, the model results in a difference of about 4 %-point.

Comparing the recovery of water and VC, in the first year water is better recovered than VC. This is presumably because in the case of VC dispersion is also included, so VC is spead. After 10 years, this effect is gone because the surroundings are also contaminated with VC so dispersion has no effect any more. After ten years, the recovery of temperature is higher than the recovery of VC, which is slightly higher than the recovery of water. This effect is probably due to retardation. More retardation means slower spreading and thus higher recovery.

Considering the difference between warm and cold wells, this is the largest in the case of temperature recovery. This has probably to do with $\bar{t}$. In the case of warm wells, the long injection period is negative for the recovery, because the water might flow that far that it can not be recovered any more. However, with a higher retardation water spreads not that far, so this negative effect is declined. The positive effect of β is still there for the warm well. This combination results in a larger difference between the recovery of the cold and warm well.

The lower recovery ratio of the cold well implies both a lower energy efficiency and more spreading of contamination, as less (contaminated) injected water is recovered.